THE UNIVERSITY OF WARWICK

University of Warwick institutional repository: http://go.warwick.ac.uk/wrap

A Thesis Submitted for the Degree of PhD at the University of Warwick

http://go.warwick.ac.uk/wrap/66780

This thesis is made available online and is protected by original copyright.

Please scroll down to view the document itself.

Please refer to the repository record for this item for information to help you to cite it. Our policy information is available from the repository home page.

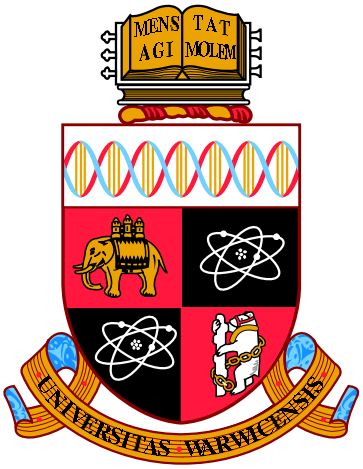

Opinion Dynamics: from Local Interactions to Global Trends

by

Anthony James Christopher Woolcock

Thesis

Submitted to the University of Warwick

for the degree of

Doctor of Philosophy

Centre for Complexity Science and Mathematics Institute

July 2014

THE UNIVERSITY OF WARWICK

Contents

Acknowledgments

I would like to thank all those who have helped me in the last few years. Annette Woolcock has provided unquantifiable support for which I will always be grateful. I am indebted to my supervisors, Dr. Colm Connaughton and Yasmin Merali, both at Warwick University, for their many suggestions and fruitful discussions. Their help and guidance has been a source of inspiration and motivation. There are many others within Warwick and Complexity who deserve a mention for many reasons: Paul, Matt, Jamie, Q, Sam, Adnan, Ben, Marcus, Martine, Dan, Dan, Olly, Monica, Phil, Jen, Jenny and family, and others too. I wish to thank them for: scientific discussions, floor space, spare bedrooms, excellent meals, suggestions, explanations, coffee, GLTron, coffee discussions, but most of all friendship and encouragement which has helped me on my way. And to all those others I would like to thank but do not have room: Thank you.

Declarations

This work has been composed by myself and has not been submitted for any other degree or professional qualification. Work from Chapter 3 was done in collaboration Dr Colm Connaughton and Dr Federico Vazquez. Work from Chapter 6 was done in collaboration Dr Colm Connaughton and Yasmin Merali.

Abstract

We study the dynamics of consensus formation in a finite two-state voter model in which each agent has a confidence in their current opinion, k. The evolution of the distribution of k–values and the opinion change rules are coupled together to allow the opinion dynamics to dynamically develop heterogeneity of agent states in a simple way. We introduce two models. In both models pairs of agents with different opinions interact, which means k–values are compared and, with probability p, the agent with the lower value adopts the spin of the one with the higher value. In our nonconserved confidence model the agent with the higher k–value increments their confidence by one. In our conserved confidence model, additionally, the agent changing opinion reduces their k–value by one, so total confidence is conserved. The only parameter in both models is the probability p. We study the nonconserved model on the complete graph and compare the consensus time with the case $p = \frac{1}{2}$ in which the opinion dynamics are decoupled from the k–values and are equivalent to standard voter model dynamics. When $\frac{1}{2} < p < 1$, agents with higher k–values are more persuasive and the consensus time is increased relative to the standard voter model although it still scales linearly with the number of agents, N. When $p = 1$, the consensus time scales as N^α with $\alpha \approx 1.4$. When $0 < p < \frac{1}{2}$, agents with higher k–values are less persuasive and the consensus time is greatly decreased relative to the standard voter model and appears to be logarithmic in N. We provide some partial explanations for these observations using a mean-field model of the dynamics and a low-dimensional heuristic model which tracks only the sizes and mean k–values of each group. We also study the conserved model on the complete graph. When $\frac{1}{2} < p < 1$ this model also has consensus time that scales linearly with N and when $p = 1$ it scales as N^α with $\alpha \approx 1.4$. However when $0 < p < \frac{1}{2}$ this conserved confidence model does not behave in the same way as the nonconserved model and the consensus time scales linearly with N. We compare the mean-field model dynamics with those of the nonconserved confidence model to partially explain model behaviour differences. We find consensus times for the nonconserved confidence model on low dimension regular lattices and compare with the complete graph. When $\frac{1}{2} < p < 1$, the consensus for the model on a 2d lattice is slower than the fully connected model, but in 3d results suggest that it is comparable. When $p = 1$, the population is prevented from reaching consensus by stable locally coordinated confidence arrangements. When $0 < p < \frac{1}{2}$, the consensus time is slow compared to the fully connected model and we notice spatial structures in the simulations. Also we implement a modification to the Axelrod model to introduce heterogeneity in the opinion space. We implement a bias in which opinions (features) are updated and separately a bias in the weight of influence of opinions on whether interaction occurs. Despite affecting the dynamics of the opinions and the time to absorbing state, we find the state, consensus or coexistence, the model typically reaches is robust under the effect of these two types of heterogeneity.

Abbreviations

General

- N population size, i.e. number of agents
- d system dimension
- t time
- τ_N mean time taken to reach consensus (or frozen fragmented) state, with a population N, averaged over simulations

Voter models

- s the choice (opinion) of the agent (s $= \pm$)
- k the confidence the agent has in their own choice (opinion)
- n^s number of population with choice s
- f_k^s fraction of population with choice s and confidence k, $f = n/N$
- F_k^s fraction of population with choice s and confidence up to k, nonconserved model: $F_k^s = \sum_{j=0}^{k-1} f_j^s$, conserved model: $F_k^s = \sum_{j=-\infty}^{k-1} f_j^s$
- G_k^s fraction of population with choice s and confidence above k, nonconserved model: $G_k^s = \sum_{j=k+1}^{+\infty} f_j^s$, conserved model: $G_k^s = \sum_{j=k+1}^{+\infty} f_j^s$
- ρ^s fraction of population with choice s, nonconserved model: $\rho^s = \sum_{j=0}^{+\infty} f_j^s$, conserved model: $F_k^s = \sum_{j=-\infty}^{\infty} f_j^s$
- $\rho^{\pm} = F_{\infty}^{\pm} = F_k^{\pm} + G_k^{\pm} + f_k^{\pm}$ holds in non-conserved and conserved models

- conservation of mass is given by $\rho^+ + \rho^- = 1$
- p the parameter defining the probability that a more confident agent wins (persuades the other agent) in an interaction
- total mean + confidence, $\mu^+ = \sum_{k=0}^{+\infty} k f_k^+$ in non-conserved model, $\mu^+ = \sum_{k=-\infty}^{+\infty} k f_k^+$ in conserved model,
- total mean - confidence, $\mu^- = \sum_{k=0}^{+\infty} k f_k^-$ in non-conserved model, $\mu^- = \sum_{k=-\infty}^{+\infty} k f_k^-$ in conserved model,

Axelrod models

- f the opinion (feature)
- F number of opinions (features)
- q number of choices (traits) for each feature to choose from
- C_i^f cultural choice of the fth feature of the ith agent
- m the overlap between two agents
- $\langle S_{max} \rangle$ mean size of the largest cultural region
- $\langle R \rangle$ mean number of cultural regions
- α parameter defining the level of linkedness in the Biased Outcome model
- β parameter defining the level of importance of opinions (features) in the Biased Topic model

Chapter 1

Introduction

"Sociophysics" is a branch of complexity science which aims to use methods from statistical physics to provide conceptual explanations for social phenomena. Within this field of study, much attention has focused on opinion dynamics which is the study of consensus formation in idealised agent-based models of social interaction in which the effects of social influence and opinion formation are encoded into simple stochastic interaction rules between agents. This thesis investigates the effects of various forms of heterogeneity on two of the most elementary models of opinion dynamics (the voter model and the Axelrod model) and explores the importance of coexistence states in which groups of agents with differing opinions coexist in the population.

Agent based models in this context can be "used to perform highly abstract thought experiments that explore plausible mechanisms that may underlie observed patterns" [40, p.147]. And these models do not necessarily "...aim to provide an accurate representation of a particular empirical application. Instead the goal of agent-based modelling is to enrich our understanding of fundamental processes that may appear in a variety of applications" [5, p.25]. In this spirit we investigate the effect of the introduction of specific forms of heterogeneity into the voter and Axelrod models.

Research has shown that changes to the voter model, which at first sight might seem innocuous, can lead to significant changes in the statistics of consensus times. In particular, the introduction of various forms of heterogeneity can have far–reaching consequences. Heterogeneity here means that not all agents are equivalent. The introduction of even a single "zealot" [45] – an agent with a finite probability to unilaterally change opinion back to a preset preference – greatly increases the consensus time (although the scaling exponents remain the same). If all agents

are assigned flip rates which are sampled from a probability distribution then, by choosing this distribution appropriately, one can make the approach to consensus arbitrarily slow [41]. This model is called the Heterogeneous Voter Model. On the complete graph, one can have $\tau_N \sim N^\beta$ with $\beta > 1$ arbitrarily large. This occurs because τ_N is dominated by the (slowest) flip rates of the "stubbornest" agents. A related model is the Partisan Voter Model [41]. In this model, heterogeneity is introduced by randomly endowing all agents with a preferred opinion. The interaction rules are modified so that agents have a higher rate for switching to their preferred opinion. The consensus time on the complete graph was then found to be even longer and grow exponentially with N. In contrast to these examples, heterogeneity can also accelerate the formation of consensus. For example, if the agents acquire temporal memory such that their flip rates decrease the longer they remain in a given state then, depending on the strength of this effect, the scaling exponent of τ_N can decrease [57]. Even more extremely, if the underlying graph is replaced by a random, scale-free network (a network that has a degree-distribution that follows a power law), then depending on the properties of the degree distribution of this network, τ_N, can scale sub-linearly with N and can even become logarithmic or independent of N [56]. This effect is known as "fast consensus".

Our research goal is to investigate the effects of various forms of heterogeneity on two of the most elementary models of opinion dynamics (the voter model and the Axelrod model) and explore the importance of coexistence states in which groups of agents with differing opinions coexist in the population. We use the mean consensus time of the finite size models as a way to test the effect of the introduction of heterogeneity we make.

We implement heterogenous opinions in the two simplest ways. Firstly we introduce and study an adapted voter model that incorporates agents with self-confidence in their current opinion, which is coupled with the voter dynamics through a parameter p which assigns the probability that a less confident agent changes opinion. Secondly we study the effect of heterogenous opinions in the interaction rules between agents, with multiple opinions (features), in an adapted Axelrod model. We investigate the modified voter and Axelrod models by finding the time to consensus. We test whether a coexistence state of mixed opinions is reached in the adapted Axelrod models. The voter and Axelrod models are chosen because both stochastic models reach a frozen state in finite time so we are able to find the mean consensus time. Also the Axelrod model contains many frozen (absorbing) states which are not consensus so this model is natural to investigate the ability for the model to reach coexistence as opposed to consensus. Also both

models incorporate specifically nominal opinions.

In Chap. 2 we provide an introduction to similar models from the literature before firstly introducing the non-conserved confidence model in Chap. 3. This model is a finite two-state voter model on the complete graph in which each agent has a confidence in their current opinion, k, in addition to its opinion. In this way we incorporate fitness as self-confidence and the evolution of the distribution of k–values and the opinion change rules are coupled together to allow the opinion dynamics to dynamically develop heterogeneity and memory in a simple way. Pairs of agents with different opinions interact, which means k–values are compared and, with probability p, the agent with the lower value adopts the spin of the one with the higher value. At the same time the agent with the higher k–value increments their confidence by one. The only parameter in the model is the probability p. We refer to this as the non-conserved confidence model. We compare the consensus time with the reference case $p = \frac{1}{2}$ in which the opinion dynamics are decoupled from the k–values and are equivalent to standard voter model dynamics. We find that when $\frac{1}{2} < p < 1$, agents with higher k–values are more persuasive and the consensus time is increased relative to the standard voter model although it still scales linearly with the number of agents, N. When $p = 1$, the consensus time scales as N^α with $\alpha \approx 1.4$. When $0 < p < \frac{1}{2}$, agents with higher k–values are less persuasive and the consensus time is greatly decreased relative to the standard voter model and appears logarithmic in N. We provide some explanations for these observations using a mean-field model of the dynamics and a low-dimensional heuristic model, in Sec. 3.8, which tracks only the sizes and mean k–values of each group. In this work a 'heuristic model' is a model that is simplified relative to the full model but still captures the characteristic behaviour of the full model. The purpose of creating the heuristic model is to help understand the behaviour of the model.

We find that the mean-field equations posses a coexistence state. This exists only at the mean-field level because the stochasticity in the finite size model helps the system reach an absorbing consensus state. The stability of the coexistence state in the mean-field model depends on the confidence dynamics. This stability depends on the value of p. When $p > \frac{1}{2}$ the coexistence state is stable and at $p = 1$ it is extremely attractive. We suggest that this influences the consensus time and is the reason for increasingly slow average consensus in the finite size model and the slow exponent when $p = 1$. When $p < \frac{1}{2}$ the coexistence state is unstable and we suggest that this influences the consensus time in the finite size model, to cause the fast consensus (consensus times that are logarithmic in N) found in this model.

In Chap. 4 we adapt only the interactions in the non-conserved confidence

model to include the consequence that the agent changing opinion also reduces their own k–value by one, so the total confidence in the model is conserved. When $\frac{1}{2} < p < 1$ this model also has consensus time that scales linearly with N and when $p = 1$ it scales as N^{α} with $\alpha \approx 1.4$. However the model with $0 < p < \frac{1}{2}$ does not behave in the same way as the non-conserved confidence model and the consensus time is not fast but scales linearly with N. We compare the mean-field model of the dynamics with those of the non-conserved confidence model to partially explain the differences in the model behaviour. We see that when $p > \frac{1}{2}$ there is a coexistence state, and when $p < \frac{1}{2}$ non-equal coexistence state which is different. We suggest these coexistence states in the mean-field model influence the consensus times in the finite size model.

We make a numerical study of the non-conserved confidence model placed on regular lattices in low dimensions in Chap. 5. We find the average consensus time from Monte Carlo simulations and compare these with the model on a fully connected network. When $\frac{1}{2} < p < 1$, the consensus time in 2d is different to the fully connected model, but in 3d results suggest that it is comparable. When $p = 1$, the population is prevented from reaching consensus by stable locally co-ordinated high low confidence agent arrangements. When $0 < p < \frac{1}{2}$, the consensus time is slow compared to the model on a fully connected network and we notice spatial structures in the simulations.

In order to study the effect of heterogenous confidence space we implement a modification to the Axelrod model to introduce heterogeneity in the opinion space, and specifically the importance of the opinions, Chap. 6. We implement a bias in which opinions (features) are updated and separately a bias in the weight of influence of opinions on whether interaction occurs. In the original Axelrod model, when an interaction occurs, there is an equal update probability for each unshared feature, between two agents. There is no bias in which feature is updated. We implement bias in which feature is updated by introducing a rule, for all agents, that increases the probability of updating features, which are both linked and have the linked feature currently shared by both agents. In this way if agents agree on a feature the linked feature is more likely to be updated. In the original Axelrod model the probability of interaction occurring is given by the sum of number of shared features, relative to the total. We introduce a weight to the contribution of each feature to the sum, and therefore the probability of interaction.

The coexistence states in the Axelrod model are different to the ones found in the mean-field level of the non-conserved and conserved confidence models. In the Axelrod model they are truly absorbing states because they freeze the system in the

stochastic model. We find that despite affecting the dynamics of the opinions and the time to absorbing state, the state, consensus or coexistence, that our adapted Axelrod model typically reaches is robust under the effect of these two types of heterogeneity. We highlight the differences in the heterogeneity introduced to the voter model and the Axelrod model. The heterogeneity we implement in the voter model is dynamic and at the level of agents. The heterogeneity we introduce into the Axelrod model is static and at the level of features. We suggest that the dynamic aspect of the changes to the voter model help the system reach a coexistence state: it is the changes in the confidence distributions that enable the coexistence state to be reached in the mean-field model and as a consequence, we suggest, the consensus time in the finite size model is affected.

Chapter 2

Background

2.1 Social influence

The focus of this work is to understand the effect of heterogeneity in the voter model, through the dynamically confident agents, and in the Axelrod model through biased opinions. Because both of these models capture elements of social influence theory which has been based on empirical research, we discuss a brief overview of the key theories from the area of social influence. The focus of our work is on how quickly a population reaches consensus given the changes made to the model in introducing the respective heterogeneity. Therefore we focus on research which considers social influence as a process in which individuals change their opinion to agree with another individual or a group, often described as conformity.

The research on individuals in groups and the social influence they are affected by initially focused on the effect of a majority influencing a passive minority. Research by Asch [3] on conformity showed that individuals holding an opinion which is correct can change their opinion when they are part of a group of individuals who hold the opposing (incorrect view). This work intended to show the effect of the preference of the individual to modify their own opinions towards social conformity. A group of students were shown a card with lines of different lengths and asked to compare and correctly identify the line with the same length as shown on a second card. One subject sat with actors who identified the incorrect line unanimously. Thus they were situated in a group of a majority holding an opinion they knew was incorrect (given the context of the task). Asch repeated the experiment with different majority sizes, from one to 15, and found that the subjects would on average give the incorrect answer (i.e. agree with the majority) roughly one third of the times when the number in the majority was more than three. This work showed

that it is possible for a majority to change the opinion of a minority through the presentation of their unanimous (incorrect) opinion and thus achieve conformity.

The view of social influence as a majority affecting a passive minority ignores the effect a minority may have. A theory of minority influence was introduced by Moscovici [47] that described the influence made by a minority is different to that made by a majority. This different mode of influence was that a minority presents a novel view, relative to the opinion of the majority, and therefore provides a reason for individuals to be influenced. However this theory was also in a sense one sided because it only considered a minority group influencing a passive majority. A composite theory which combines both majority and minority influence is Social Impact theory, introduced by Latané [38]. Social Impact theory is a model designed to quantify the amount of social impact in social situations through capturing the effect of social forces, a psychosocial law and the multiplication/division of impact. These three effects are implemented as three rules in the model. Social forces are implemented as a rule that the quantitative effect of the social impact is determined by the strength, immediacy and number of people in a simple multiplicative function. The psychosocial law states that the initial increase in number of people in the source from none to one gives the greatest increase in the social impact. As more people are added to the source the increase in social impact levels off. The rule is that the effect is given by the number of people to some power, multiplied by a scaling constant. The effect of a greater number of targets (that the source acts on) is that the social impact is divided between more individuals. Therefore the rule implementing the multiplication/division of impact is that the effect of the source is reduced and therefore divided by the strength, immediacy and number of the target.

The dynamic Social Impact theory, introduced by Nowak et. al. [50], is an extension of the Social Impact theory, and is constructed from a number of model elements: attitude; persuasiveness; supportiveness; immediacy; and the model rules. Attitude is the opinion and is a binary (nominal) choice. Persuasiveness is the strength (in the range 0-100) of ability to persuade members that hold a different attitude (opinion) and as a result of the interaction the persuasiveness value is changed to a random value (between 0 and 100). Supportiveness is an additional characteristic to persuasiveness and accounts for the ability of an individual to support another individual, with the same opinion, to resist changing opinion. Supportiveness is also given by a number between 0 and 100 and is randomly changed after interaction. Immediacy is the physical distance between agents. These elements are combined in a multiplicative way, to find the total persuasiveness of the source, so that the impact of a group of members is the square root of the number of group members

times the average force (persuasiveness divided by square of the distance) of each of those members. The impact of support is given by the same formula but with support replacing persuasiveness. Individuals change opinion when the impact of support (from their own opinion group) was less than that impact of persuasiveness from the opposite opinion group. Our model is formulated differently but addresses a question that one could consider in the Dynamic Theory of Social Impact, which is the introduction of a resistance-to-change parameter.

An alternative approach to understanding social influence is to investigate the changes in the strength of attitudes or polarisation. James Stoner in unpublished work (1961) found that the decisions taken by a group were more risky, or extreme, than those made by the same members as individuals. Research by Moscovici [48] found that attitudes in a group were shown to become more extreme through a process of group discussion. The similar 'persuasive arguments' theory provides another example of conformity. Research by Myers [49] found that when individuals hear new arguments in favour of their current opinion they take a more extreme stance in favour of the same view. Another process which results in polarisation is the effect of taking an extreme view, that is in line with the current group preference, in order to be viewed like a leader. This process of comparison and change is included in the Social Comparison theory.

The theories of social influence, discussed in this section, motivate the simple interaction rules used by socio-dynamics models. The simplest rule capturing social influence is that one agent copies a neighbour and it is this rule that both the voter and Axelrod models incorporate.

Social influence and the voter model

The voter model is a simple model which incorporates social influence because an agent copies the opinion of one of their neighbours. This is the simplest way that social influence can be implemented. Social influence is an effect motivated by the research described in the previous section and the seminal research to show social influence between individuals by Festinger [21]. Festingers study was into the attitudes towards and the activity in a tenant organisation by those living in two housing projects. The responses to questionnaires and interviews as to whether individuals attitudes were favourable, neutral or negative and whether they were active in the organisation or not showed that there were patterns of uniformity within groups. These groups of individuals were friends who lived geographically close to one another. Festinger suggested that standards developed in the groups and the uniformity in attitudes resulted from social influence, although he did not

address how this process works. The conclusion was that social pressure between individuals living in proximal locations and within friendship groups resulted in individuals adopting the same attitude or opinion as the others in their group.

Self-esteem in relation to changing opinions has been studied. We consider self-esteem in the context of the influence of others to be self confidence. Research by Janis [28] showed that people with low self-esteem are persuaded more easily than others. She compared self-rating scores of personality factors, of college students with their results of how influenced they were by persuasive communications. And found high correlation between those who self-rated highly in the social inadequacy responses, a representative of self-esteem in this test, and those who changed their opinion more. Rhodes and Wood [52] highlight in a meta-review the research that shows that people with low self-esteem are persuaded more easily than people with high self-esteem. More recently research by Kearns et. al. [29] showed that in the context of specific networks of voters that those individuals who are less likely to change their own opinion can effect the ability for a group to reach consensus. This work did not use confidence as a factor but found that, in experiments where participants had to reach a consensus in order to receive a payment, those more stubborn individuals were more likely to be involved in experimental runs that finished in consensus. The ability for stubbornness to affect the group dynamics is motivation to study dynamic confidence which has the consequence that agents are less likely to change opinion, i.e. act in a stubborn way.

Social influence and the Axelrod model

Like the voter model, the Axelrod model updates agents as a result of interaction to include the concept of social influence. Research by McPherson et. al. [44] showed that those who are similar are more likely to have social links, described as homophily. Empirical studies by Billy et. al. [9] found that in junior high school friendship groups there was homogeneity bias in relation to sexual behaviour. Research by McPherson and Smith-Lovin [43] found that in work-related groups individuals have a preference for friendships between those with similar status. Both studies finding examples of homophily. The Axelrod model includes the rule that if agents are more similar then they are more likely to interact, thus also incorporating the effect of homophily.

We provide two modifications of the Axelrod model. We link opinions (features) so that if one is shared between agents then the other is more likely to be updated than the other, regular, opinions. Motivation for linking the features in our adapted Axelrod model comes from the empirical research that shows that some

opinions are correlated [20]. Separately we include a weighted bias to opinions in the interaction stage of the Axelrod model. The consequence of the bias is that the weight of importance of that opinion when deciding whether to interact is greater. There is motivation for this model characteristic from research by Asch [2]. His research finds that not all traits are equal when forming an impression of personality. Asch found that central characteristics were more important than peripheral ones when subjects in two groups were read exactly the same words describing a personality. One group were also read the word 'warm' and the other group 'cold'. The brief sketches the subjects then wrote demonstrated that the difference in the one word read to them resulted in a change in the entire impression formed. The results showed that the central characteristic of warm/ cold was able to transform the other characteristics.

2.2 Modelling approaches

Two related approaches to investigating simple models are computational Agent Based models (ABMs) and statistical physics methodology. ABMs are highly simplified, 'bottom-up', models of processes which occur within, usually large, populations of agents. Statistical physics is useful when studying systems of large numbers of entities which follow simple local interaction rules. These are both useful when studying our models. There are two aspects to ABMs which motivate their use: the typical approach and the nature of the results. Firstly we note that the typical approach one uses for ABMs is 'bottom-up'. This approach is commensurate with our research question. We want to define the local rules and then make observations at the population level. Secondly ABMs are a test-bed for implementing mechanisms of social influence. This means that social interactions observed in the real world can be implemented and their, possibly surprising, consequences found (for example in Schelling's' models of segregation [53] where it is only a small amount of preference in an agents choice to move that result in a global segregation between the different agent types). Also theoretical assumptions can be implemented and their effect tested. In this way models help perform 'virtual experiments' that test macro-sociological theories. Furthermore when the assumptions tested are not empirically based they can still improve understanding of the social model studied because these models do not necessarily "aim to provide an accurate representation of a particular empirical application." [5, p.25]. The aim of ABMs is to further understanding of the processes that occur within the dynamics of the systems studied. Limitations of ABMs are that that the simplicity of the model definition which is

required to simulate it fully mean that the accuracy of the model definitions can be challenged. There is also the problem presented by the introduction of additional parameters that requires more validation. However it is the power of ABMs to provide examples of surprisingly subtle and complex phenomena arising from models with plausible, simple and implementable model rules, for example population wide patterns of segregation emerging despite only limited tendency for agents to seek local homogeneity [53].

2.3 Models of Opinion Dynamics

We now introduce two opinion dynamics models, the voter and Axelrod models. Both are simple models with rules based on empirically observed phenomena. They are the simplest models which allow us to incorporate model adaptations that help us ask our research question because the stochastic, finite models will always reach a frozen state, either consensus or, in the case of Axelrod model, frozen coexistence state. Therefore we can measure the consensus time for both models and investigate whether a coexistence state is reached. Also they exhibit behaviour that is dependent on simple model parameters. Whether the dynamics reach consensus or not and the time taken to reach consensus are dependent on these parameters. Therefore we are able to obtain results of the time to consensus or alternative frozen state as a way of investigating the effect of including the confident agents compared to the dynamics of the original voter and Axelrod models respectively. They have been studied previously and after our brief introduction we summarise some relevant previous work. In the following chapters we present: our new modifications to these models; motivation for these modifications; how we tested them; and the results obtained.

The phenomena of social influence is simpler than homophily, therefore we firstly introduce a model which includes social influence (but not homophily): the voter model [39]. The model was named 'voter model' because the opinion can be taken to mean the voter's attitude on one subject, but was originally created as a model for the competition of species [13] (where opinions represented occupation at that site of one of two species competing for territory and where individuals from both species are equally matched). This model is constructed of agents which interact repeatedly. The agents reside on nodes in a network of connections between neighbouring agents which can interact with each other. Each agent has an opinion which is a preference between, only, two different choices (for example between Labour and Conservative). Each turn an agent i is selected at random. Also one

of the neighbours of i is selected at random. The agent i then takes the opinion of the neighbour, and this directly implements social influence. So directly after the interaction the two agents share the same preference, and have therefore become more similar. We discuss the key results previously obtained for the original model in Section 2.4.

The Axelrod model [4] is more complicated. Again the agents reside on the nodes of a network of connectivity, typically a lattice where each agent has exactly four connected neighbours. However in this model the agents have a range of choices available to them. Each agent is represented by F, ordered, 'opinions' (synonymous with 'features') each with q 'choices' (synonymous with 'traits'). (Therefore $F = 1$, $q = 2$ is the voter model's range of opinion choices). Also the interaction rules are more subtle in the Axelrod model. Both homophily and social influence are implemented. Each turn an agent i is selected at random and one of its neighbours j is also selected. Then the probability of interaction is calculated. The probability of interaction is the proportion of overlap of features (the number of features with respectively shared traits between the two agents, an integer between 0 and F) divided by the total number of features (F). Therefore agents who are more similar (with more features with matching traits) are more likely to interact. This is the implementation of homophily: more similar individuals spend more time together and are more likely to interact. With the probability calculated an interaction occurs and the first agent of the pair selected copies one of the traits of the features of the second (selected at random from all the features without the same trait). Therefore directly after an interaction the two agents are more similar: social influence has been implemented.

In both the voter and Axelrod models the interactions are repeated. The interaction steps are followed in both models until no further interactions are possible, when the system has reached an absorbing state, for example when all agents have the same opinion so no further updates are possible and the system is 'frozen'. The voter model has only two absorbing states: consensus for one choice or consensus for the other. The Axelrod model has many absorbing states which are either consensus (all agents have exactly the same set of opinions) or a diverse frozen state (a more complicated state where interactions are not possible because each pair of agents either have exactly the same opinions are they share exactly none). There are many consensus type absorbing states, in the Axelrod model, exactly one for each combination of q different choices for each F feature, q^F. There are many more absorbing states of the diverse type where connected regions of agents all sharing the same agent state of features (looking like local consensus) lie next to other regions which

share no trait for their respective features. In this type of state no reaction occurs because the overlap of features is zero (for example a model with $F = 3$, $q = 4$ would have no interactions between an agent with state 442 and one with 134).

Furthermore the model specifications of the number of features (opinions), F, and traits (choices for each opinion), q, specify the typical type of absorbing state reached for multiple simulations. In cases with fewer traits, for example $F = 10$, $q = 2$, the population of agents is more likely to reach consensus in the simulations. Whereas cases with fewer opinions (features) and with more traits, e.g. $F = 2$, $q = 10$, are more likely to reach a diverse absorbing state. Fewer traits mean that it is more likely that agents will share some or all and continue to interact until consensus is reached. More traits means there are more combinations where no features share a trait and it is more likely that the population will reach a state where neighbouring agents are either the same or have each feature different, i.e. a diverse absorbing state is reached.

It is the relative choice of F and q which determines the typical absorbing state reached. Previous work has highlighted the transition in typical absorbing state when q is changed and F is held constant [4]. However it is possible to hold q constant and show the transition when F is changed.

The two models we study have only interactions between paris of agents, and both include opinions which are discrete (in the sense that the opinion is held or not). There are models which provide different examples of social dynamics where these criteria are different. For example the Axelrod model includes homophily in the calculation of the probability of interaction between two agents. This calculation measures the similarity of the features of those agents. Another model which allows for the comparison of two agents before interaction occurs is the Bounded Confidence model [18], [17]. In these models each agent is characterised by a single decimal value between 0 and 1 representing their opinion. Comparison between agents is simply made by finding the difference between their opinion values. If this difference is above some set bound then they do not interact. If it is less then the agents do interact. In this way homophily is included. (When the agents do interact both their opinion values become the average of their previous ones, and therefore social influence is also included in the model). We study modified versions of the voter and Axelrod models because they both reach consensus in the finite size models which means we are able to measure the time to consensus (or frozen coexistence state in the case of the Axelrod model). Although they incorporate different aspects of social influence they are similar in the sense that they both incorporate nominal opinions.

2.4 Voter model

The voter model, introduced in the previous chapter, is a collection of N agents, each with an opinion (from a binary choice), sitting on the nodes of a network. Interactions result in an agent copying the opinion of their neighbour. We only consider networks with a single connected component. The model then has only two absorbing states of consensus for one opinion or the other. A natural global characteristic of voter models is the variation of the time taken to reach consensus.

The voter model when viewed as a simplified spin model, where opinions are spins, has be studied on lattices where the agents sit on the vertices of regular lattices [54], [23]. These models include the notion of the distance between spins through the specification of the lattice. Using this structure for the connectivity was mathematically useful because the regularity of the spatial model meant some models were mathematically tractable. Essentially each pair of individual spins could be viewed in the same mathematical way due to the equality of the distance between them. Given the absorbing states present in the voter model, of consensus for either opinion, a natural question is 'How does the model reach consensus?'. Therefore research has focused on understanding whether these fully ordered states of all agents holding the same opinion are reached and what are the process by which the model reaches them.

It was shown that starting from a disordered initial condition the dynamics mean that on average the system will move to a state where there is less disorder and agents are increasingly likely to be surrounded by those with the same opinion. The typical cluster size will grow with the square root of time, and so the voter model increases in order [54]. This increase of order indicates a coarsening process where the characteristic length scale of the size of a cluster increases with time. The coarsening process stops when the system reaches one of the two symmetric absorbing states. These are the consensus states (in which all agents have the same spin, "opinion") and the time to consensus is a way of understanding the speed of the ordering process. The size of the system, i.e. number of agents, and the dimension of the system both have an effect on the consensus time of the voter dynamics.

An inactive interface is the bond (connection) between two agents of the same opinion. An active interface is a bond between two agents of different opinions. The concentration of active interfaces is the number of different bonds between agents of different opinions relative to the total number of bonds. Frachebourg and Krapivsky [23] showed that the density of active interfaces (between agents with different opinions) was asymptotically finite in dimensions greater than 2. They

used the spin-flip rates (for an agent copying a neighbour) to write down the Master Equation for the probability distribution of all the agents opinions. From this they found the average correlation of opinion, between two agents at a given distance. This was then used to find an asymptotic solution for the density of the active interface (between agents with different opinions). They found that when $d \leq 2$ the asymptotic behaviour of the density of active interfaces is to decrease with time, so the voter model in these low dimensions will reach consensus through a coarsening process. They found that the density of active interfaces does not tend to zero as time increases when $d > 2$. Instead the density of active interfaces tends towards non-zero constant so there is a finite density of active interfaces and therefore not consensus in the infinite population model when $d > 2$. However in all dimensions the finite population model does reach consensus asymptotically. The mean time to consensus in the finite population models depends on the size of the population, N. Specifically, for finite populations of size N, the mean time to consensus is $\tau_N \simeq N^2$ when $d = 1$, $\tau_N \simeq NlnN$ when $d = 2$ and $\tau_N \simeq N$ when $d > 2$ (see [35, chap. 8]), [14].

In general surface tension is a force that arises from the local curvature of the interface between two clusters (connected groups of agents with the same opinion). To minimise the free energy the system reduces the area of the interface. This surface tension is typically found in models with an energy dependent on the local state of the system. The process of reducing the area of the interface has a consequence that numerous smaller clusters in an initial disordered state will become part of larger clusters. These larger clusters will have a characteristic length scale. Whether surface tension is present in the voter model has been investigated relatively recently [19]. Domain lengths are the size of the regions of agents with the same opinion. Scheucher and Spohn [54] found from simulations of the voter model that there was no single domain length in 2d. This suggested that there is no typical domain length which would be found in a system coarsening through surface tension. Specific initial conditions were used to show whether there is surface tension present. Dornic et. al. [19] simulated the voter model in 2d with initial condition of a droplet of agents with one opinion in a sea of agents starting with the other opinion. In a curvature driven model the radius of the droplet would reduce in order to reduce the concentration of active interfaces. However they found that while the interface became less smooth ('roughened') the average radius remained the same. This indicates that the coarsening process was not curvature driven. Therefore the voter model coarsens through a process driven by interfacial noise and does not include surface tension.

2.4.1 Voter model variations

A large number of variants of the voter model have been studied in the literature, the examples that make the key departures from the voter model specification are: Sznajd model [6], Majority Rule model [34], voter model on heterogenous graphs [56]. Below we provide more detailed discussion of several variants which are relevant to the 'confident voter model' which we introduce in Chap. 3.

2.4.2 Zealots, weak-willed and heterogeneous agents

Mobilia [45] introduced heterogeneity into the standard voter model by incorporating a single zealot to the voter model. A zealot means an agent which favours + and therefore is allowed to change to this state, from −, with a fixed rate. All other agents are standard and it is through the interactions with the others that the zealot agent affects the dynamics. The zealots are agents which spend more time in the favoured opinion and are more likely as a consequence to cause their neighbours to take the favoured opinion. Mobilia analytically studied this model on regular lattices with infinite populations and found that the models in 1d and 2d reached consensus given by the choice of the zealot. The consensus time for large populations, i.e. as $N \to \infty$, in 1d, 2d, and 3d scale with N in the same way as the original voter model.

In further work on the effect of zealots Mobilia et. al [46] studied a finite density of zealots. Heterogeneous agents are included that are either in favour of one opinion or the other. This is different to the single zealot model [45] because now the zealot nature is incorporated by never allowing them to change their opinion. There are therefore in fact four heterogeneous agents: zealot +, susceptible +, susceptible −, and zealot − where zealots never change and susceptibles can. Mobilia et. al. studied the stochastic model on the complete graph where all agents are connected to all others. When the number of zealots with both opinions was equal they found that averaging over many simulations the distribution of the magnetisation (i.e. the difference in the number of − agents and + agents) was a Gaussian centred at zero (i.e. equal number of agents with both opinions). However there are time-dependent fluctuations in the single simulations that fluctuate about the steady state of equal coexistence of + and − agents (zero magnetization). Mobilia et. al. show that the more zealots present the smaller the fluctuations about the zero magnetisation, and that it is only a small proportion of zealots ($\simeq 1/10$) that are required to maintain the steady state with only small fluctuations about it. The consequence is that the width of the Gaussian that is the magnetisation averaged over many simulations is

more narrow with a greater number of zealots. When there are an unequal number of agents in favour of opinion $+$, Z_+, and Z_- (in favour of $-$) the steady state (average of simulations) magnetisation is $m^* = (Z_+ - Z_-)/(Z_+ + Z_-)$. Mobilia et. al. found that the model on 1d with two zealots of opposite opinion would result in magnetisation that was peaked at zero (equal numbers of $+$ and $-$ agents) for both the analytical and result average over simulations. However the case with many zealots in 1d (with periodic boundary conditions, i.e. a ring) provides the opportunity for two situations. These are the dynamics where: zealots of the same type to 'book-end' a segment which over time reaches consensus for their opinion; and where opposing zealots 'book-end' a segment which never reaches consensus but contains a domain wall (that separates opposing opinions) that diffuses freely within the segment. Therefore the Gaussian magnetisation depends on the initial conditions (whether segments are bookended by zealots of the same or different opinions). They find that distributions of magnetisation in 2d (with equal numbers for each opinion) are similar to the mean-field (for a range of total number of zealots, from 2 to 512, in population of $N = 1000$). Overall the result is that the presence of zealots which favour of both opinions (who never change their opinion) prevent consensus and keep the numbers of agents with each opinion roughly equal. The work does not consider agents which have confidence in their own opinion which can change over time.

Another way to introduce a single type of heterogeneous agent, that have different confidence in their own opinion, is to include weak-willed agents. These agents are more likely to change opinion, in contrast to the zealots in the work of Mobilia et. al. [46] which never change opinion. Weak-willed agents, as those which vacillate, have been incorporated to the voter model by Lambiotte [36]. These agents are different to the standard voter agent because in the interaction they change opinion if either of two (randomly selected neighbours) hold an opinion different to their own. Therefore the model is different to the voter model in two respects. There are heterogeneous agents and the number of neighbours involved in the interaction is different. In the voter model only one agent is considered in the interaction. Lambiotte finds the mean-field dynamics and identifies a stable fixed point of equal numbers of agents with each opinion. To study the stochastic dynamics they find the probability of reaching consensus, in 1d and 2d, for a given initial condition of proportion of agents with one opinion, for example $+$. They find that the probability of reaching consensus is different to the voter model, and that for larger populations the exit probability (the probability of reaching consensus) is reduced, even for initial conditions close to consensus , reflecting the ability of

the model to drive the dynamics away from consensus by anti-coarsening increasing the size of the minority group. Overall the inclusion of agents which vacillate, i.e. change opinion if either of two randomly selected neighbours disagrees with their current opinion, inhibits global consensus by driving the system to the state where there are equal numbers of agents with each opinion (zero magnetisation). This work does not find the mean consensus time for this model, or dynamically weak-willed agents. Although having agents which are weak-willed means some agents have more self-confidence than others and therefore seems comparable with the zealot agents model [46] there is a difference in the interaction stage which means the model is different. This difference is that the vacillating agent model [36] has agents which compare up to two neighbours in the interaction, and not strictly only one agent as in the original voter model and the zealot agents model [46].

So far we have only discussed introducing single types of heterogeneous agents to the voter model. A model which includes a range of different agents is the Heterogeneous voter Model [41]. In this model all agents are assigned flip rates (which are the rate at which an agent will change opinion) that are sampled from a probability distribution. Masuda et. al. analytically studied the fully connected model and found that the inclusion of a power-law distribution of flip rates has the consequence that the consensus time is slower. The flip rate distributions with more stubborn voters (those with slowest flip rates) result in mean consensus times that are arbitrarily slow so $\tau_N \simeq N^\beta$ where $\beta > 1$ (the choice of β is given by the distribution and can be arbitrarily large). Masuda et. al. also investigate a Partisan voter Model (PVM) [41]. In this case there are fewer types of heterogeneous agents which are specified as concordant or discordant agents favouring the two different opinions. This is similar to the voter model with zealots [46] because there are now four types of agent, however the rates in the PVM are different. In this zealot model [46] the rate at which the agents change opinion is zero, whereas the PVM includes a strength of preference ϵ for a fixed choice of the two opinions. This strength of preference determines the rate at which an agent which is not currently in its preferred opinion will flip. Masuda et. al. find that on the fully connected network the consensus time increases with population size, N, and with the strength of preference for their own opinion choice. This reflects the result in the mean-field case where they show that the dynamics are driven away from the consensus state and towards the state with equal number of agents of both opinion due to the presence of the discordant agents (those with increased rate of aligning with its preferred state).

2.4.3 Agents with fitness

The models presented above introduce heterogeneity through introducing agents with fixed rates of changing opinion. An alternative to this is to incorporate a relative fitness that each agent holds and that can be compared when agents interact. Here 'fitness' means simply a numerical attribute of an agent which influences the outcome of an interaction with another agent. Typically the fitness of each agent is compared and the agent with the higher value benefits from the consequence of the interaction. This fitness can be compared to confidence if the interaction consequences are commensurate with this interpretation. A model which includes agents with fitness in a simple way has been proposed by Ben-Naim et. al. [7] as a way to build a model of dynamic wealth in a population. In their model of competitive societies each agent has a fitness value but no opinion, so there are no voter dynamics. However the fitness is introduced in a way that corresponds to confidence. Interactions between agents result in the more confident agent (with a relatively higher fitness) increasing their confidence (fitness) with a fixed probability p set at the outset of the dynamics. Also with a fixed, different, rate r the confidence of agents reduce their confidence. They find that the choice of these two parameters determine the distribution of confidence values that evolve in the system. They solve the master equation and find that the fixed probability, p, that more confident agents advance determines the shape of the confidence distribution. When the probability p is higher the distribution is wider, because the most confident agents continue to advance and increase the maximum confidence. When p is chosen so that the less confident (less fit) agent advances their confidence with higher probability the resulting confidence distribution is much more narrow and 'delta like'. (Also when the rate r of decline is high the proportion of agents in the population with low confidence is non-zero). They interpret the population with high advancement probability and low rate of confidence reduction as a middle-class society with a relatively wide confidence (wealth) distribution and no agents with low confidence (zero poor agents). However the model can also be interpreted as a population with confidence but only one opinion. Therefore an alternative but related model would be to incorporate voter agents with fitness levels that are updated by the interaction rules of the model.

A voter model with agent fitness has been studied on heterogeneous degree networks by Antal et. al. [1]. Each agent has an opinion from a binary choice as before, but now one opinion ($s = 1$ where s is a parameter) has relative fitness 1 and the other, fitter, type ($s = 0$) has relative fitness $1 - s$, where $0 < s < 1$. The agents with the more fitness $(1 - s)$ change opinion less often and are able to influence their

neighbours more. When the structure of the network is such that all agents have the same number of neighbours (degree) the choice of whether the agent selected (at random) updates or the neighbour of the agent selected (at random) updates has no consequence for the dynamics. In the homogeneous degree case the probability of selecting any pair of agents in a particular order is exactly the same as picking that pair in the opposite order. However the situation is different in models with degree-heterogeneous networks. Antal et. al. study three subtly different models on degree-heterogeneous networks. When the agent to update is selected the three models pick them in different ways. In the first model it is a link which is selected at random from all the agent pairs, the second selects at random an agent (VM) who copies a neighbour, and thirdly it is the neighbour that copies the agent (IP). They study the probability of reaching consensus from an initial state of a single fitter agent with degree k, in a model with a power-law degree distribution. They find that increasing the degree increases the probability of reaching consensus in the model where the agent (VM rule) is updated, and decreases it when the neighbour (IP rule) is updated. This is understandable given the influence of the update is from the agent selected to their neighbour in their VM model. An extension to this work could consider a voter model with agents on a regular degree network.

2.4.4 Agents with memory

An alternative way to introduce agents which have heterogeneity is to include a memory dependent transition rate. This can be done with a counter which records the number of times an agent has not interacted [57]. The model is interpreted as including inertia for those agents which have aged because the rate of updating reduces as the counter recording the time spent in the current state increases. The inertia (decrease in the transition rate to change their current state) increases linearly with the time spent in the current state and proportional to a strength μ, up to a maximum. The strength μ and the maximum is the same for each agent. The rate that the inertia grows is therefore μ and gives the number of time steps before the maximum inertia is reached for an agent which has not updated their opinion. An agent's inertia is reset to zero as soon as an agent changes opinion. Stark et. al. find that the mean consensus time of their stochastic model depends on the strength μ. They study regular lattices with 1d, 2d, 3d and small-world networks (obtained by rewiring a 2d regular lattice) and the fully connected network. The relationship between consensus time, τ_N, and μ is non-linear and there is a minimum, μ^*, within the range $0 < \mu < 1$ (where $\mu = 0$ is the voter model). The consensus time at the strength giving the minimum is less than the voter model consensus time for

each the corresponding network constructions, and different population sizes tested. There is also slower consensus times when the strength of increase in inertia is increased beyond the respective μ^*. They find two processes that are dominant at different μ values by investigating the stability of the rate equations of the size of the opinion groups and the average inertia of the voters with the two states. When μ is small the inertia in the system helps the majority reach consensus. When μ is large enough the rate that the minority group agents change is also reduced, thus slowing down the consensus time. This model does not strictly include agents with confidence levels because each agents counter affects each agents rate independently of the agent they are interacting with. Also the reseting of the counter after an agent changes opinion means that the counter is different to our k–value which is an agents personal confidence level in their current opinion.

2.4.5 Agents with intermediate states

A consequence of introducing zealot agents to the voter model is that there are four types of agent (both zealot and regular voter agents for each of the two opinions) [46]. An alternative approach is to construct a model with three types of agents which correspond two two extreme types and one intermediate type. Intermediate agents have been introduced in models with three states studied in a variety of work [59] [11] [16]. In general the dynamics leading to consensus have been shown to be different to that for the voter model.

Vazquez et al. [59] considered the opinion formation in a model with three agent types: leftists; centrists; and rightists. The interactions were restricted to the agents with a difference of only one type only so leftists can become centrists but not rightists. They set an initial condition of a density of centrists which controlled probability of the type of final frozen states reached. They studied the 1d model by considering the domain walls between the three agent types. Domains between leftists and rightists do not move because they do not interact and domains between centrists and either of the extreme agents will be mobile because these pairs of agents can interact. They consider the change when domain walls meet and find the rate equations the describe the change in the relative amounts of the stationary and moving domain walls. They find that for an initially uncorrelated state the density of the stationary domain walls decay algebraically, i.e. slowly.

Castello et al. [11] show that in a similar model with A, AB and B labeled agents that in 2d the system reaches dynamical metastable states. They found that in 2d the presence of the intermediate agents, AB, caused the dynamics of coarsening to change. The typical voter model coarsens by interfacial noise but the dynamics

with the intermediate state were characteristic of curvature driven coarsening (shown by inspecting the shape of the regions for a single simulation). The spatial structures created by these dynamics were then dynamically metastable and the system only reached consensus slowly. In separate work an apparently different model has given similar results. The inclusion of memory has been made with a model with each agent additionally having separate counters for each type of opinion [15]. These record the number of times that an agent has interacted with an agent with that respective opinion. The agent will only change their own opinion when the counter has reached a set threshold. Therefore this model is different to the one proposed by Stark et. al. because here the effect is not one of inertia where agents are less likely to change after time has passed, but instead one where it is only after a number of interactions will the agent change opinion. Dall'Asta et. al. find the density of interfaces in stochastic results of the model on the regular 2d lattice [15] and they find that the density scales with $t^{-1/2}$ which is found when curvature-driven coarsening is present. This suggests that the memory effects, through the effective reduction in noise, has introduced surface tension in to the voter model. The link between this result and the spatial coarsening seen in the model by Castello et. al. [11] is that the memory model introduces an intermediate state into the voter model and therefore the spatial coarsening seen is similar.

More recently in the work by Dall'Asta and Galla [16] a model with intermediate states was studied and the density of the intermediate state (of the three states in the model) found, and used as a measure of the density of interfaces. They found that the density of intermediate states decayed algebraically (compared to the voter model which decreases logarithmically [23]). This form of decay of the density of interfaces, agreed to a theoretical result found using field theoretic methods, indicates coarsening by surface tension.

2.5 Axelrod model

The Axelrod model is more complicated than the voter model, and therefore it is understandable that there are far fewer related analytical results. The model is made of agents, each with a vector of F 'opinions' (synonymous with 'features'), each opinion with q 'choices' (synonymous with 'traits'). The vector of the choices for each of the F opinions for an agent is referred to as their 'culture'.

Numerical results show that when F is fixed there is a phase transition of the type of absorbing state reached by the model, either consensus or fragmented frozen groups, which depends on q (the number of choices, traits, for each opinion,

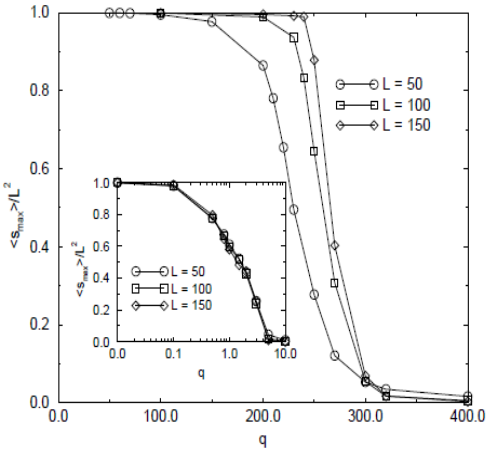

Figure 2.1: Size of the largest group in the frozen state for 2d Axelrod models with $F = 10$ (and $F = 2$ inset) for a range of q, for system size L^2. (Results reproduced with permission from [10]).

feature) [4]. In consensus the mean size of the largest group will make up the entire population, N. Therefore a suitable order parameter is the mean proportion of agents in the largest group in the frozen state, $\langle S_{max} \rangle / N$, this is given by the average of a large number of simulations and is found from the mean number of agents in the largest group $\langle S_{max} \rangle$ in proportion to the total number of agents N. Alternatively one can use the number of different groups, R, in the final frozen, state as this will vary between the ordered and disordered phase so $\langle R/N \rangle$ approaches zero, in the large N limit, in the consensus phase.

Considering the transition with fixed F (number of opinions) and q (choices for each opinion) at the relevant critical value, there is a dimensional dependence. In one-dimension, for all F, the transition is continuous in the order parameter [30]. Research by Castellano et. al. [10] found, using numerical results of the density of active bonds, a phase transition between the consensus state and the frozen coexistence state (of groups of different cultural states) when changing the parameter q. This transition was different depending on F and when $F = 2$ there is a continuous transition, but with $F > 2$ it is discontinuous. We illustrate this with a reproduction of the 2d model with $F = 2$ and $F = 10$ numerical results from [10], Fig. 2.1.

The analytical results which have been found focus on Axelrod models with a only few features and traits, i.e. mean-field treatments for judicious parameter choices. Work studying the master equations of a simple model with $F = 2$ considers

the density of bonds because there are only three possible ones (sharing none, one or two of the F features). Vazquez and Redner [58] find an analytic explanation for the non-monotonic time dependence of the density of active links. The non-monoticity is because which q is higher than the critical value q_c (which determines the whether the system reaches a frozen phase) density of active bonds quickly reduce do to small enclaves of interacting agents which then reach local consensus but are frozen due to the difference of the surrounding background and the whole system freezes. When q is lower there is less diversity and more possibility for interactions. In this case there is partial coarsening into interacting domains and those that are locally in the same.

Recent analytical work has been performed on the dependence on both these parameters and the 1d spatial model is shown with $F = 2$ and $q = 2$ to result in consensus, while models with q sufficiently greater than F result in frozen fragmented states [37]. This dependence on both F and q indicates that it is possible to highlight the transition between consensus and fragmented frozen states by changing F when q is kept constant. In these results, Fig. 2.1, we see that when q is small, for example $q = 100$ when $F = 10$ main plot Fig. 2.1, the dynamics reach consensus and the mean largest group size in the frozen state, scaled by the system size ($N = L^2$), is $\langle S_{max} \rangle / N = 1$. We also see that when q is large, for example $q = 400$ when $F = 10$ main plot Fig. 2.1, that the size of the mean largest group in the frozen state is very small so the typical frozen state reached by the dynamics is a fragmented state with many groups with different opinion states. The explanation for this result is that when there are many q states it is easier for the agents to find themselves in complete disagreement with their neighbour and hence reach the fragmented frozen state. However when q is smaller there are fewer options to to able to disagree so the dynamics for the entire system can find a way to consensus with more ease. Because it is the relative number of features and traits that determine the likely state the system will reach then it is possible to hold q constant and change F.

2.5.1 Modifications to the Axlelrod model

The changes that have been made to the Axelrod model that are most similar to the modifications we introduce are those that incorporate heterogeneity to the way the features are involved in the interactions. This has been studied by introducing an external field, as a mass media effect, and by changing the probability of interaction based on the traits the pair of agents share. These models are different to ours and we describe them here. Mass media influencing individuals has been implemented as an external field acting on the agents. Here an agent can interact, with some

probability B, with an external vector of opinions (features) (the external field) instead of another agent. Counterintuitively the application of a field with larger B helps the model reach a multicultural (disordered) state [24]. While the value of q is still critical and increasing this number of traits decreases the chances of reaching consensus. An alternative, indirect mass media influence, has been introduced in two other ways. Firstly Shibanai et. al [55] introduced a generalised other which is an effective agent that has a cultural state that is made up of the most popular traits (from the whole population) for each respective feature. Secondly they introduce a global media that filters the influence of the usual agent-agent interactions. The typical cultural state is recorded and compared to agents own cultural state. If an agent does not share the trait with the typical cultural state, for the specific feature they are trying to update their neighbour on, then they do not update. This means that the ability for an agent to influence their neighbours is dependent on having traits the same as the typical cultural state. In this way the population through the most popular cultural state has an effect on the local interactions, although the updates themselves are strictly still between the neighbours. Both the generalised other and the filtered global media resulted in simulations that maintained diversity (number of regions didn't go to zero) despite the largest group quickly reaching dominance. The Axelrod model interaction step includes using the proportion of common traits as the probability of interaction. So more similar agents are more likely to interact. An additional rule has been suggested, constraining the situations in which interaction can occur. A parameter, between 0 and F, above which the overlap of number of common traits must be for interactions to occur, introduces 'non-conformity' to the model [51]. As expected a non-zero choice of this parameter leads to disordered states.

A wide range of other Axelrod model variations have been studied, many suggested in the paper describing the original model [4]. As with the voter model the network on which the agents reside has been changed. Noise both in the interaction and affecting the opinions has been introduced. We briefly describe them here.

Axelrod models on static networks have been modelled with similar networks to those used with the voter model. Placing the Axelrod model in a small-world network results in the order-disorder transition being shifted as a result of the disordered networks favouring consensus [32]. This means that in order to achieve consensus in an Axelrod model (on a small-world network) with a high rewiring rate you can choose q to be higher (relative to the q choice with a lower rewiring rate). This is because the long range connections in the rewired network help the system reach consensus by connecting regions. Dynamic networks have also been

studied recently [60] and [12]. Results show the usual transition between disordered and ordered frozen states but also a second transition to states where the groups are isolated by the changes made to the network but contain locally ordered opinions. This second transition is only possible because of the changing connectivity. It is the third type of state that is new in this model, where the groups are unconnected but locally ordered in their cultural states.

Noise has been introduced to the Axelrod model in a variety of ways and in general small random fluctuations facilitate the dynamics so that the ordering time is reduced. Cultural drift is modelled by features (opinions) being randomly changed to take another random trait. This is independent of any interaction and can therefore prevent a model reaching a frozen state if the rate of fluctuations is large enough [33]. In one-dimension there is a noise induced transition between the ordered and dis-ordered state [31]. This transition is relatively independent of q (the number of choices for each opinion) but does vary with N. The reason for the transition is that small noise helps the local agents explore close configurations of their opinions. But higher rates of noise the system reaches a disordered and noisy state. In other work noise has been included in Axelrod models with thresholds controlling the level of similarity agents must be before they interact [17]. Including external noise, the same as cultural drift, and a threshold controlling the similarity before interaction did not affect the qualitative effect of noise. It is still the case that high noise favours order and low noise favours disorder. Also the two effects of noise and mass media have been studied. Here mass media is different, to previous work [24], and can also interact with the agents that share no traits with it. These different interactions give rise to alternative results. When noise rates are low consensus is reached. However when noise rates are high ordered and disordered states are obtained, with the external field inducing consensus [42].

Another extension to the Axelrod model interaction step is to include a comparison of an agent with agents within a local or extended communication range. The increase in communication range was found to reduce the average number of cultures (distinct vectors of features) [27]. While a co-evolving network and extended communication ('geographical') range has been studied. As expected an increasing range of communication favours the ordering process [61].

Axelrod's model contains agents with vectors of integer values: 'features' ('opinions'). However models with a metric choice for the opinion also allow for agents' opinion state to be compared in the interaction stage. models with the metric opinion state, which include a bounded confidence parameter have been introduced [18], and more recently [22]. When the difference in two agents' opinions is greater

than this parameter interactions do not occur. And when interactions do occur the two agents take a new opinion equidistant between their current values. For larger choices of bounded confidence an ordered state is reached, but with a narrow range of bounded confidence multiple opinion states make up the long time state of the model.

Mobile agents have been introduced to the Axelrod model. In these models there are sites with agents and empty sites that agents are able to move into. In the context of the rule for movement given in the Schelling model of racial segregation (where movement is more likely where there are differences in the agent states in a local neighbourhood) [53] mobile agents have been included in the Axelrod model [26]. When the number of empty sites is low the addition of mobile agents increases the speed to ordered states, but when the number of empty sites is large enough there is a new phase of locally ordered states separated spatially, analogous to the third phase in the co-evolving networks Axelrod model [60].

2.6 Our modifications

We make novel modifications to both the original voter and Axelrod models. Our voter model modifications include the attribute of confidence to each agent. This value informs the probability of the outcome of the interaction (i.e. which of the pair of interacting agents is the influencer) and is also updated as a result of that interaction. This is the most simple way to implement a model which dynamically creates zealot-like agents. The interaction steps are that two neighbours are selected at random and the agent with the greater value of confidence has a probability of influencing their neighbour (i.e. the neighbour copies their opinion) given by p, where $0 \leq p \leq 1$. Also the agent which influences the other (i.e. has their opinion copied) increases their self-confidence by one unit. In this way agents who successfully influence others become more confident. While agents which change their opinions as a result of interactions do not.

We implement dynamic confidence in the voter model. Another model, introduced by Ben-Naim et al. [7], with a dynamic agent attribute that influences the interactions is the model of a single population, with no opinions (therefore not like the voter model). The agents increase their confidence (referred to as fitness in their work) after interactions. This model is different because the agent attributes do not include an opinion. Our model is also different to the model in the work by Antal et. al. [1] where the confidence values are constant and associated with the opinion values, so when a site has their opinion updated the confidence value is

updated to the corresponding one. In our model each confidence value is the respective attribute of agents which are static on their sites at the vertices of the network structure specified in the model. This is also different to a recent voter memory model [15] because our update rules compare the confidence of the two neighbours who may interact to see which is more confident. Whereas in the Dall'Asta and Castellano model, [15], the interaction only occurs when a specified threshold has been reached by the agent's counter.

In the models with $p > \frac{1}{2}$, as the self-confidence of individual agents grows, relative to the respective self-confidence of other agents, they become more likely to persuade those other agents to change their opinion. Therefore they are becoming more zealot-like because they are more likely to persuade other agents, which have lower confidence, and the alternative opinion to them. Zealot agents have been studied in recent work by Mobilia [46] and these agents who never change their opinion prevent the population from reaching consensus. We note that our model has dynamic self-confidence values so is different to models with zealots with fixed opinion. Furthermore we note that a single population version of our modified voter model is described by Ben-Naim et al. [7] and [8]. In this model a single population of agents interact, each with only one single attribute, their respective confidence parameter.

We make two different novel Axelrod model modifications. Both modifications make changes to the interaction rules of the original Axelrod model. We introduce a new probability of interaction rule based on biased opinions. This means that there is a weighting to each feature which means that their contribution to the probability of interacting is no longer equal (as in the original Axelrod model). Separately we introduce new update rules based on linked features which are more likely to be updated. These rules are defined in detail in Chap.6. Both modifications are to how the features (opinions) affect the updates to the agents opinion states.

We note that the Axelrod model with a global mass media - filtered through the local agents [55], [25] is different to our changes but does also, implicitly, modify the update rules in relation to the specific features. Research by Parravano [51] has introduced a constraint which modifies the probability of interaction and the consequence is that the proportion of agents in the largest group is reduced. Although this model is different to ours we note that is does also introduce heterogeneity at the level of the features in the interaction step, when calculating the probability of interaction. Therefore both our modified voter and modified Axelrod models are novel. We firstly describe in detail and investigate our modified voter model before also considering the adapted Axelrod model.

Chapter 3

Non-conserved confidence model on fully connected networks

3.1 Introduction

In this Chapter we present a novel variant of the voter model with agents possessing confidence in their current opinion. We define interactions between agents such that the result is the less confident agent changes opinion with probability p, and the more confident agent increases their confidence. The more confident agent changes opinion with probability $1-p$, when the less confident agent increases confidence. In this way we are able to dynamically introduce confident agents to the voter model. To understand the effect of these dynamically confident agents we find the mean consensus time of the stochastic model on the fully connected network and the mean-field equations describing the dynamics on the same fully connected network.

We find that the consensus time depends on p. When $1 > p > \frac{1}{2}$ the mean consensus of the stochastic model scales with N, like the voter model, but the pre-factor depends on p, and that consensus time is greater with increased p. At $p = 1$ there is a jump to a different, slower, exponent and $\tau_N \simeq N^a$ where $a \approx 1.4$. Furthermore we find that when $p < \frac{1}{2}$ the mean consensus time is fast, $\tau_N \simeq lnN$, when compared to the $p = \frac{1}{2}$ voter model, $\tau_N \simeq N$ [14], (see [35, chap. 8]).

We find the mean-field equations Eqn. 3.1, 3.2 and show that the ensemble average of the stochastic model dynamics are the same as those of the numerical solutions of the mean-field equations. We see in the numerical solutions of the mean-field equations that when $p > \frac{1}{2}$ the model dynamics create zealot-like agents

Sec. 3.7 (who have more confidence than others) and there are damped oscillations in the opinion group size towards a coexistence state. The fully connected model is described by many ODEs in the mean-field case therefore we create and solve a simple 3 dimension heuristic model that captures the same qualitative dynamics as the full ODEs, Sec. 3.8. We show that the stability of the equal coexistence state in the heuristic model depends on p. The closer p is to 1 the greater the coexistence state stability and at $p = 1$ the stability of the equal coexistence is much stronger than for all other p values. In the stochastic model it is only through random fluctuations away from the coexistence state that the system reaches consensus. Therefore the increase in stability of this state we suggest is related to the slower consensus time.

3.2 The non-conserved confidence model

We introduce a novel mechanism for dynamically evolving heterogeneous agents that hold a confidence in their current opinion. There are many ways one could design a model which achieves this, and we present the simplest one here. Each agent is represented by an integer value of the self-confidence they have in their respective opinion in their own group choice. There is a probability p which controls the importance of confidence in determining the outcome of the interaction. Each turn an agent i randomly selects one of its neighbours j. If they are different then we determine the outcome which in our model depends on the parameter p (If the agents have the same opinion there is no interaction). If an agent from group $+$ with confidence m interacts with one from group $-$ with confidence n (and the first agent is more confident, so $m > n$) then the two possible outcomes of the interaction are:

$$(m, +) \oplus (n, -) \to (m + 1, +) \oplus (n, +) \text{ with probability } p,$$

$$(m, +) \oplus (n, -) \to (m, -) \oplus (n + 1, -) \text{ with probability } 1 - p.$$

In the case where $p = 1$ the more confident agent always wins and when $p = 0$ the less confident agent always succeeds in persuading the other. (We note that immediately after an agent changes their opinion, they hold the new opinion with the same confidence with which they previously held the other opinion). If the agents have the same confidence then there is an equal chance that either wins. So these outcomes are:

$$(m, +) \oplus (m, -) \to (m + 1, +) \oplus (m, +) \text{ with probability } 1/2,$$

$$(m,+) \oplus (m,-) \rightarrow (m,-) \oplus (m+1,-) \text{ with probability } 1/2.$$

In the Voter model [39], there is a fixed probability of $\frac{1}{2}$ that an agent will win an interaction and persuade the other to change group choice. We have more subtle interaction step with a parameter p: the probability that the more confident individual will persuade the less confident one to change groups.

The idea is that as the simulation progresses those agents which have previously persuaded agents to adopt their own opinion are more confident in their own view. Therefore these agents are more likely to persuade other agents in the future and are more zealot-like in their interactions, relative to those agents with low confidence. The dynamics mean that agents which start with low confidence have a chance to persuade others and increase their own confidence and become more confident. Therefore we introduce a model where agents with heterogeneous confidence are dynamically created by the interactions in the model. It is possible to construct a model with conserved global confidence by keeping the same model rules but also reducing the confidence of the agent which changes opinion and we study this model in Chap. 4.

When $p > \frac{1}{2}$ the natural interpretation of the k–value is that it represents the confidence an agent has in their current opinion. If the agent wins more interactions their k–value increases and they become more zealot-like relative to lower confidence agents (with the opposing opinion view). When $p = \frac{1}{2}$ we have the voter model because each choice of which agent updates is independent of the confidence values.

The natural interpretation of the k–value is that it represents confidence an agent holds in their opinion. However when $p < \frac{1}{2}$ the k–value can be considered to be a counter. In this model the agent with the lower k–value is more likely to win an interaction. Therefore it represents a scenario where the agent which has won fewer interactions in the past is more likely to win in the future. When the interaction takes place the k–value is considered to be a confidence value. But it can also be considered to be a counter representing the number of times an agent has persuaded other agents to change. This is not the same model described by Stark et al. [57] because their model has a counter which records how long is has been since that agent had its own opinion changed, up to a globally defined maximum. The counter in the inertia model [57] is reset to zero when an agent does change opinion. However our counter retains more memory because once an agent has persuaded many other agents their confidence value is high. This does not fall to zero when they eventually lose an interaction for the first time. Instead they take their high confidence with them over to the other opinion group. The specific agent retains the 'memory' of not having lost an interaction. Furthermore our confidence is a value

which is relative because two agents are compared in the interactions.

As discussed in the Chap. 2 there has been research into zealots with fixed confidence [46] and permanently weak-willed agents [36] which can separatley inhibit global consensus. Also heterogenous agents with fixed rates for changing opinion that are given by a specific distribution can slow the consensus time down arbitrarily [41]. We, however, seek to understand what the effect of *dynamically* confident agents play in the ability to reach consensus. The idea of confidence is similar to agent fitness and the model by Ben-Naim et. al. [7] can be considered to a single population of agents with confidence updated as a result of interactions. Their model has agents with no explicit opinion so is not a voter model. Our model has a similar update rule for the confidence but is coupled to the voter dynamics. Other recent work has studied models with one explicit intermediate agent, between two extreme opinions and shown that coarsening behaviour is different to the voter model [11], [16]. In Chap. 5 we seek to understand what effect the agents with dynamic confidence have on the consensus time in the model on regular lattices.

There are two salient approaches to probing our model. These are through: analytical analysis of the deterministic mean-field equations; and stochastic simulation results. We employ both methods here. Firstly we consider the mean-field equation and the consequences of these to gain an initial understanding of the model. Secondly we employ a stochastic simulation of the model to investigate the behaviour of finite sized versions of the model.

3.3 Mean-field description of the model

We describe the dynamics of the model by considering the distribution of proportion of agents $f_k^{\pm}$ over the confidence values k, for the opinion group $+$ and $-$. The distributions for both groups, f_k^+ and f_k^-, of the integer confidence values k will change as the model dynamics progress. Also the proportions of agents in each group ρ^+ and ρ^- will change, where the number of agents in each group are n^+ and n^-. So $\rho^+ = n^+/N$ where the total population is N, and $N = n^+ + n^-$. In order to write the dynamic equations we consider the elemental processes in the model and collect the terms which change the distribution of confidence with their respective probability of occurrence, as represented in Fig. 3.1. We define the cumulative distribution is F_k^+ and that the total population is normalised so that $F_{k+1}^+ + G_k^+ + F_{k+1}^- + G_k^- = 1$. Taking the thermodynamic limit we can write the

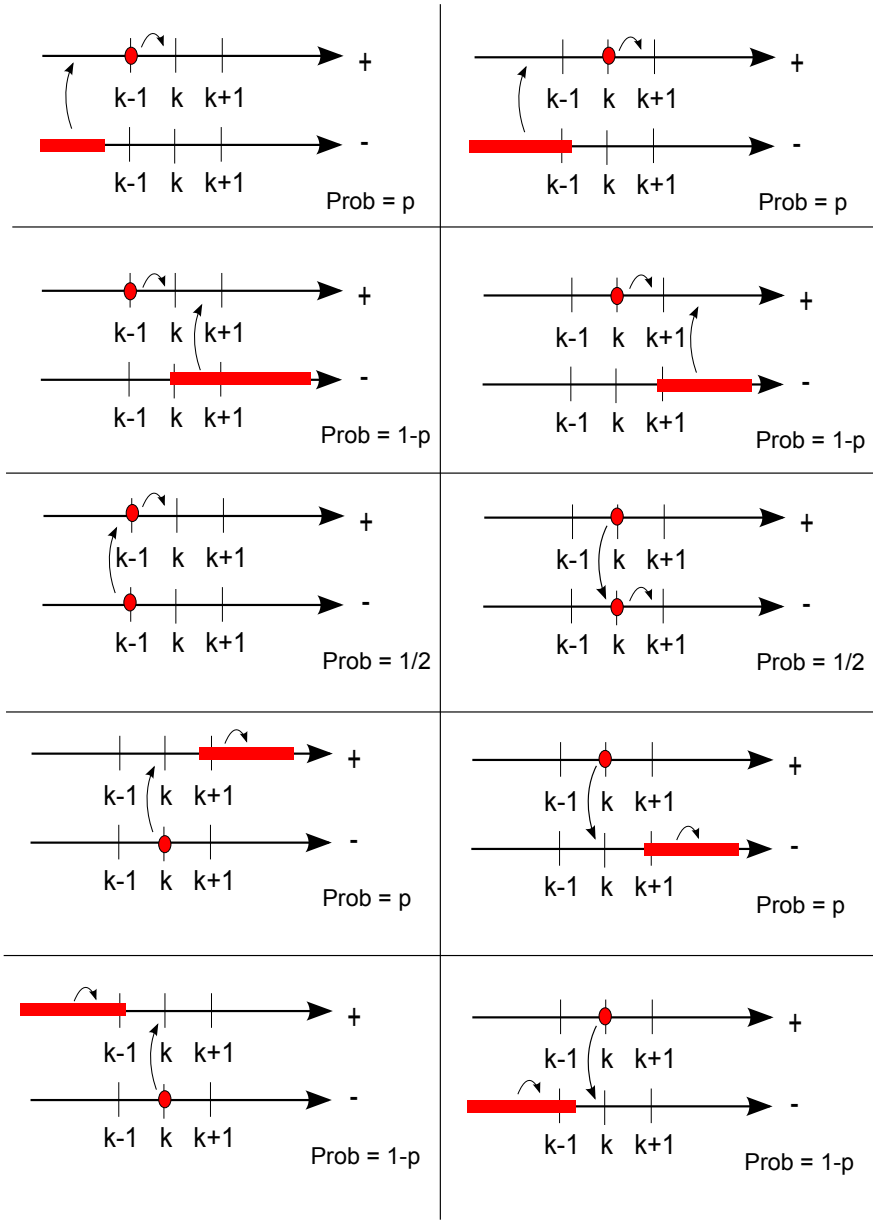

Figure 3.1: The possible changes for any interaction given with their associated probability. The probability that a more confident agent wins an interaction is p. As a result of the interaction the winner becomes more confident (e.g. $k-1 \to k$) and the loser change group (e.g. $- \to +$). The red bar represents the sum of all possible agents that have confidence either lower ($F^{\pm}$) or higher ($G^{\pm}$) than the other agents confidence value. The first box shows f^{+}_{k-1} on the top line (red dot) and F^{-}_{k-1} on the bottom line (solid red line).

mean-field equations for the confidence distributions:

$$\begin{aligned}\frac{d}{dt}f_k^+ \quad =&p\left(f_{k-1}^+F_{k-1}^- - f_k^+F_k^-\right) + (1-p)\left(f_{k-1}^+G_{k-1}^- - f_k^+G_k^-\right) + \frac{1}{2}\left(f_{k-1}^+f_{k-1}^- - f_k^-f_k^+\right)\\ &+p\left(f_k^-G_k^+ - f_k^+G_k^-\right) + (1-p)\left(f_k^-F_k^+ - f_k^+F_k^-\right),\end{aligned} \tag{3.1}$$

$$\begin{aligned}\frac{d}{dt}f_k^- =&p\left(f_{k-1}^-F_{k-1}^+ - f_k^-F_k^+\right) + (1-p)\left(f_{k-1}^-G_{k-1}^+ - f_k^-G_k^+\right) + \frac{1}{2}\left(f_{k-1}^-f_{k-1}^+ - f_k^+f_k^-\right)\\ &+p\left(f_k^+G_k^- - f_k^-G_k^+\right) + (1-p)\left(f_k^+F_k^- - f_k^-F_k^+\right).\end{aligned} \tag{3.2}$$

The interpretation of the terms on the right hand side in Eq.(3.1) is that they contribute all the ways that the proportion of agents with confidence k and opinion + (or opinion - in Eq.(3.2)) can be increased or reduced. These gain and loss terms are collated by common pre-factors of p or $(1-p)$ or $\frac{1}{2}$. The first term in Eq.(3.1) is the probability p that the more confident agent wins multiplied by the proportion of agents with opinion + and confidence one less than k. In this term these interact with the proportion of agents with opinion - and confidence less than themselves (i.e. the sum of all those with two less than k, $\sum_{j=0}^{k-2} f_j^- = \sum_{j=0}^{k-1} f_{j-1}^- = F_{k-1}^-$ by definition). The result of this interaction is that the proportion of agents with confidence k, and opinion +, increases hence the pre-factor for this term is positive. A stylised representation of this interaction is shown in the first section of Fig. 3.1. The second term is the case where the proportion of agents with opinion + and confidence k is reduced as a result of agents with confidence k and opinion + winning an interaction with those with opinion - and confidence less than k (as shown in the second box, in the top right section, of Fig. 3.1). The other terms contribute all the other possible ways of changing the proportion of agents with opinion + and confidence k. For example the fifth term corresponds to the case where agents with the same confidence interact and the result is that the proportion of agents with confidence k and opinion + increases, which is shown in the fifth stylised diagram in Fig. 3.1.

The boundary conditions are $f_{-1}^+(t) = 0$ and $f_{-1}^-(t) = 0$ for all time, i.e. a no flux boundary condition at $k = 0$. We also enforce the reasonable boundary condition that the distribution diminishes to zero at very large confidence values, i.e. $f_{k=\infty}^{\pm} = 0$ (because we know there is finite confidence in the population when

the dynamics are considered in finite time). The initial conditions can be written

$$f_k^+(t=0) = \left(\frac{1}{2}+\epsilon\right)\delta_{k,0}, \qquad f_k^-(t=0) = \left(\frac{1}{2}-\epsilon\right)\delta_{k,0},$$

where ϵ is the difference from the symmetric initial condition case where there is initially half the total population in each of the two groups. We note that $F_{k+1}^+ = F_k^+ + f_k^+$ and $G_k^+ = F_\infty^+ - F_{k+1}^+ = F_\infty^+ - F_k^+ - f_k^+$.

The dynamics of the proportion of agents in each group is found by using $\rho^\pm = \sum_{k=0}^{k=\infty} f_k^\pm$ and the mean-field equations. We notice that when we sum Eq.(3.1) or (3.2) from $k=0$ to $k=\infty$ the first six terms (in pairs of fF or fG or ff) of Eq.(3.1) and separately of Eq.(3.2) on the right hand side will cancel inside the sum to leave terms with a pre-factor of $f_{-1}^\pm$. We substitute $G_k^\pm = F_\infty^\pm - F_k^\pm - f_k^\pm$ into terms 7 and 8, then use the boundary conditions and find that

$$\begin{aligned}
\frac{d}{dt}\rho^+ &= 2(p-1/2)\sum_{k=0}^{\infty}\left(f_k^+F_k^- - f_k^-F_k^+\right), \\
\frac{d}{dt}\rho^- &= 2(p-1/2)\sum_{k=0}^{\infty}\left(f_k^-F_k^+ - f_k^+F_k^-\right).
\end{aligned} \tag{3.3}$$

We see that when $p = \frac{1}{2}$, the change of group size is independent of the confidence distributions. This is expected from the micro-dynamics which allocate equal probability of choosing either group to copy in the interaction. Furthermore we note that cumulative confidence distribution follows

$$\begin{aligned}
\frac{d}{dt}F_k^+ =& (-f_{k-1}^+)[F_{k-1}^-(2p-1) + (1-p)(F_\infty^- - f_{k-1}^-) + 1/2 f_{k-1}^-] \\
&+ (2p-1)\sum_{j=0}^{k-1}(f_j^+F_j^- - f_j^-F_j^+) - \sum_{j=0}^{k-1}(f_j^+F_\infty^- - f_j^-F_\infty^+)
\end{aligned} \tag{3.4}$$

and the average confidence, obtained from the first moment of Eq.(3.1),

$$\begin{aligned}
\frac{d}{dt}\mu^+ =& \sum_{k=0}^{\infty}(2p-1)((k+1)f_k^+F_k^- - kf_k^-F_k^+ + 1/2 f_k^+f_k^-) \\
&- p((k+1)f_k^+F_\infty^- - kf_k^-F_\infty^+) + f_k^+F_\infty^-
\end{aligned} \tag{3.5}$$

Taking the sum over k we find that

$$\begin{aligned}\frac{d\mu^+}{dt} &= (1-p)\,\rho^+\rho^- + p\,\left(\rho^+\mu^- - \rho^-\mu^+\right) \\ &\quad +(2p-1)\sum_{k=0}^{\infty} k\,\left(f_k^+F_k^- - f_k^-F_k^+\right) \\ &\quad +(2p-1)\sum_{k=0}^{\infty} f_k^+F_k^- + \frac{1}{2}(2p-1)\sum_{k=0}^{\infty} f_k^+f_k^-\end{aligned} \tag{3.6}$$

The total mean confidence k of the whole population satisfies

$$\begin{aligned}\frac{d(\mu^+ + \mu^-)}{dt} &= 2\,(2p-1)\sum_{k=0}^{\infty}\left(f_k^+F_k^- + \frac{1}{2}f_k^+f_k^- + f_k^-F_k^+\right) \\ &\quad +2(1-p)\,\rho^+\rho^-.\end{aligned}$$

It is not clear how the total mean confidence relates to the opinion group size or the confidence distributions. However further algebraic manipulation of the equation reveals a simpler expression and the total mean confidence k of the whole population satisfies

$$\frac{d(\mu^+ + \mu^-)}{dt} = \rho^+\rho^-. \tag{3.7}$$

This is commensurate with the model description. On average, in the fully connected model, the confidence will increase at a rate proportional to the number of active bonds (between agents of different opinions). Therefore the total average confidence will increase with a rate $\rho^+\rho^-$.

It is difficult to tell a-priori how the k–values in the system will behave since it has a complicated dependence on the distribution of k–values in the two groups. We note, however, that when $p = \frac{1}{2}$, $\mu^-(t) + \mu^+(t)$ grows linearly since $\rho^\pm$ are constant and given by their initial values.

3.4 Mean-field dynamics

We consider three parameter regimes when investigating the mean-field dynamics. These were $p = \frac{1}{2}$, which corresponds to a voter model (in group allocation) and decoupled dynamics of the confidence values. Then the $p > \frac{1}{2}$ model which exhibits early time oscillations in group density, ρ, and a scaling solution in the long time

limit for the confidence distribution, f_k. (A scaling solution identifies that for large times the shape of the appropriately scaled solution tends towards a fixed form given by the parameters of the model. We find the exact shape of the fixed form analytically and compare the large time numerical solutions of the full equations to confirm this result.) We also find that the $p < \frac{1}{2}$ model which generates absorbing confidence distributions which display p dependent stability.

3.4.1 $p = 1/2$ and symmetric initial conditions

We use a continuum limit in k-space (the confidence range) because this make the mathematical analysis more tractable. We are able to do this because the distribution of confidence values change slowly relative to the confidence values themselves, i.e. is smooth, at long times. When t is small the limit is less accurate because we use initial conditions of a delta spike at zero confidence. However the results that we consider are at $t > 1$, and we find good agreement between the analytical results with continuous k and the numerical solutions of the full ODEs (Eq.(3.1), (3.2)) in discrete confidence.

The $p = \frac{1}{2}$ case has dynamics which are the most simple of our three parameter choices. The proportion of agents in each of the two groups are unchanging, i.e. $\frac{d\rho^-}{dt} = 0 = \frac{d\rho^+}{dt}$ (as is clear from Eq.(3.3)). We therefore focus on the analysis of the confidence distributions, f_k^- and f_k^+. The confidence distribution is decoupled from the dynamics of any group choice because each interaction is independent of the confidence of the two agents (i.e. probability of more confident agent winning is $p = \frac{1}{2}$ and the probability of a less confident agent winning is $1 - p = 1/2$).

When $p = \frac{1}{2}$ many of the terms in the mean-field equations (Eq.(3.1), (3.2)) cancel, i.e. the terms in the last two brackets cancel ($f_k^+ G_k^- = f_k^- G_k^+$ etc.). We also notice that $F_k^+ + G_k^+ + f_k^+ = F_\infty^+$, and $F_\infty^+ + F_\infty^- = 1$ always. Therefore Eq.(3.1) becomes

$$\frac{df_k^+}{dt} = \frac{1}{2}(f_{k-1}^+ - f_k^+)F_\infty^- + \frac{1}{2}f_k^- F_\infty^+ - \frac{1}{2}f_k^+ F_\infty^-.$$

But we know that when $p = \frac{1}{2}$ there is no change in the proportions in each group, from Eq.(3.3) that is $\frac{dF_\infty^\pm}{dt} = 0$. So $F_\infty^\pm(t) = \rho^\pm(t) = \rho^\pm(0)$. We have

$$\frac{df_k^+}{dt} = \frac{1}{2}(f_{k-1}^+ - f_k^+)\rho^-(0) + \frac{1}{2}f_k^- \rho^+(0) - \frac{1}{2}f_k^+ \rho^-(0).$$

We consider the case with $p = \frac{1}{2}$ and $f_k^+(0) = f_k^-(0)$, so that $\rho^+(t) = \rho^-(t) = \frac{1}{2}$ and $f_k^+(t) = f_k^-(t)\ \forall t$. This simplifies the mean-field equations (Eq.(3.1), (3.2))

greatly. We find that

$$\frac{df_k}{dt} = \frac{1}{2}(f_{k-1} - f_k)F_\infty, \tag{3.8}$$

where we write $f_k = f_k^+ = f_k^-$. Now we consider a continuous confidence distribution $f(k,t)$, where

$$f_{k-1} = f_k - \Delta k \frac{\partial f}{\partial k} + \frac{1}{2}(\Delta k)^2 \frac{\partial^2 f}{\partial k^2} + O(\Delta k)^3. \tag{3.9}$$

Therefore, writing $f_k(t) = f(k,t)$, and using $F_\infty = 1/2$, substituting Eq.(3.9) into Eq.(3.8), and assuming $\Delta k = 1$, we find

$$\frac{\partial f}{\partial t} = -\frac{1}{4}\frac{\partial f}{\partial k} + \frac{1}{8}\frac{\partial^2 f}{\partial k^2}, \tag{3.10}$$

which is the advection with diffusion equation with, drift term (i.e. speed of the mean of the confidence distribution), and the diffusion term respectively $u = 1/4$ and $D = 1/8$. We solve Eq.(3.11) in several steps. First we take an unbounded domain in confidence ($-\infty < k < +\infty$), then solve the advection and diffusion equation using a moving co-ordinate, with speed of the advection term, to give us a pure diffusion equation in this new co-ordinate. Then we solve this diffusion equation, Eq.(3.10), before substituting back in for our original co-ordinates and inserting our initial conditions. Lastly we account for the no flux boundary condition at $k = 0$ by using the method of images to finally obtain our solution for the confidence distribution. We consider a general equation with advection and diffusion

$$\frac{\partial f}{\partial t} + u\frac{\partial f}{\partial k} = D\frac{\partial^2 f}{\partial k^2}, \tag{3.11}$$

and we firstly solve Eq.(3.11) with ($-\infty < k < +\infty$) and $t > 0$ and initial condition $f(k,0) = (1/2)\delta(k-0)$. We use a moving co-ordinate, x which has speed u, so $x = k - ut$. We find the appropriate partial derivatives of $f(x,t)$, using the chain rule, and rewrite Eq.(3.11) as

$$\frac{\partial}{\partial t} f(x,t) = D\frac{\partial}{\partial x^2} f(x,t). \tag{3.12}$$

We solve Eq.(3.12) by means of the Fourier Transform with respect to x. We define the Fourier Transform of a function to be

$$\hat{f}(\omega,t) = \mathcal{F}(f) = \frac{1}{\sqrt{2\pi}} \int_{-\infty}^{\infty} f(x,t) e^{-ix\omega t} dx.$$

We take the Fourier Transform of the terms in Eq.(3.12) so that $\mathcal{F}(\partial_t f) = D\mathcal{F}(\partial_{xx} f) = D(i\omega)^2\mathcal{F}(f) = -D\omega^2\hat{f}$. We can also reorder the differentiation and integration to give $\mathcal{F}(\partial_t f) = \partial_t \hat{f}$. We now write the initial condition in a general form $\hat{f}(\omega, 0) = \hat{g}(\omega)$ and Eq.(3.12) becomes

$$\partial_t \hat{f}(\omega, t) = -D\omega^2 \hat{f}(\omega, t), \tag{3.13}$$

and the solution to this first order ODE is simply

$$\hat{f}(\omega, t) = \hat{g}(\omega) e^{-D\omega^2 t}. \tag{3.14}$$

But we know that the initial condition $f(x, 0) = 0.5\delta(x - 0)$ (because $f(k, 0) = 0.5\delta(k - 0)$ and $x = k - ut$). Therefore in Fourier space this initial condition is

$$\hat{g}(\omega) = \mathcal{F}(f)(\omega, 0) = \frac{1}{\sqrt{2\pi}} \int_{-\infty}^{\infty} f(x, 0) e^{-ix\omega t} dx = \frac{1}{2} \frac{1}{\sqrt{2\pi}}.$$

(We highlight the use here of unconventional notation, of ω as the variable in Fourier space, not angular frequency, because k has previously been allocated to denote the confidence variable in the model in "real" space.) Therefore the full solution to Eq.(3.12) is found by performing an inverse Fourier Transform, i.e.

$$f(x, t) = \frac{1}{\sqrt{2\pi}} \int_{-\infty}^{\infty} \frac{1}{2} \frac{1}{\sqrt{2\pi}} e^{-D\omega^2 t} e^{+ix\omega t} d\omega = \frac{1}{2} \frac{1}{\sqrt{4\pi D t}} e^{-\frac{(x^2)}{4Dt}}.$$

Thus in our original co-ordinates we have, for the infinite domain k case,

$$f(k, t) = \frac{1}{2} \frac{1}{\sqrt{4\pi D t}} e^{-\frac{(k-ut)^2}{4Dt}}.$$

However we have a boundary condition at $k = 0$. This condition is that no confidence values drop below zero. Therefore we have a no flux condition, $\frac{\partial f}{\partial k}|_{k=0} = 0$. Therefore, as illustrated in Fig. 3.2, we use the method of images to superimpose two symmetrically positioned solutions, and obtain the true solution for the $k \geq 0$ domain. The two solutions will have identical initial conditions but opposite velocity in the advection term so our solution obeying the no flux condition is (for $k \geq 0$)

$$f(k, t) = \frac{1}{2} \frac{1}{\sqrt{4\pi D t}} \left[e^{-\frac{(k-ut)^2}{4Dt}} + e^{-\frac{(k+ut)^2}{4Dt}} \right].$$

We test this solution against numerical results for f_k^+ and f_k^- of the mean-field equations (Eq.(3.1), (3.2)) and find good agreement Fig. 3.3.

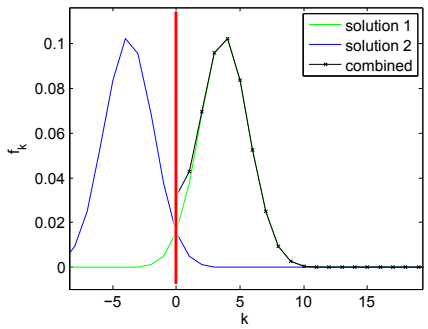

Figure 3.2: An example of using the mirror images technique with a no flux condition at $k = 0$.

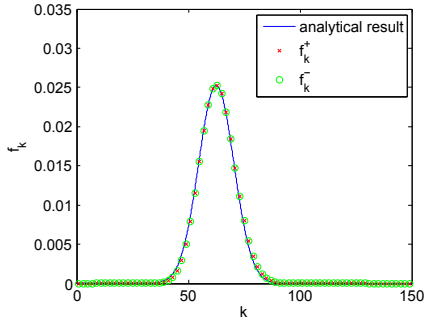

Figure 3.3: A comparison of the analytical and numerical results for a model with $p = \frac{1}{2}$ and symmetric initial conditions, at $t = 250$.

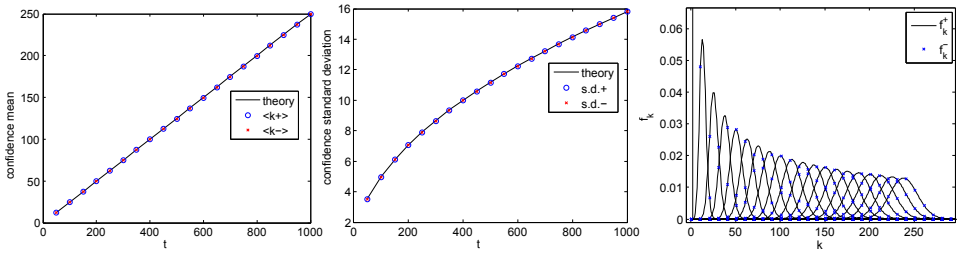

(a) (b) (c)

Figure 3.4: When $p = \frac{1}{2}$ (a) the mean of the confidence distribution increases linearly with time and (b) the standard deviation follows a $\sqrt{t}$ relationship, so (c) the confidence distribution (for $t = 50, 100, 150, .., 950, 1000$) appears to follow dynamics of drift with diffusion.

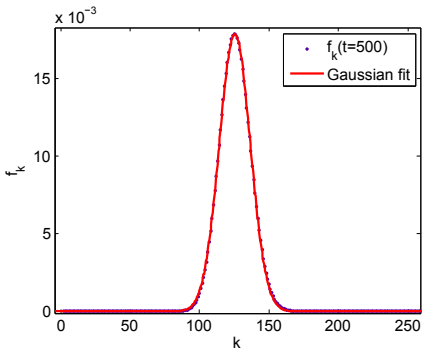

Figure 3.5: When $p = \frac{1}{2}$ the confidence distribution fits a Gaussian distribution.

We note that the dynamics of the $p = \frac{1}{2}$ model with symmetric initial conditions does not lead to the emergence of zealot-like agents. The confidence distributions evolve in a way which stay peaked close to the mean, as shown in Fig. 3.4c. Therefore there are no agents who evolve confidence which is far from the mean confidence of either their own group or the other.

Table 3.1: $p = \frac{1}{2}$ Confidence Distribution Fitting

Coeff	Fit	Lower confidence	Upper confidence
A	0.01788	0.01785	0.0179
μ	125.4	125.4	125.4
σ	15.78	15.75	15.80

The summary of these results are that when $p = 1/2$, and the distributions of confidence are equal, we have equal and constant sizes of the two groups. Furthermore there is both a drift and a diffusion of the confidence distribution. Therefore the mean increases and we have a Gaussian distribution at time $t > 0$ from the initial condition $f_k(t = 0) = \delta(k - k_0)$. We now consider a model with non-symmetric initial conditions.

3.4.2 $p = 1/2$ and non-symmetric initial conditions

We consider the case when $p = \frac{1}{2}$ but with non-symmetric initial conditions. In this parameter regime there is constant group size (as we see from Eq.(3.3)) so $\rho^{\pm}(t) = \rho^{\pm}(0)$, but $\rho^{+}(0) \neq \rho^{-}(0)$. The mean-field equations (Eq.(3.1), (3.2)) for the case when $p = \frac{1}{2}$ are

$$\frac{df_k^+}{dt} = \frac{1}{2}(f_{k-1}^+ - f_k^+)F_\infty^- + \frac{1}{2}f_k^- F_\infty^+ - \frac{1}{2}f_k^+ F_\infty^-.$$

Taking the continuous approximation of the confidence distribution, and writing $f_k(t) = f(k,t)$,

$$f_{k-1} = f_k - \frac{\partial f}{\partial k}\Delta k + \frac{1}{2}\frac{\partial^2 f}{\partial k^2}(\Delta k)^2 + O(\Delta k)^3,$$

and writing $\rho^{\pm} = F^{\pm}_{\infty}$ we have

$$\frac{\partial f^+}{\partial t} = \frac{1}{2}\rho^- \left(-\frac{\partial f^+}{\partial k} + \frac{1}{2}\frac{\partial^2 f^+}{\partial k^2}\right) + \frac{1}{2}\rho^+ f^- - \frac{1}{2}\rho^- f^+,$$

and

$$\frac{\partial f^-}{\partial t} = \frac{1}{2}\rho^+ \left(-\frac{\partial f^-}{\partial k} + \frac{1}{2}\frac{\partial^2 f^-}{\partial k^2}\right) + \frac{1}{2}\rho^- f^+ - \frac{1}{2}\rho^+ f^-.$$

Now we take the Fourier Transform, of both the confidence distributions, $f^+(k,t)$ and $f^-(k,t)$, and the initial conditions $f^{\pm}(k, t=0) = (0.5 \pm \epsilon)\delta(k-0)$. We note that $\mathcal{F}(\partial_t f^{\pm}) = \partial_t \hat{f^{\pm}}$, $\mathcal{F}(\partial_k f^{\pm}) = -ip\hat{f^{\pm}}$, $\mathcal{F}(\partial_{kk} f^{\pm}) = -p^2\hat{f^{\pm}}$. Therefore we can write the coupled equations in Fourier space:

$$\frac{\partial \hat{f}^+}{\partial t} = \frac{\rho^-(0)}{2}\left(-\frac{1}{2}p^2 - ip - 1\right)\hat{f}^+(p,t) + \frac{\rho^+(0)}{2}\hat{f}^-(p,t)$$

and

$$\frac{\partial \hat{f}^-}{\partial t} = \frac{\rho^+(0)}{2}\left(-\frac{1}{2}p^2 - ip - 1\right)\hat{f}^-(p,t) + \frac{\rho^-(0)}{2}\hat{f}^+(p,t).$$

To solve these we seek to decouple the equations. To do this we rewrite the equations in matrix form and then diagonalise this. Written in matrix form we have

$$\begin{bmatrix} \partial_t \hat{f}^+ \\ \partial_t \hat{f}^- \end{bmatrix} = \begin{bmatrix} A & B \\ C & D \end{bmatrix} \times \begin{bmatrix} \hat{f}^+ \\ \hat{f}^- \end{bmatrix}.$$

Where the coefficient matrix is defined by

$$A = \frac{\rho^-(0)}{2}\left(-\frac{1}{2}p^2 - ip - 1\right), B = \frac{\rho^+(0)}{2}, C = \frac{\rho^+(0)}{2}\left(-\frac{1}{2}p^2 - ip - 1\right), D = \frac{\rho^-(0)}{2}.$$

We diagonalise this coefficient matrix to obtain a system of equations given by, distinct eigenvalues λ^+ and λ^-, in the form

$$\begin{bmatrix} \partial_t \hat{f}^+ \\ \partial_t \hat{f}^- \end{bmatrix} = \begin{bmatrix} \lambda^+ & 0 \\ 0 & \lambda^- \end{bmatrix} \times \begin{bmatrix} \hat{f}^+ \\ \hat{f}^- \end{bmatrix}$$

We simplify notation by defining $c(p) = 1/2p^2 + ip + 1$, $E = \rho^+/\rho^-$, and

$$M = \begin{bmatrix} A & B \\ C & D \end{bmatrix}.$$

As standard, to find the eigenvalues of M, we find the determinant, $|(M - \lambda I)|$. We find the eigenvalues are

$$\lambda^{\pm} = 1/2(E-1)c \pm \sqrt{(E-1)^2c^2 + 4E}.$$

We also find that the initial conditions in Fourier space are

$$B^{\pm}(p) = \frac{\rho^-}{2} \pm \left(-\frac{\rho^-}{2} + \frac{\rho^+ - (Ec + \lambda^-)\rho^-}{\lambda^+ - \lambda^-} \right),$$

and find the full solution in Fourier space:

$$\begin{aligned} \hat{f}^+(p,t) &= (Ec + \lambda^+)B^+ e^{\lambda^+ t} + (Ec + \lambda^-)B^- e^{\lambda^+ t}, \\ \hat{f}^-(p,t) &= B^+ e^{\lambda^+ t} + B^- e^{\lambda^+ t}. \end{aligned} \tag{3.15}$$

Comparing the Inverse Fourier Transform of Eq.(3.15) with the numerical solutions of the original mean-field equations (Eq.(3.1), (3.2)) shows good agreement, Fig. 3.6. We have solved for $f^{\pm}$ using an inverse Fourier Transform in *Matlab* and compare this with the numerical results of the ODEs (Eq.(3.1), (3.2)) for the same time, $t = 500$, in Fig.3.6. Finding the inverse Fourier Transform results in the confidence distributions f_k^+ and f_k^-, for the time chosen. Therefore we have found the exact confidence distribution for the $p = \frac{1}{2}$ case of the non-conserved confidence model when the initial conditions are all agents with zero confidence and one opinion group larger (i.e. $\rho^+(t = 0) = 0.7$).

3.4.3 $p > 1/2$ Oscillating populations and scaling solutions

Now we consider the mean-field dynamics of the case where $p > 1/2$. In these models the local interactions represent the case where a more self-confident agent is more likely to persuade a neighbour of their own opinion (i.e. have their opinion copied in the interaction). We expect the mean confidence of the groups to increase because each interaction will increase the confidence of one of the agents by a single unit. We also expect that the distribution of the confidences of both groups to widen because the most confident agents will interact and a proportion of the time persuade others and increase their confidence, hence increasing the maximum confidence of both

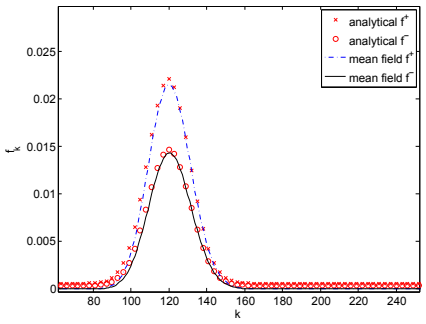

Figure 3.6: Confidence distributions (when $t = 500$) for models with $p = \frac{1}{2}$ and non-symmetric initial conditions $f^{\pm}(k, t = 0) = (0.5 \pm \epsilon)\delta(k - 0)$ for $\epsilon = 0.2$.

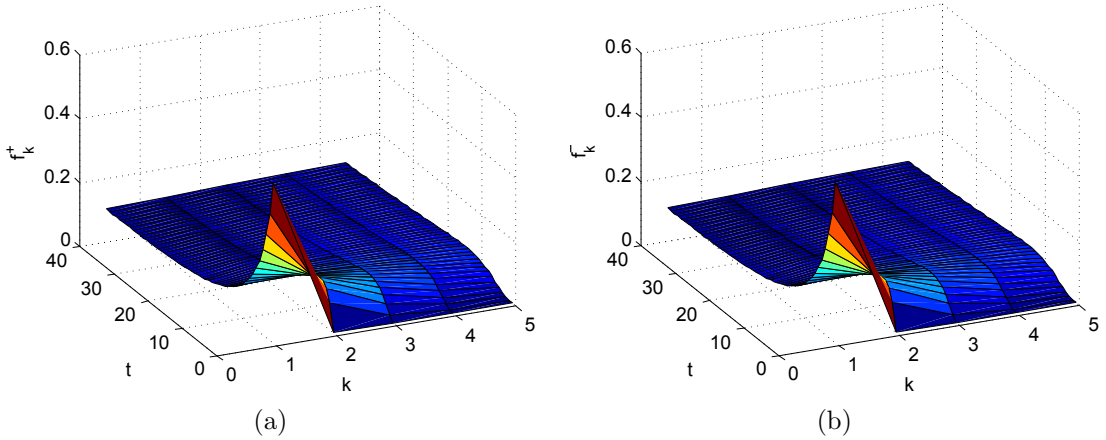

Figure 3.7: Confidence distributions (a) f_k^+ and (b) f_k^- from numerical results of the mean-field equations (Eq.(3.1), (3.2)) for $p = 0.8$, with initial conditions $f_k^{\pm}(t = 0) = (0.5)\delta_{k,0}$ (symmetric initial conditions).

groups. One would also naively expect that a group with more agents may exert more influence over the other group. However we find an unexpected result for the group fraction dynamics: that of oscillating group size.

We obtained numerical results of the mean-field equations Eq.(3.1) and (3.2) using ode45 in *Matlab*. We used an initial condition of all agents with zero confidence and a p value greater than $\frac{1}{2}$. For the case with equal numbers of agents in both groups we notice how the distributions of confidence values appear to be identical and the distributions widen with time Fig. 3.7a and 3.7b.

Similarly we obtained numerical results for a model with initial conditions with all agents with zero confidence and one group (+) with a proportion (2ϵ) more agents than the other group (-). For the example with $p = 0.8$ and $\epsilon = 0.1$, Fig. 3.8a and 3.8b we see that the confidence distribution broadens in time and the mean

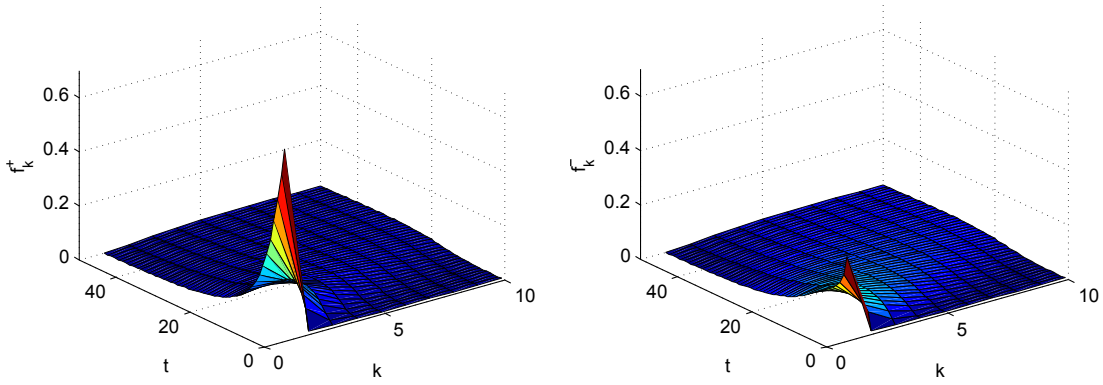

Figure 3.8: Confidence distributions (a) f_k^+ and (b) f_k^- from numerical results of the mean-field equations (Eq.(3.1), (3.2)) for $p = 0.8$, with initial conditions $f_k^{\pm}(t = 0) = (0.5 \pm 0.2)\delta_{k,0}$.

confidence appears to increase.

It appears that the confidences for both opinion groups with non-symmetric initial conditions, in the $p = 0.8$ mean-field ODE numerics results, may converge to a similar distribution, Fig. 3.8a and 3.8b. This is a surprise given that our naive assumption was that the opinion group with more agents would reach consensus. However it is unclear from these plots what the early time dynamics are. To observe the dynamics in more detail we firstly consider the fraction of agents in the two groups, for early times, and then the confidence distributions in the long time region.

3.4.4 $p > 1/2$ Early time results

Considering first the group membership dynamics we obtained results for the model with $\epsilon = 0.2$ to highlight the oscillations and a range of p to show the different dynamics. As expected from Eq.(3.3) the group proportions are unchanging with $p = 0.5$. We find that numerical results of the mean-field equations (Eq.(3.1), (3.2)) demonstrate early time oscillations about the long time state of equal group size, Fig. 3.9a and 3.9b .

3.4.5 $p > 1/2$ Long time scaling solutions

We have seen that the long time numerical solutions to the mean-field equations (Eq.(3.1), (3.2)) for $p > 1/2$, Fig.s 3.9a and 3.9b, reaches a state where the proportion of agents in each group are the same, i.e. $\rho^+ = \rho^- = 1/2$. We tested the numerical results of the confidence distributions in these long time states and found

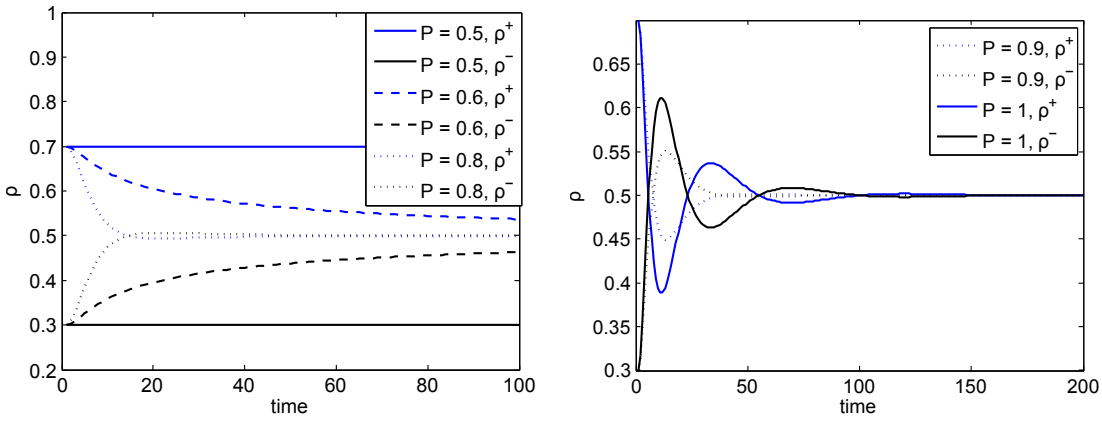

(a) (b)

Figure 3.9: Models with larger probability, p, of the more confident agent winning any single interaction, show group proportion, ρ, dynamics that are increasingly oscillatory. Demonstrated by group fraction dynamics for a range of p choices from numerical solutions to the mean-field equations (Eq.(3.1), (3.2)) of confidence distributions, f_k^+ and f_k^-, with initial conditions of $\epsilon = 0.2$ where $f_k^+(t=0) = (0.5+\epsilon)\delta_{k,0}$ and $f_k^-(t=0) = (0.5-\epsilon)\delta_{k,0}$.

that they were identical, i.e. $f_k^+ = f_k^- \; \forall k$. This suggests that the dynamics converge to a universal solution. Therefore there is effectively only one distribution, when $t \to \infty$, that the dynamics follow that of the single population. Analysis was made of the dynamics for the long time $p > \frac{1}{2}$ case, in the same way as Ben-Naim et al [7] for their single population model. Firstly we note that Eq.(3.1) and Eq.(3.2) can be written more simply under the conditions described above, $f_k^+ = f_k^-$ and therefore $f_k^- G_k^+ = f_k^+ G_k^-$ and $f_k^- F_k^+ = f_k^+ F_k^-$. So we can cancel the last two pairs of terms. Writing $f_k = f_k^+ = f_k^-$ this gives us

$$\frac{d}{dt} f_k = p\left(f_{k-1}F_{k-1} - f_k F_k\right) + (1-p)\left(f_{k-1}G_{k-1} - f_k G_k\right) + \frac{1}{2}\left(f_{k-1}f_{k-1} - f_k f_k\right). \tag{3.16}$$

We recognise this as the master equation for the single population (without the decline term r) in Ben-naim et al [7]. We then follow the same steps followed in their paper to find a scaling function. We rewrite Eq.(3.16) using $f_k = F_{k+1} - F_k$ and $G_k = F_\infty - F_{k+1} = 1/2 - F_{k+1}$ (where the maximum group size is $F_\infty^+ = 0.5$ or

$F_\infty^- = 0.5$). This gives the equation for the cumulative distribution:

$$\frac{d}{dt}F_k = pF_{k-1}(F_{k-1} - F_k) - \frac{1}{2}\left(F_k - F_{k-1}\right)^2 + (1-p)(1/2 - F_k)(F_{k-1} - F_k), \tag{3.17}$$

where the boundary conditions are $F_0 = 0$ and $F_\infty = 0.5$. Next we take a continuum limit of Eq.(3.17) where $F_{k+1} - F_k \to \frac{\partial F}{\partial k}$. Considering only the first order terms of $\frac{\partial F}{\partial k}$ we have

$$\frac{\partial F}{\partial t} = \left[\frac{1}{2}(p-1) + (1-2p)F\right]\frac{\partial F}{\partial k}. \tag{3.18}$$

Having observed for equal distributions, $f_k^+ = f_k^-$, for example in Fig. 3.4c, that the mean confidence increases linearly for the numerical solutions to the original mean-field equations Eq.(3.1) and (3.2) we know empirically that $< k > \propto t$ so we make a scaling ansatz $F_k(t) \simeq \Phi(\frac{k}{t})$. So we rewrite Eq.(3.17) using the scaling form and the variable $x \equiv k/t$ to give

$$\left[\frac{1}{2}(p-1) + x + (1-2p)\Phi(x)\right]\frac{d\Phi}{dx} = 0, \tag{3.19}$$

with boundary conditions $\Phi(0) = 0$ and $\Phi(\infty) = 0.5$. Solving Eq.(3.19) gives

$$\Phi(x) = 0 \text{ or } \Phi(x) = \frac{\frac{1}{2}(p-1)}{2p-1} + \frac{x}{2p-1}.$$

As in Ben-naim et al. [7] we use the boundary conditions and monoticity of F_k. Assuming that Φ changes continuously with p we analyse the solution to Eq.(3.19). We restrict ourselves to the model space with $0.5 < p \leq 1$. Using the bounds on Φ we find the upper and lower bounds on x:

$$x_- = \frac{1}{2}(1-p) \text{ and } x_+ = \frac{1}{2}p.$$

Therefore we have

$$\Phi(x) = \begin{cases} 0 & \text{if } 0 < x < x_- \\ \frac{\frac{1}{2}(p-1)}{2p-1} + \frac{x}{2p-1} & \text{if } x_- < x < x_+ \\ \frac{1}{2} & \text{if } x_+ < x \end{cases} \tag{3.20}$$

We compared the scaled cumulative distribution of the confidences with the long time result from numerical simulations to Eq.(3.1) and (3.2) and found they agreed,

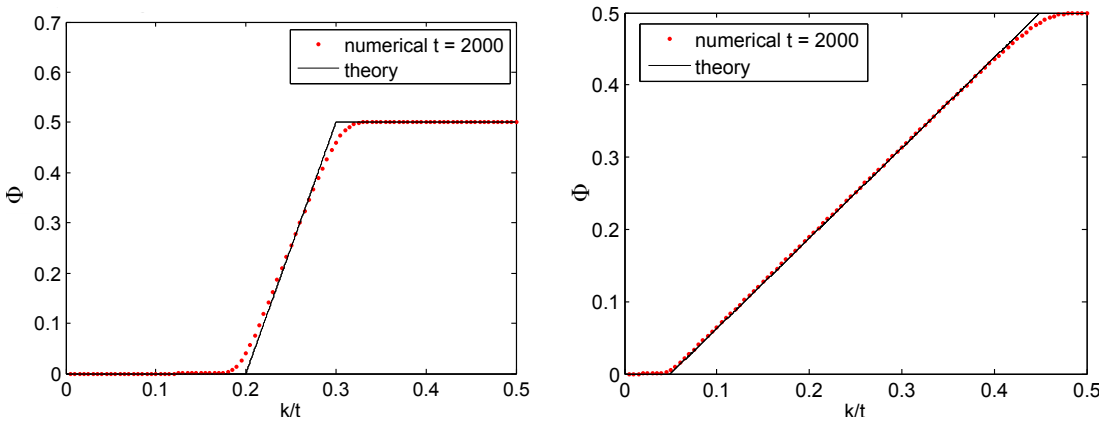

(a) (b)

Figure 3.10: The scaled cumulative distribution of the confidence values for (a) $p = 0.6$ and (b) $p = 0.9$. Numerical results (from solutions to the mean-field equations (Eq.(3.1), (3.2)) of the confidence distributions, f_k^+ and f_k^-) are compared to the theoretical result for $p > \frac{1}{2}$ and the long time limit.

Fig. 3.10a and 3.10b. The form of the results are comparable to the "middle class society" of the single population model presented in Ben-Naim et al. [7] (when the decline term r is zero). We notice that the numerical results do not exactly agree with the theoretical result. This is because there are higher order terms omitted from the theoretical result (we consider only the first order terms when we obtain Eq.(3.18) from Eq.(3.17)). Furthermore the higher order terms in Δk are 'diffusion like' (as seen in the previous chapter) therefore cause the confidence distribution to spread out and consequently smooth the cumulative confidence distribution. This would then 'smooth out' the corners in the theoretical result, Eq.(3.20), and this explains the difference in the numerical and theoretical result in Fig. 3.10a and 3.10b.

We now consider the model with $p = 1$. To visualise the confidence distribution we plot both the original, Fig. 3.11a, and the cumulative, Fig. 3.11b, confidence distributions for a range of p values up to and including $p = 1$. We observed that there was a qualitative difference in the distribution at the parameter choice $p = 1$. Here the distribution always includes a non-zero term for $f_{k=0}$, as seen in Fig. 3.11a and Fig. 3.11b which means there is always a proportion of agents with zero confidence for this model.

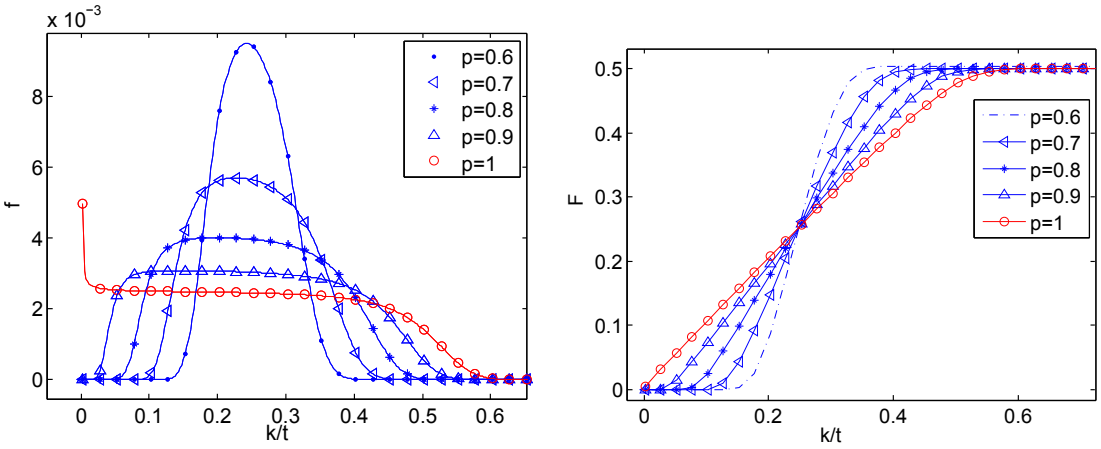

(a) (b)

Figure 3.11: The scaled distribution of the confidence values for (a) $p = 0.6$ to $p = 1.0$ and (b) the cumulative distributions for the same parameters, for a model with $\epsilon = 0.1$ initial conditions, plotted at $t = 400$.

3.4.6 $p < 1/2$ Absorbing states

We now consider the numerical results of the mean-field equations Eq.(3.1) and Eq.(3.2) for models with $p < 1/2$. In this parameter regime the k–value can be considered to be a counter of the number of times that agent has persuaded another agent to change opinion (i.e. interacted and not changed opinion). This interpretation is comparable to the different model that incorporates inertia [57]. In our $p < \frac{1}{2}$ model the agents with the least times they have persuaded others are more likely to persuade others in future interactions. Alternatively one can say that the agents that have spent relatively more time with their current opinion are more likely to change opinion in the future.

We firstly obtained numerical results of the model with half the agents in both opinion groups and all with zero self-confidence. We used a value of $p = 0.2$ and found that both the mean confidence and also the minimum confidence value increase with time as expected Fig. 3.12a and 3.12b. Furthermore the confidence distributions appear to stay the same throughout time. Again this agrees with our expectation from the mean-field equations (Eq.(3.1), (3.2)).

Then we obtained numerical results of the mean-field equations (Eq.(3.1), (3.2)) for the model with $p = 0.2$ and initial conditions of all agents with zero self-confidence and a greater proportion (0.4) in one of the confidence groups (+) than the other (-). We see a clear decrease in the group size, of opinion -, which was initiated with fewer agents Fig. 3.13b. This group reduces to zero while the other

group reaches consensus Fig. 3.13a.

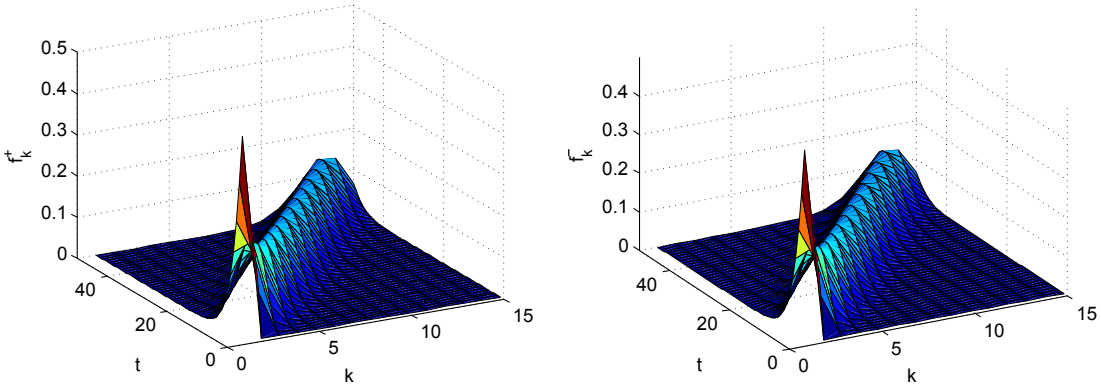

(a) (b)

Figure 3.12: Confidence distributions (a)f_k^+ and (b) f_k^- from the numerical solutions of the mean-field equations (Eq.(3.1), (3.2)) when $p = 0.2$ and with initial conditions $f_k^{\pm}(t = 0) = (0.5)\delta_{k,0}$ (symmetric initial conditions).

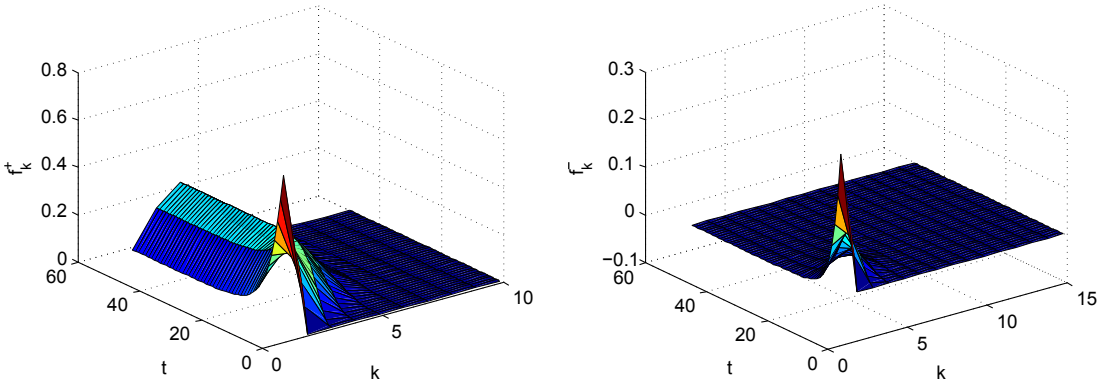

(a) (b)

Figure 3.13: Confidence distributions (a)f_k^+ and (b) f_k^- from the numerical solutions of the mean-field equations (Eq.(3.1), (3.2)) when $p = 0.2$ and with initial conditions $f_k^{\pm}(t = 0) = (0.5 \pm 0.2)\delta_{k,0}$.

To highlight the change observed in opinion group proportion we plotted the group proportion, ρ, for the numerical results of the mean-field equations (Eq.(3.1), (3.2)). We did this for a selection of p values and initial conditions with all zero self-confidence and non-symmetric group size (opinion group + having 0.4 more than opinion group -) Fig. 3.14. We notice that the group with more agents initially (here opinion +) is the group which reaches consensus. Also that the value of p used determines the time the model takes to reach consensus, with values closer to $p = \frac{1}{2}$ taking longer. Furthermore we find that the confidence distribution the consensus

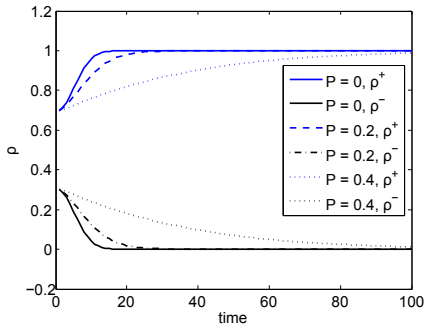

Figure 3.14: Numerical solutions of the mean-field equations (Eq.(3.1), (3.2)) for a range of parameter choices below $p = 1/2$. Initial conditions are $f_k^+(t=0) = (0.5+\epsilon)\delta_{k,0}$ and $f_k^-(t=0) = (0.5-\epsilon)\delta_{k,0}$ and $\epsilon = 0.2$.

group is made up of depends on the p value (and also the ϵ value). The model cases where consensus is reached faster have a confidence distribution which is a closer approximation to the initial conditions, i.e. close to zero confidence. In summary we have found absorbing states for $p < \frac{1}{2}$ which depend on both p and the initial conditions, ϵ.

We notice that our results of the mean-field equations (Eq.(3.1), (3.2)) suggest different consensus times for the different model parameter choices. Models with p closer to 0 approach the absorbing state faster, Fig. 3.14. When $p > \frac{1}{2}$ the suggestion is that consensus time in the stochastic model may be greater in models with p closer to 1, due to oscillations observed in the opinion group sizes Fig. 3.9b.

We highlight here the way the group size oscillates most for the $p = 1$ model compared to lower p choices. We also notice a difference in the confidence distribution arising in the $p = 1$ model, compared to the lower p parameter models. Therefore we anticipate that the consensus time results for this model may be different to those with $p < 1$. We investigate this further in later sections by finding the mean consensus times for $p = 1$ and comparing these to the same result for models with $p < 1$. We also go on to study a heuristic model which is simpler than the full set of ODEs (Eq.(3.1), (3.2)), captures the qualitative dynamics and the solution of which highlights the discontinuity at $p = 1$.

3.5 Stochastic simulations method

The definition of the algorithm we followed to simulate our non-conserved confidence voter model, in continuous time, is to implement the following update rule:

- select an agent at random from the population, i,

- select an agent, j, at random from the neighbours of agent i,
- if they have the same opinion then go to the next update,
- if they have different opinions then compare confidence values, and
  - if confidence equal, then change opinion i and increase confidence j with probability $\frac{1}{2}$
  - if confidence equal, then change opinion j and increase confidence i with probability $\frac{1}{2}$
  - if confidence i greater than j, then change opinion j and increase confidence i with probability p
  - if confidence i greater than j, then change opinion i and increase confidence j with probability $1-p$
  - if confidence j greater than i, then change opinion i and increase confidence j with probability p
  - if confidence j greater than i, then change opinion j and increase confidence i with probability $1-p$.

With each update we increment time, on average, by $1/N$ so that in each time increment each agent has a chance to change opinion on average once. In practice we choose a time increment, for each update, that is drawn from an exponential random variable with mean $1/N$. This captures the time increment of the continuous time voter model which is that update events for agents occur periodically, at independent exponential times. We continue to update until all agents share only one of the two opinions. At this point consensus has been reached an no further updates are possible.

The method above will select agents which have the same opinion, in which update there is no interaction. This computation will take a finite amount of time and when the simulation is close to consensus, i.e. one opinion group is close to making up the entire population, will be repeated many times. This is because the most likely pairing selected at random would be both agents from the group with near consensus opinion. This fact makes simulations slow when the algorithm is followed as above. Therefore we employ a modified version which is quicker to implement a slightly modified version which selects pairs which have different opinions and also increases time an appropriate amount. This modified version:

- keeps track of the number of active bonds, N_a (of pairs of agents connected and with different opinions) and which agents they are made of

- selects an active bond (pair) at random
- we choose a time increment that is drawn from an exponential random variable with mean $1/(2N_a)$. This gives the time increment of the continuous time voter model which is the update events for agents occur periodically, at independent exponential times.
- follows the algorithm for agents with different opinions, above.

3.6 Stochastic simulation results

3.6.1 Ensemble average of simulation dynamics and consensus times

There are two key approaches to probing our model. These are through: analytical analysis of the deterministic mean-field equations (Eq.(3.1), (3.2)); and stochastic simulation results. We have considered the mean-field equation and the consequences of these to gain an initial understanding of the model. Now we employ a stochastic simulation of the model to investigate the behaviour of finite sized versions of the model. The mean-field equations (Eq.(3.1), (3.2)) are written in the large N limit ($N \to \infty$). The simulations are all with a finite number of agents. Furthermore each simulation has noise in the each interaction step as per the update rules. We therefore expect each simulation to be different and also different to the mean-field results (for example the $p = 1/2$ simulations will reach consensus even though the mean-field dynamics do not for this parameter choice). However we expect that the results of an ensemble average (an average over many simulations) will approximate the results from the mean-field equations. We therefore compared the results from 1000 simulations with the mean-field equation results, for the opinion group fractions, $\rho^{\pm}$, and parameter choices $P = 0.6$, $P = 0.9$ and noticed that there are virtually exact Fig. 3.15a and 3.15b.

We see that when $p = 1$ the ensemble average of the stochastic simulations is the same as the numerical solutions to the mean-field equations (Eq.(3.1), (3.2)), Fig. 3.16a, and that there are stronger oscillations than in the $p = 0.9$ plot of $\rho^{+}(t)$, Fig. 3.15b. We also notice that a plot of a single simulation, Fig. 3.16b has the character which is a little like a noisy oscillation.

The results from the numerics of the mean-field equations (Eq.(3.1), (3.2)) suggested different consensus times for different p values. We therefore examine the results from single simulations. We expect that consensus time to increase with increasing p and we see that in Fig.s 3.17a, 3.17b and 3.17c.

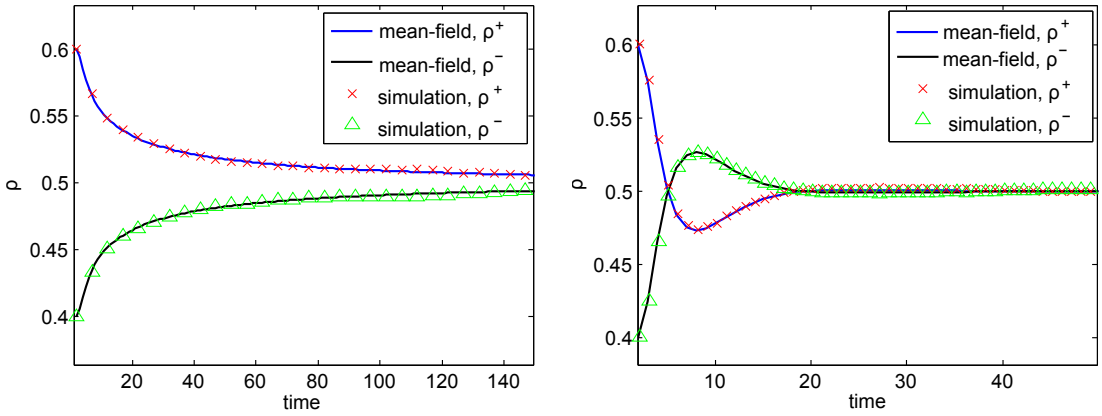

(a) $\rho(t)$, $p = 0.6$ (b) $\rho(t)$, $p = 0.9$

Figure 3.15: Numerical solutions of the mean-field equations and ensemble average (over 1000 simulations) of the stochastic simulations (with $N = 12800$). Initial conditions $\epsilon = 0.1$ for both. Parameter choices were (a) $p = 0.6$ and (b) $p = 0.9$.

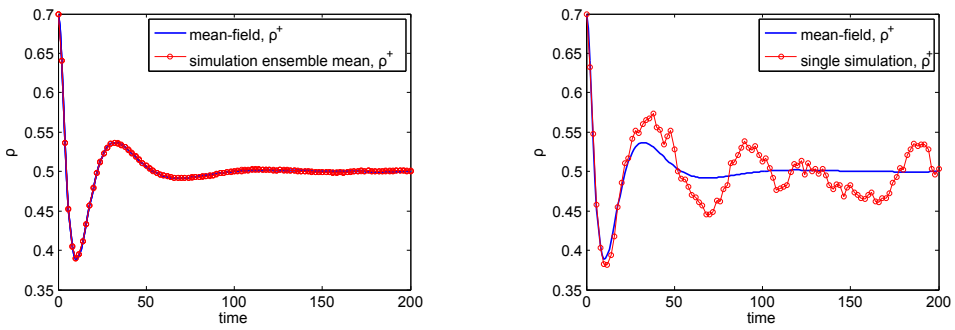

(a) (b)

Figure 3.16: Model parameter choice $p = 1$ (a) $\rho^+(t)$ ensemble average (red circles) of 1000 stochastic simulations and with the mean-field solution (blue line) ($N = 6400$, and initial condition of $\epsilon = 0.2$). (b) $\rho^+(t)$ single simulation (red circles) and the mean-field (blue line).

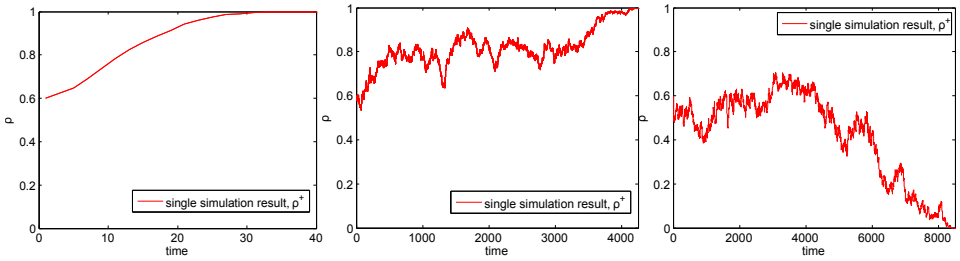

(a) $\rho^+(t)$, $p = 0.2$ (b) $\rho^+(t)$, $p = 0.5$ (c) $\rho^+(t)$, $p = 0.8$

Figure 3.17: Three examples of single stochastic simulations of the model. (a) $p = 0.2$ (b) $p = 0.5$ (c) $p = 0.8$. Population size is $N = 6400$ with non-symmetric initial conditions ($\epsilon = 0.1$ so that $f_k^+(t = 0) = 0.6$ and $f_k^-(t = 0) = 0.4$).

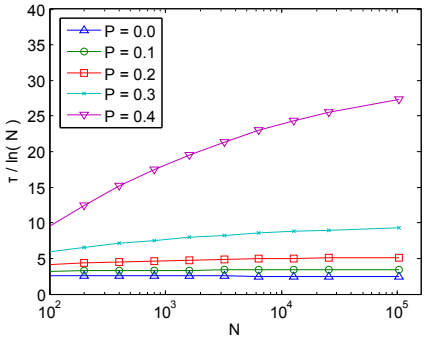

Figure 3.18: Average consensus times for $p < 1/2$ are approximately proportional to lnN. Mean consensus time, τ, plotted as τ/lnN averaged over 1000 simulations with N=6400 and symmetric initial conditions, $f_k^{\pm}(0) = 0.5\delta_{k,0}$.

To find the average consensus time for the model with a range of parameter choices we ran multiple simulations and found the mean time to absorbing state. As the absorbing states are symmetric we took the mean over all absorbing times. We used symmetric initial conditions of half the population in each opinion group ($\pm$) and all agents with zero confidence. 1000 simulations were averaged for a range of total population size, N, and parameter choices $p = 0, 0.1, 0.2, 0.3, 0.4$ and the results plotted Fig. 3.18.

We noticed that, for models with $0 \leq p < 0.5$, as expected the greater p the longer the time to consensus, in agreement with our expectation from the numerics of the mean-field equation (Eq.(3.1), (3.2)) and the single simulations.

We see that consensus time, τ, increases with population size, N, see Fig. 3.18 and Fig. 3.19a. The results in Fig. 3.18 and Fig. 3.19a suggest that the relationship between N and τ is:

$$\tau_N \propto \begin{cases} lnN & \text{if } p < \frac{1}{2} \\ N^1 & \text{if } \frac{1}{2} \leq p < 1 \\ N^{1.4} & \text{if } p = 1 \end{cases}$$

Where for the model with $p = 1$ we find that the exponent, $\tau_N \simeq N^a$, with a least squares fit and find that with 95 percent confidence bounds $a = 1.416(\pm 0.001)$.

Furthermore the results in Fig. 3.19a suggest that there is a jump in the exponent for the mean consensus time between $p = 0.9$ and $p = 1$. We tested whether this was the case by additionally finding the mean consensus time for p values between 0.9 and 1, Fig. 3.19b and we note that the is a jump at $p = 1$.

We observed in the mean-field results that the model with $p = 1$ exhibited qualitatively different behaviour to the other models. We suggest that the jump

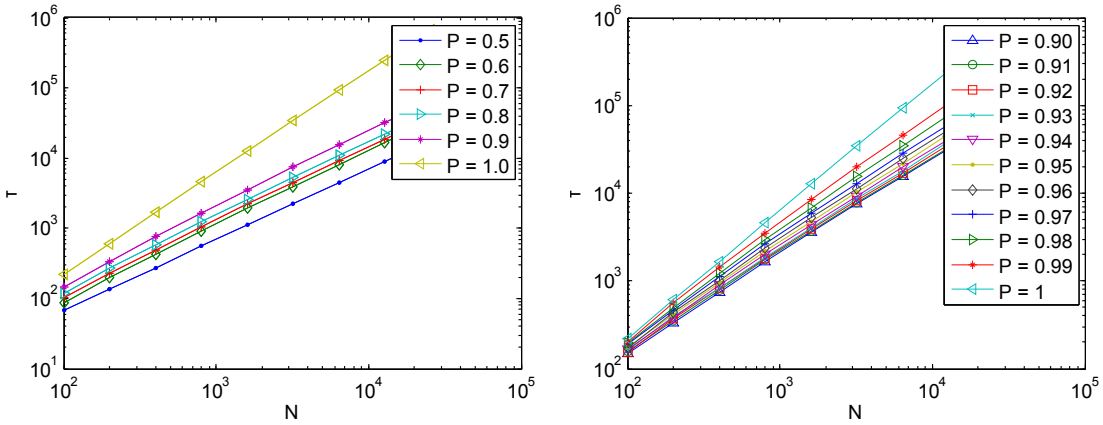

(a) (b)

Figure 3.19: The mean consensus time of simulations is dependent on p, the probability that a more confident agent wins a local interaction. We see a jump in the consensus time at $p = 1$. Results are for 1000 simulations, each with symmetric initial conditions.

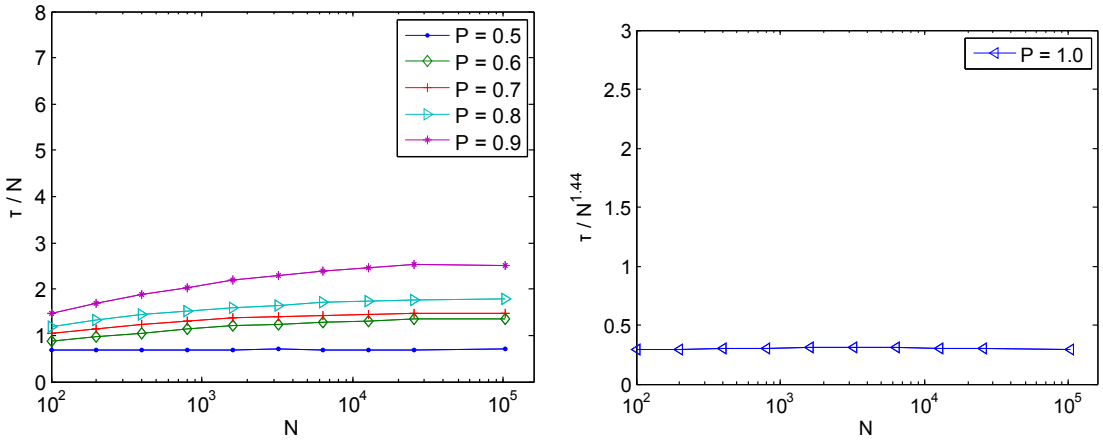

(a) (b)

Figure 3.20: Mean consensus times, τ depend on p. It appears that (a) $\tau \propto N^1$ for $0.5 \leq p < 1$ and (b) $\tau \propto N^{1.4}$ for $p = 1$. Results for 1000 simulations, each with symmetric initial conditions.

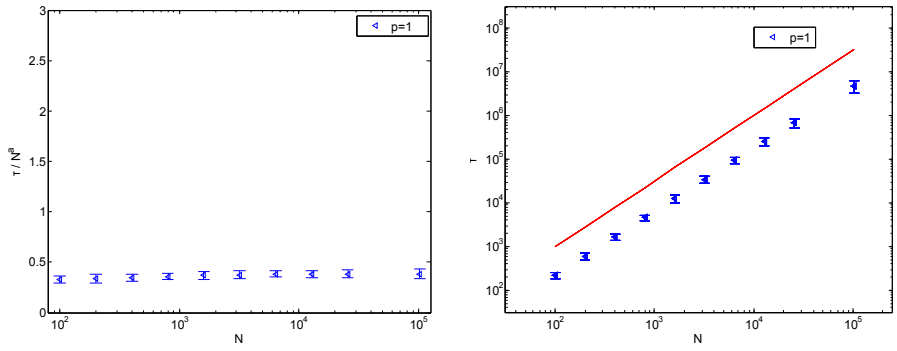

(a) (b)

Figure 3.21: Mean consensus time $\tau(N)$, for the $p = 1$ non-conserved confidence stochastic model, (a) scaled by $N^{1.416}$, and (b) $\tau(N)$ plotted and $N^{3/2}$ (red line) plotted for comparison. Mean consensus time (blue triangles) with error bars of 3 standard error (SEM).

in a, where $\tau \propto N^a$, between the results for models with parameters $p = 0.9$ and $p = 1$ is partly due to the qualitatively different behaviour of the minimum of the confidence distribution in model with $p = 1$ which retains a non-zero proportion of agents with zero self-confidence, Fig. 3.11a.

3.7 Oscillations and fast consensus

We now consider the fast consensus, when $p < \frac{1}{2}$, and the increasing consensus time with p, when $p > \frac{1}{2}$, from the perspective of the confidence distributions $f_k^{\pm}$. We find that the confidence distributions help us make some insights into the dynamics.

3.7.1 Non-conserved model $p > \frac{1}{2}$ oscillations

In the non-conserved model we observe oscillations in both the group size $\rho^{\pm}$ and the mean confidence $\mu^{\pm}$, when $p > \frac{1}{2}$. These damped oscillations in the mean-field equations (Eq.(3.1), (3.2)) and the average stochastic results are greatest when $p = 1$. The oscillations are the cause of the slow consensus time when $p = 1$ and can be explained by considering the dynamics of the mean confidence of the opinion groups.

We explain the oscillations in several short steps. The initial conditions are that one group of opinions is larger than the other. For example $\rho^+ > \rho^-$. It is also the case that during the simulation one group will be larger in size than the other at most times, for example Fig. 3.22a. Now we recall that only the agents with different opinions interact. So the rate at which the minority group have conversations,

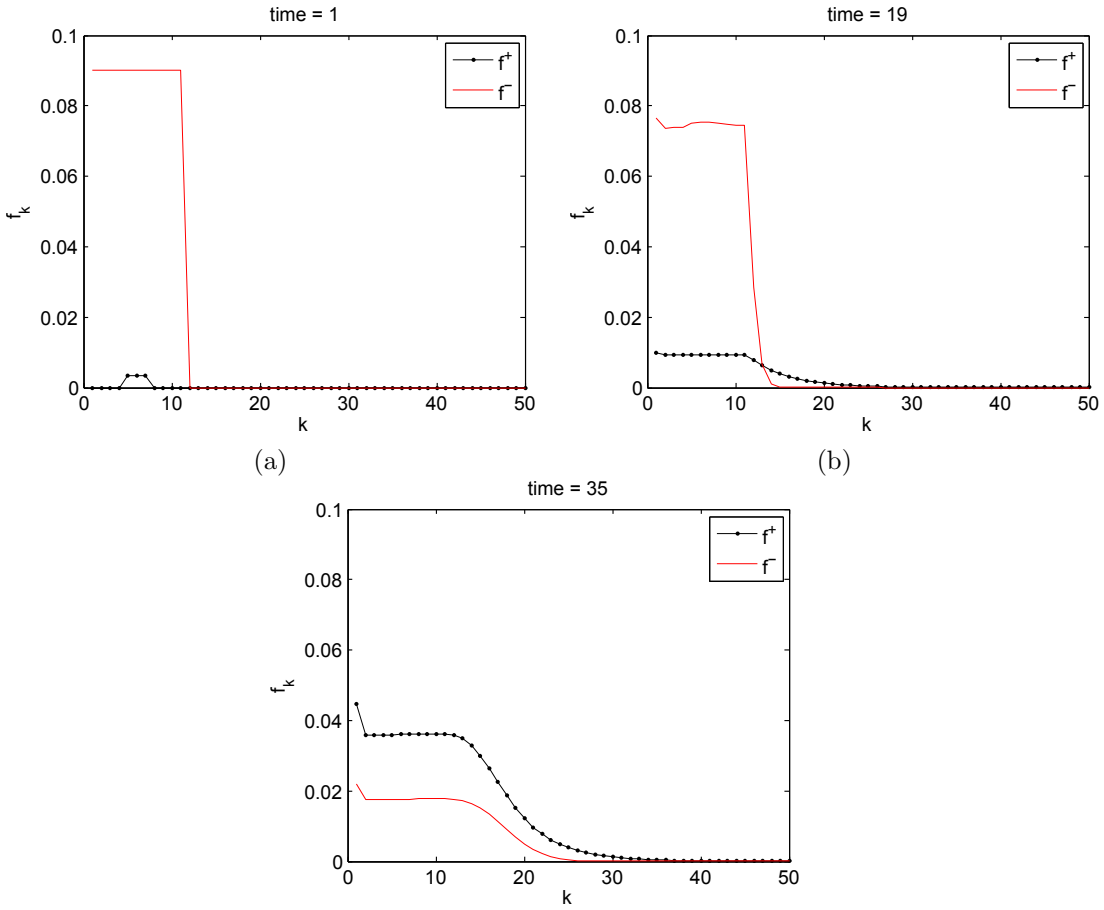

(a) (b)

(c)

Figure 3.22: $f_k^{\pm}(t)$, numerical solutions of mean-field equations (Eq.(3.1), (3.2)), with $p = 1$, initial condition $f_k^+(t = 0) = 0.01(\delta_{5,k} + \delta_{6,k} + \delta_{7,k})/3$, $f_k^-(t = 0) = 0.99(\delta_{1,k} + \delta_{2,k} + \delta_{3,k} + \delta_{4,k} + \delta_{5,k} + \delta_{6,k} + \delta_{7,k} + \delta_{8,k} + \delta_{9,k} + \delta_{10,k} + \delta_{11,k})/11$, at times (a) $t = 1$, (b) $t = 19$ and (c) $t = 35$.

relative to the size of the minority group, is greater than the rate at which the majority group have conversations relative to the size of the majority group. The consequence of this is the mean confidence of the minority group increases faster than the majority. To explain this increase in mean confidence we consider a state in which the two groups have the same distribution of k–values but slightly different sizes. Suppose the $+$ group has size n and the $-$ group has size m, with $n > m$. Since the two groups have the same distributions of k–values, an interaction will result in a transfer from $+$ to $-$ with probability $\frac{1}{2}$ and from $-$ to $+$ with probability $\frac{1}{2}$. If the mean k–values are each μ before interaction, a short calculation shows that after interaction the changes in the mean k–values of the two groups are

$$\Delta\mu^+ = \frac{n(\mu+1)+\mu-1}{2(n^2+1)} \quad \text{and} \quad \Delta\mu^- = \frac{m(\mu+1)+\mu-1}{2(m^2+1)}$$

Therefore $\Delta\mu^- > \Delta\mu^+$ if $n > m$. Thus the average k–value of the smaller group has actually increased which will bias future interactions in its favour thereby stabilising the coexistence state. When $p < \frac{1}{2}$ this mechanism works in reverse. It would be nice to be able to demonstrate this heuristic mechanism analytically although this is complicated by the fact that Eqs. (3.1), (3.2) constitute an infinite-dimensional nonlinear dynamical system so an analysis of its stability properties is not straightforward. In Sec. 3.8 we will introduce a 3-dimensional dynamical system which mimics much of the required behaviour but is more tractable.

The mean confidence of the minority group increases until the maximum confidence of the minority is greater than the maximum confidence of the majority group, Fig. 3.22b. (We use maximum to mean the maximum confidence at that specific time, rather than a maximum for the entire simulation). At this point the choice of p is important. We have the situation where there is a minority group with a maximum confidence greater than the majority group, and $p > \frac{1}{2}$. The p value means that the more confident agents are more likely to persuade the other agents to join their opinion group. Those specific agents in the minority group that have the greatest confidence will now win any conversations they have with agents from the majority group with the probability given by p. When $p = 1$ it is with certainty that these high confident agents in the minority group will win their conversations.

The dynamics are now dominated by the high confidence agents persuading the majority group to join them in their opinion. The opinion group proportions change rapidly (as seen in the mean-field equations (Eq.(3.1), (3.2)) and the average of the simulations) until the previous minority group has become the new majority group Fig. 3.22c.

In summary the oscillations cause slow consensus because they help the group size oscillate about $\rho^+ = 0.5 = \rho^-$. Therefore the dynamics only get close to consensus when there are large deviations, in the stochastic model, towards one of the two absorbing states $\rho^+ = 1$, $\rho^- = 0$, or $\rho^+ = 0$ and $\rho^- = 1$.

3.7.2 Non-conserved model $p < \frac{1}{2}$ fast consensus

In the non-conserved model we see a fast consensus time for the $p < \frac{1}{2}$ model on a fully connected network. (Typical consensus time for the voter model is $\tau \simeq N$, so times less than this are 'fast', for example $\tau \simeq lnN$.) We also see that as p approaches zero the consensus time is reduced. Therefore we consider the confidence distribution for $p = 0.4$ model provides the details that explain the fast consensus time. We explain why the majority group quickly reaches consensus, Fig. 3.23a. We see that the weighted mean, Fig. 3.23d, of the minority opinion group ($z = \frac{\mu^-}{\rho^-}$) is consistently higher than that of the majority group weighted mean confidence ($y = \frac{\mu^+}{\rho^+}$). This means that the distribution of the majority group is on average lower in confidence than the minority group (when the group size has been accounted for). However the parameter choice is $p < \frac{1}{2}$ so we expect that the agents with lower confidence to persuade those with higher confidence to join their group. On average there are more agents of lower confidence in the majority group. So the majority group is more likely to persuade individuals from the minority group. At no point does the minority group find themselves with the least confident agent. This would provide them with the mirror of the zealot-like agents seen the in the $p > \frac{1}{2}$ case. Instead they find that their minimum confidence agents do win enough conversations to keep their weighted mean (z) higher than the weighted mean confidence of the majority group. Therefore the majority group continues to win agents at a faster rate than the minority group until consensus has been reached. Furthermore when p closer to 0 the rate at which the majority group wins interactions is greater so this provides the faster consensus time.

3.8 Heuristic model

In order to better understand the confidence distribution dynamics described by the mean-field equations, Eq. (3.1) we introduce a reduced model which captures most of the essential features of Eq. (3.1) but is simple enough to allow some insight to be obtained. If we think of the $f_k^{\pm}$ as being analogous to probability distributions, then their specification is equivalent to the specification of all their moments. We have already seen, however, that even the first two moments, $\rho^{\pm}$ and $\mu^{\pm}$, satisfy compli-

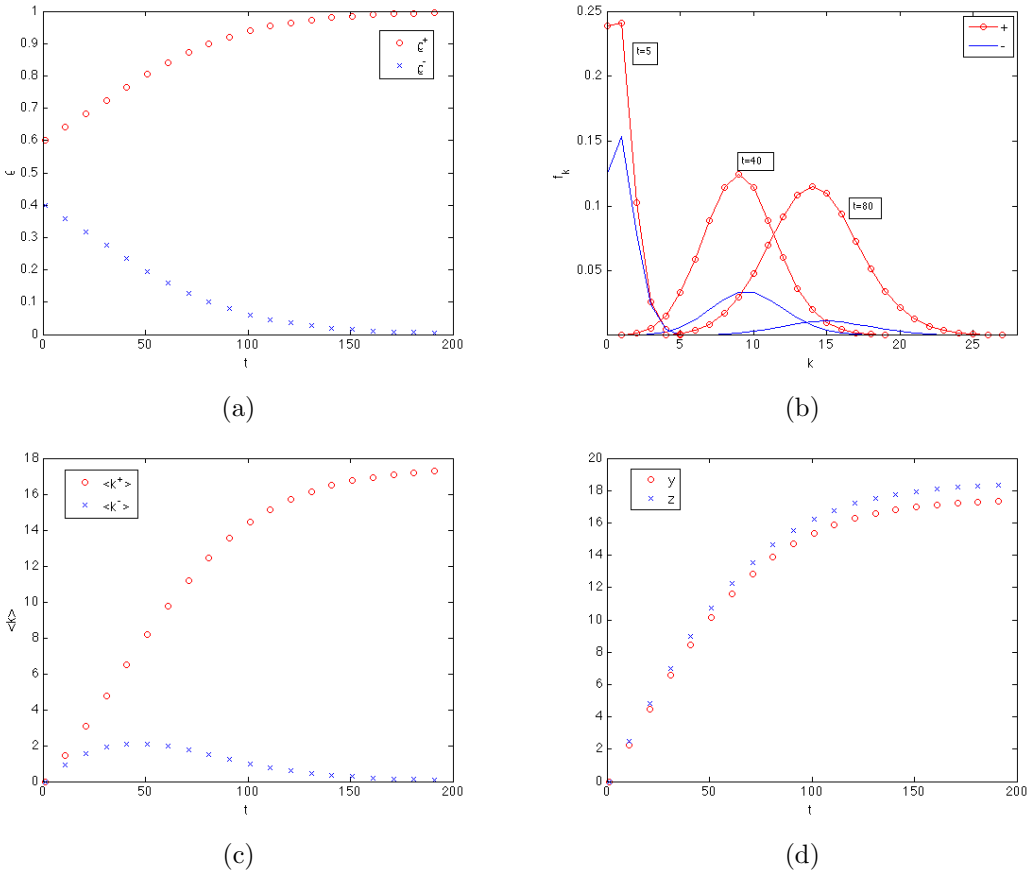

(a) (b)

(c) (d)

Figure 3.23: (a) $\rho^{\pm}(t)$, (b) $f_k^{\pm}$ snap shots, (c) $\mu^{\pm}(t)$, (d) $\mu^{\pm}/\rho^{\pm}(t)$ for the numerical solutions of the mean-field equations when $p = 0.4$. We see that the distribution for both opinion groups drifts away from zero confidence, but the opinion group with the largest mean confidence does not change.

cated equations, Eqs. (3.3) and (3.6) involving cross-correlations between f_k^+ and f_k^-. In principle, one could use the dynamical equations to write evolution equations for these cross-correlations but such equations would involve triple correlations and so on. Such an approach is unlikely to lead anywhere. Instead we suggest to close the system at the level of the first order (in $f_k^\pm$) quantities $\rho^\pm$ and $\mu^\pm$. That is to say, we attempt to "approximate" the RHS of Eqs. (3.3) and (3.6) with functions of $\rho^\pm$ and $\mu^\pm$ only. This would yield a simple three dimensional dynamical system (because we know there is conservation of total number of agents so $\rho_+ + \rho_- = 1$ and therefore not four dimensional) in place of the infinite hierarchy of equations in Eq. (3.1). This cannot be done exactly because of the terms of summations of pairs of f_k and F_K over confidence k therefore the trick in obtaining useful closures is to choose a sensible proposal for these functions should be.

Inspired by the k–value distributions in Fig. 3.11a and aiming to construct the simplest possible model, we introduce the following model for the f_k:

$$\widetilde{f}_k^\pm = \frac{(\rho^\pm)^2}{2(\mu^\pm)^2}\,\Theta\left(\frac{2\mu^\pm}{\rho^\pm} - k\right), \tag{3.21}$$

where $\Theta(x)$ is the Heaviside theta function. We therefore treat the distributions $f_k^\pm$ as being uniform on an interval $[0, K]$. The width, K, of this interval and the value of the function on the interval are chosen such that we have the following properties

$$\begin{aligned}\int_0^\infty \widetilde{f}_k^\pm\, dk &= \rho^\pm \\ \int_0^\infty k\, \widetilde{f}_k^\pm\, dk &= \mu^\pm,\end{aligned}$$

where, in order to simplify things, we shall treat the k–value as a continuous variable from this point on. We can now integrate Eq. (3.21) to get a model for the cumulative distribution, $F_k^\pm$:

$$\widetilde{F}_k^\pm = \rho^\pm + \left(\frac{(\rho^\pm)^2}{2\mu^\pm}k - \rho^\pm\right)\,\Theta\left(\frac{2\mu^\pm}{\rho^\pm} - k\right). \tag{3.22}$$

We now substitute Eqs. (3.21) and(3.22) into Eqs. (3.3) and(3.6) and perform the integrations on the RHS in order to obtain expressions which depend only on $\rho^\pm$ and $\mu^\pm$. This is a surprisingly tedious process given the deceptive simplicity of Eq. (3.21). Using *Mathematica* and rearranging the terms, we obtained the following

dynamical system

$$\begin{aligned}
\frac{d\rho_+}{dt} &= (2p-1)\, R_1^+ && (3.23)\\
\frac{d\rho_-}{dt} &= [+ \leftrightarrow -] && (3.24)\\
\frac{d\mu_+}{dt} &= (1-p)\,\rho^+\rho^- + p\,(\rho_+\mu_- - \rho_-\mu_+) \\
&+ (2p-1)\left(R_2^+ + R_3^+ + R_3^+\right) && (3.25)\\
\frac{d\mu_-}{dt} &= [+ \leftrightarrow -]\,, && (3.26)
\end{aligned}$$

where

$$\begin{aligned}
R_1^+ &= \int_0^\infty \left(\widetilde{f}_k^+ \widetilde{F}_k^- - \widetilde{f}_k^- \widetilde{F}_k^+\right) dk \\
&= \frac{1}{2\mu^+\mu^-}\left[\left(\left(\mu^+\rho^-\right)^2 - \left(\mu^-\rho^+\right)^2\right) + \left|\mu^+\rho^- - \mu^-\rho^+\right|\right] \\
R_2^+ &= \int_0^\infty k\,\left(\widetilde{f}_k^+ \widetilde{F}_k^- - \widetilde{f}_k^- \widetilde{F}_k^+\right) dk \\
&= \frac{2}{3}\frac{1}{\mu^+\mu^-\rho^+\rho^-}\left[2\left(\left(\mu^+\rho^-\right)^3 - \left(\mu^-\rho^+\right)^3\right)\right. \\
&\quad -\frac{1}{2}\left(\mu^+\rho^- - \mu^-\rho^+\right)^2\left(\mu^+\rho^- + \mu^-\rho^+\right) \\
&\quad \left. -\frac{3}{2}\left(\mu^+\rho^- - \mu^-\rho^+\right)^2\left|\mu^+\rho^- - \mu^-\rho^+\right|\right] \\
R_3^+ &= \int_0^\infty \widetilde{f}_k^+ \widetilde{F}_k^-\, dk \\
&= \frac{1}{2\mu^+\mu^-}\left[\mu^+\mu^+\rho^-\rho^- - \frac{1}{2}\left(\mu^+\rho^- - \mu^-\rho^+\right)\right. \\
&\quad \left. -\frac{1}{2}\left|\mu^+\rho^- - \mu^-\rho^+\right|\right] \\
R_4^+ &= \frac{1}{2}\int_0^\infty \widetilde{f}_k^+ \widetilde{f}_k^-\, dk \\
&= \frac{\rho^+\rho^-}{4\mu^+\mu^-}\left[\mu^+\rho^- - \frac{1}{2}\left(\mu^+\rho^- - \mu^-\rho^+\right)\right. \\
&\quad \left. -\frac{1}{2}\left|\mu^+\rho^- - \mu^-\rho^+\right|\right]
\end{aligned}$$

This reduced model reproduces all the qualitative features of the full mean field equations, Eq.s (3.1), (3.2). In particular, the absorbing states in Eq.s (3.1), (3.2) correspond to lines of fixed points in the reduced model. We refer to these as the

consensus fixed points. They are parameterised by a single parameter, $\mu > 0$:

$$\begin{aligned} P_+ &: (\rho^+, \rho^-, \mu^+, \mu^-) = (1, 0, \mu, 0) \\ P_- &: (\rho^+, \rho^-, \mu^+, \mu^-) = (0, 1, 0, \mu). \end{aligned}$$

That these points are zeroes of the right-hand side of Eqs. (3.23)–(3.26) for any value of μ can be verified by direct substitution.

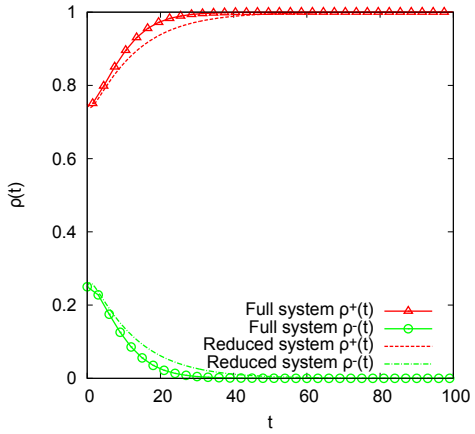

(a) $p = 0.25$, $\rho(t)$

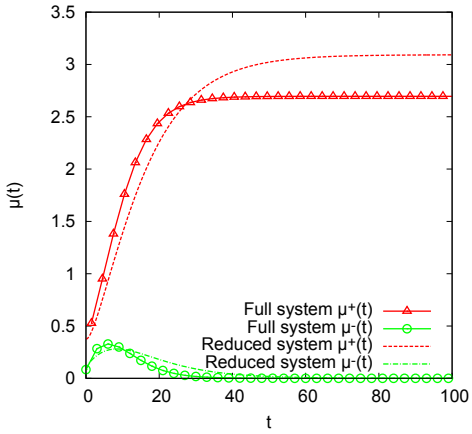

(b) $p = 0.25$, $\mu(t)$

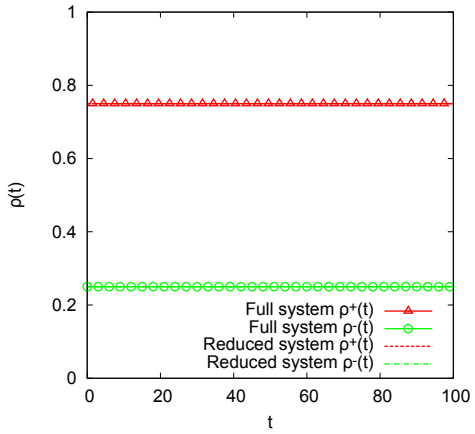

(c) $p = 0.5$, $\rho(t)$

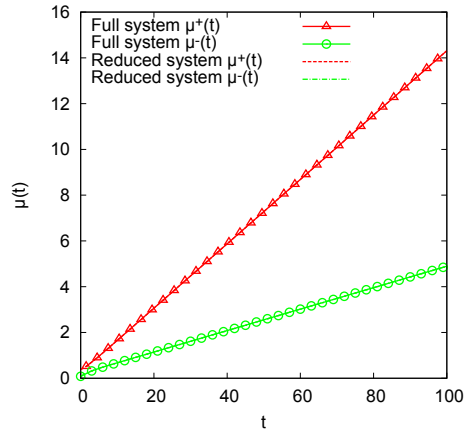

(d) $p = 0.5$, $\mu(t)$

Figure 3.24: Comparisson of the dynamics of ρ and μ between the full mean field equations, Eq.s (3.1), (3.2), and the heurisitc model, Eqs. (3.23)–(3.26),

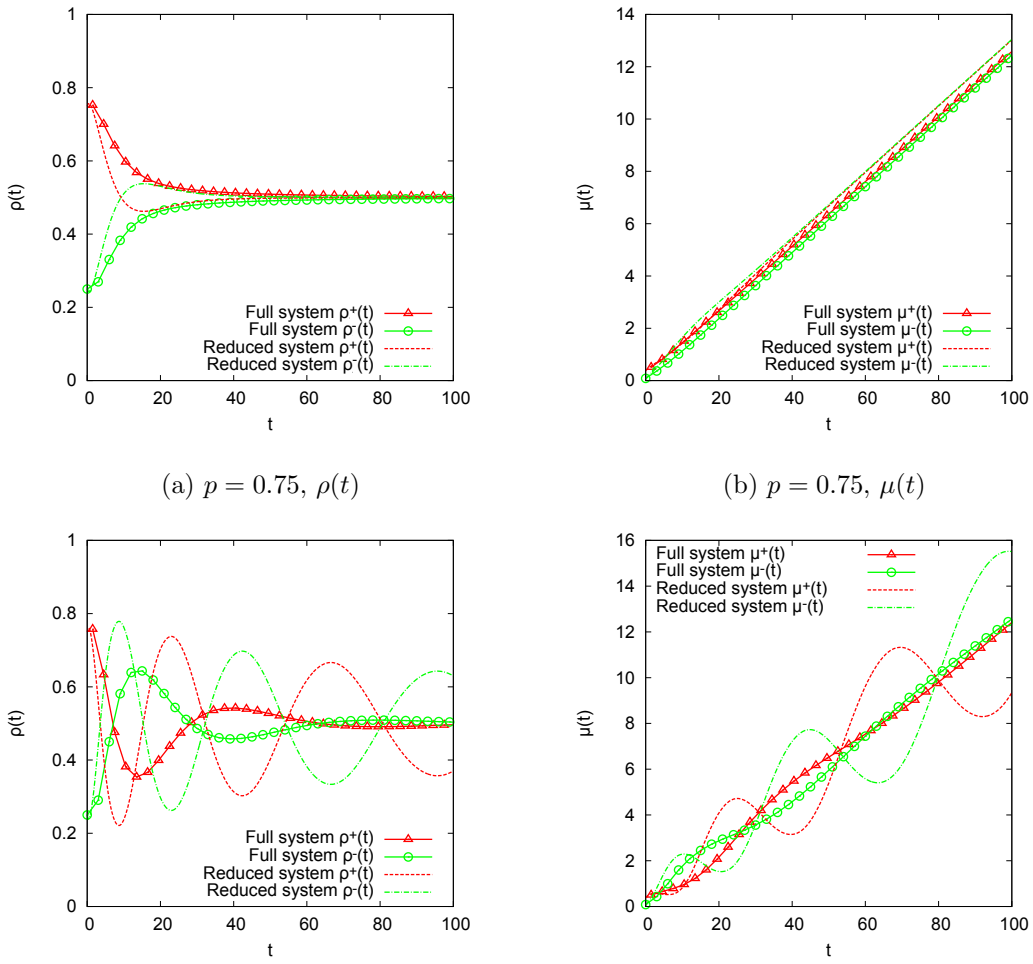

(a) $p = 0.75$, $\rho(t)$

(b) $p = 0.75$, $\mu(t)$

(c) $p = 1$, $\rho(t)$

(d) $p = 1$, $\mu(t)$

Figure 3.25: Comparisson of the dynamics of ρ and μ between the full mean field equations, Eq.s (3.1), (3.2), and the heurisitc model, Eqs. (3.23)–(3.26),

Figs. 3.24a, 3.24c, 3.25a, 3.25c demonstrate the qualitative equivalence between the two systems by comparing the evolution of the $\rho^{\pm}(t)$ obtained from numerical solution of Eqs. (3.1), (3.2) (symbols) with the $\rho^{\pm}(t)$ obtained from numerical solution of Eqs. (3.23)–(3.26) (dashed lines) for a selection of values of p. Figs. 3.24b, 3.25b, 3.25b, 3.25b do the same for the $\mu^{\pm}(t)$. The main difference between the two is that the oscillatory dynamics observed in the mean field equations for values of p near 1 is exaggerated in the reduced model.

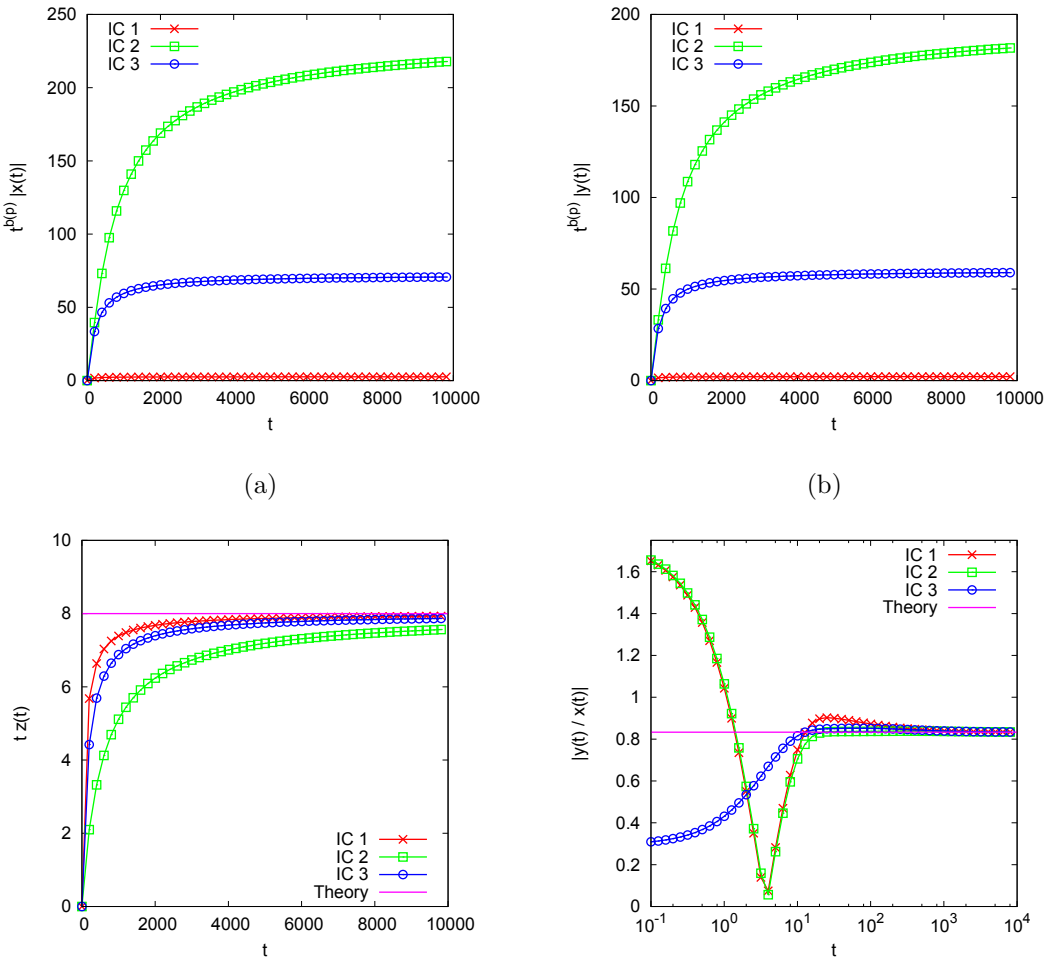

Figure 3.26: Numerical investigation of the behaviour of the reduced model, Eqs. (3.28)–(3.30), near the coexistence fixed point, P_0, for $p = \frac{7}{10}$. (a), (b) and (c) show $\widetilde{X}(t)$, $Y(t)$ and $Z(t)$ respectively for three different generic initial conditions. To make the agreement with theory clear, the data have been compensated by the t-scalings predicted by Eqs. (3.35)-(3.37) with $b(p)$ given by Eq. (3.34). (d) shows that the ratio $\widetilde{X}(t)/Y(t)$ is in agreement with Eq. (3.38).

Replacing $\rho_- = 1 - \rho_+$ throughout, it is convenient to rewrite Eqs. (3.23)–3.26) in terms of the three variables $(X(t), Y(t), Z(t))$ defined as

$$\begin{aligned} X &= \rho_+ \\ Y &= \mu^+\rho^- - \mu^-\rho^+ \\ Z &= (\mu^+\rho^- + \mu^-\rho^+)^{-1}. \end{aligned} \tag{3.27}$$

In terms of these variables, we have the system

$$\frac{dX}{dt} = \frac{2(2p-1)}{1-Y^2Z^2}\,X(1-X)YZ\,(1-Z\,|Y|) \tag{3.28}$$

$$\frac{dY}{dt} = \frac{1}{2}X(1-X)(1-2X) - (1-p)Y - \frac{2p-1}{2(1-Y^2Z^2)}\,ZF_Y(X,Y,Z) \tag{3.29}$$

$$\frac{dZ}{dt} = \frac{1}{2(1-Y^2Z^2)}\,Z^2\,\left(X - F_Z(X,Y,Z)\right), \tag{3.30}$$

where $F_Y(X,Y,Z)$ and $F_Z(X,Y,Z)$ are complicated multivariate polynomials which are written out in the App. A. The advantage of this system is that it is obvious that it has a new fixed point,

$$P_0 : (X,Y,Z) = \left(\frac{1}{2}, 0, 0\right),$$

which corresponds to the solution of the full mean-field equations, Eqs. (3.1), (3.2) found in Sec. 3.4.5. We refer to P_0 as the co-existence fixed point since it describes the situation in which both populations have size one half. Note that the consensus fixed points, P_- and P_+ are both mapped to $Z = \infty$ in these variables. Using the system, Eqs. (3.28)–(3.30), we can try to probe the stability of the coexistence fixed point. The dynamical system given by Eqs. (3.28)–(3.30) cannot be linearized about P_0. Notice, for example, that the lowest power of Z in the third equation is Z^2 so there is no linearization around $Z = 0$. Standard methods of linear stability analysis are not therefore not applicable here. Instead, let us shift the X variable, $X = \widetilde{X} + \frac{1}{2}$, and look for a scaling solution near P_0:

$$\begin{aligned} \widetilde{X}(t) &\sim X_0\,t^{-a} \\ Y(t) &\sim Y_0\,t^{-b} \\ Z(t) &\sim Z_0\,t^{-c}. \end{aligned}$$

The powers a, b and c must be all positive if the coexistence fixed point is to be attractive as $t \to \infty$. Some trial and error is required to identify the leading order terms on the RHS of Eqs. (3.28)–(3.30) due to the large number of terms but the following argument is consistent. The leading terms on the two sides of Eq. (3.30) are

$$-c\,Z_0\,t^{-c-1} \sim -\frac{1}{8}\,Z_0^2\,t^{-2c},$$

so that

$$c = 1 \quad \text{and} \quad Z_0 = 8. \tag{3.31}$$

With $c = 1$, the leading terms on the two sides of Eq. (3.28) are

$$-a\,t^{-a-1} \sim \frac{1}{2}\,(2\,p-1)\,Y_0\,Z_0\,t^{-b-c} = 4\,(2\,p-1)\,Y_0\,t^{-b-1},$$

which leads us to conclude that

$$a = b \quad \text{and} \quad \frac{X_0}{Y_0} = -\frac{4\,(2\,p-1)}{b}. \tag{3.32}$$

Finally, with $c = 1$ and $a = b$, the leading terms in Eq. (3.29) are

$$-b\,Y_0\,t^{-b-1} \sim \left(\frac{-X_0}{4} + (p-1)\,Y_0\right) t^{-b}.$$

This is impossible unless the coefficient of t^{-b} vanishes on the RHS of Eq. (3.29) (there is a subleading term of order t^{-b-1} which could then balance the LHS). Therefore we must have

$$\frac{X_0}{Y_0} = 4\,(p-1). \tag{3.33}$$

Combining Eqs. (3.32) and (3.33) we find

$$b = -\frac{2\,p-1}{p-1}. \tag{3.34}$$

Thus all three exponents are determined along with the amplitude Z_0. The amplitudes X_0 and Y_0 are arbitrary but their ratio is fixed and given by Eq. (3.33). To summarise, the reduced model predicts the following behaviour near the coexistence fixed point:

$$\widetilde{X}(t) \sim X_0\,t^{-b(p)} \tag{3.35}$$

$$Y(t) \sim Y_0\,t^{-b(p)} \tag{3.36}$$

$$Z(t) \sim 8\,t^{-1} \tag{3.37}$$

$$\frac{X_0}{Y_0} = 4\,(p-1), \tag{3.38}$$

with $b(p)$ given by Eq. (3.34). These predictions are validated against numerical solutions of Eqs. (3.28)–(3.30) in Figs. 3.26 and 3.27

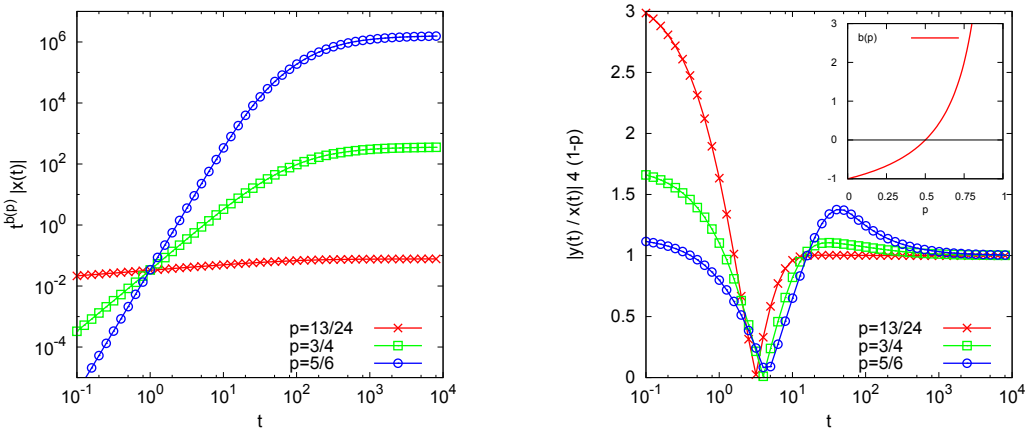

(a) (b)

Figure 3.27: Numerical investigation of the behaviour of the reduced model, Eqs. (3.28–3.30, near the coexistence fixed point, P_0, for a range of values of p for which the fixed point is attractive. (a) shows $\widetilde{X}(t)$ for p taking the values $\frac{13}{24}$(crosses), $\frac{3}{4}$(squares) and $\frac{5}{6}$(circles). The data have been compensated by the t-scaling predicted by Eq. (3.35) with $b(p)$ given by Eq. (3.34). (b) shows that the ratios $\widetilde{X}(t)/Y(t)$ are in agreement with Eq. (3.38) for each value of p. The inset graphs the dependence of $b(p)$ on p expressed in Eq. (3.34).

We find that $b > 0$ for $\frac{1}{2} < p \leq 1$ (see the inset of Fig. 3.27b). The coexistence fixed point is therefore attractive for values of p in this range and repulsive otherwise.

3.9 Conclusions

We have introduced a novel voter model with all agents holding a confidence in their current opinion. Interactions between agents result in the less confident agent changing opinion with probability p, and the more confident agent increasing their confidence. The more confident agent changes opinion with probability $1-p$, when the less confident agent increases confidence. Therefore we have introduced agent confidence which is coupled to the voter model. We found the mean consensus time of the stochastic model on the fully connected network and the mean-field equations (Eq.(3.1), (3.2)) describing the dynamics of the same model in order to understand the effect of these dynamically confident agents compared to the original voter model.

We find that when $\frac{1}{2} < p < 1$ the mean consensus of the stochastic model scales with N, see Fig. 3.20a like the voter model, but the pre-factor depends on p, and that consensus time is greater with increased p, Fig. 3.20a. At $p = 1$ there

is a jump to a different, slower, exponent and $\tau_N \simeq N^a$ where $a = 1.4$, Fig. 3.21a. Furthermore we find that when $p < \frac{1}{2}$ the mean consensus time is fast, $\tau_N \simeq lnN$, see Fig. 3.18, when compared to the $p = \frac{1}{2}$ voter model, $\tau_N \simeq N$ [14].

We find the mean-field equations Eqn. 3.1 and show that the ensemble average of the stochastic model dynamics are the same as those of the numerical solutions of the mean-field equations, Fig. 3.15a. The numerical solutions of the mean-field equations show that when $p > \frac{1}{2}$ the system reaches an equal coexistence state and find scaling solutions for these long time confidence distributions, where the confidence distributions of the two groups converge to a single distribution Sec. 3.4.5. We also see in the numerical solutions of the mean-field equations that when $p > \frac{1}{2}$ the model dynamics create zealot-like agents Sec. 3.7 (who have more confidence than others) and there are damped oscillations in the opinion group size towards a coexistence state Fig. 3.15b. The fully connected model is described by many ODEs (Eq.(3.1), (3.2)) in the mean-field case therefore we create and solve a simple 3 dimension heuristic model that captures the same dynamics as the full ODEs (Eq.(3.1), (3.2)), Sec. 3.8. We show that the stability of the equal coexistence state in the heuristic model depends on p Fig. 3.27b. The closer p is to 1 the greater the coexistence state stability and at $p = 1$ the stability of the equal coexistence is much stronger than for all other p values, see Sec. 3.8. In the stochastic model random fluctuations away from the coexistence state provide the model with a way to reach consensus. Therefore the increase in stability of this state we suggest is a reason for the slower consensus time.

We studied the mean-field equations (Eq.(3.1), (3.2)) and found analytically that when $p = \frac{1}{2}$ the sizes of both opinion groups are constant. Also when $p = \frac{1}{2}$ and there are the same proportion of agents in each group initially the decoupled confidence distributions exhibit advection and diffusion. In the same models but with non-symmetric initial conditions we have found a full solution, in Fourier space, for the decoupled equations describing the confidence distributions and agreed these to the numerical results of the original coupled mean-field equations Fig. 3.6. Because the confidence values and the choice of opinions are independent in the $p = \frac{1}{2}$ model we expect agreement with the Voter model results. We confirmed that for the stochastic model the time to consensus for $p = \frac{1}{2}$ was commensurate with the original Voter model result, i.e. mean consensus time $\tau_N \propto N$. No zealot like agents emerge from models within this $p = \frac{1}{2}$ regime because all the agents confidence values are distributed relatively close to the mean.

We identified the dynamic creation of zealot-like agents, when $p > \frac{1}{2}$ in the full ODEs (Eq.(3.1), (3.2)) and the heuristic model Sec. 3.7, 3.8. These dy-

namic zealot-like agents help explain the presence of the damped oscillations and the increase in stability of the coexistence state with increasing p. We identify the mechanism for the creation of these zealot-like agents is the increased rate at with the minority group, compared to the majority, increase the average confidence value of those agents with opinion of the minority Sec. 3.8. This causes the maximum confidence of the minority to increase faster than the maximum confidence of the majority. The zealot-like agents created help the minority group persuade many agents to leave the majority rapidly and this explains the oscillations in the opinion group size Fig. 3.15b, 3.16b.

The effect of the zealot-like agents in the $p > \frac{1}{2}$ non-conserved confidence model is comparable with specific aspects of social impact theory [38]. In the non-conserved confidence model we identify that the minority is able to affect the dynamics by increasing their confidence, per agent in the minority, and using the high confidence agents to win over many of the majority quickly. This is comparable but not identical to the minority effect in social impact theory where the minority have an influencing advantage over the majority because they are implicitly presenting a novel view (relative to the proportion who hold the view of the majority). From this position of communicating an innovative view they are able to gain greater social influence over those in the majority view.

We also identify, from the numerical solutions of the mean-field equations (Eq.(3.1), (3.2)), a non-zero proportion of weak-willed agents (with permanently zero confidence) in only the $p = 1$ case Fig. 3.11a. This also helps explain the jump consensus time at $p = 1$ because the greater the proportion of weak-willed agents the more dramatic the effect zealot-like agents will have on the change in opinion group size and therefore the greater the opinion group oscillations seen in the numerical results of the mean-field ODEs, and the less likely it is that stochastic fluctuations will allow the dynamics to reach consensus.

The continued presence of weak-willed agents with zero confidence in only the $p = 1$ model, Fig. 3.11a, suggests that these agents help the dynamics reach the equal coexistence state. A simple model with different interaction rules and the inclusion of vacillating voters captures the same model element of weak-willed agents [36]. The model of vacillating voters has an interaction step where a randomly chosen agent, i, will only stay in the same opinion group if two randomly selected neighbours both share their opinion. If either of the them hold an opposing view to the original agent then i changes opinion. The mean-field model incorporating these weak-willed agents drives the dynamics to the zero-magnetisation state, [36], the equivalent of our equal coexistence state. This vacillating voter model does

not include the range of confidence values allowed in our non-conserved confidence model, and incorporates a interaction where an agent compares themselves to two neighbours rather than one. However despite the difference the simple model helps provide an explanation for the qualitative jump in the behaviour seen at $p = 1$ in our model. In this case there are permanently low confidence agents present and this helps the dynamics move towards the coexistence state.

Furthermore the change in the stability of the coexistence state at $p = \frac{1}{2}$, from stable when $p > \frac{1}{2}$ to unstable when $p < \frac{1}{2}$ Fig. 3.27b, helps explain the fast consensus times in the stochastic model when $p < \frac{1}{2}$. We see in the numerical solutions of the mean-field equations (Eq.(3.1), (3.2)) that no zealot-like agents are dynamically created when $p < \frac{1}{2}$, Fig. 3.11a. and the majority group is able to dominate the dynamics by rapidly converting the minority group. Specifically the average confidence of the agents with the opinion of the majority group is always lower than those from the minority, Fig. 3.23d. Therefore the majority group are less likely to change opinion (because $p < \frac{1}{2}$ and those with less confidence change opinion with probability p).

If we consider the confidence value k to be a counter of the number of times that an agent has interacted and not changed group then we can compare our fast consensus in the $p < \frac{1}{2}$, seen in the consensus time, Fig. 3.18 and the mean-field dynamics, Fig. 3.14 to a similar model proposed by Stark et al. [57]. They found that a model with a counter that recorded the number of simulation steps (one per all agents having a chance to update on average) since they last changed group. Up to a maximum value the greater the counter lower the rate at which the agent would change opinion. Upon changing opinion the counter is reset to zero. They found that by reducing the rate of opinion change for agents which had not changed for a longer time the time to consensus was reduced.

We have also defined a model with state dependent rates. The effect of the k–value in the non-conserved confidence model when $p < \frac{1}{2}$ is that agents with a lower k–value are less likely to change opinion. Every time they interact and do not change opinion their confidence, k–value, increases. It is plausible that the relative changes in the k–values in the non-conserved confidence model capture some of the effects of the model proposed by Stark et al. [57]. For example if we consider the k–values in our model when $p < \frac{1}{2}$ we see that those agents with low k–values are more likely to persuade an agent with high k to change opinion and as a result will also increase their own k–value. Therefore those agents with low k–values are like agents in the Stark model that have a lower rate of changing group (and are like the high counter agents). However the consequence of the update rules are

different in our model because the previously low k agent increases their k–value. Furthermore our non-conserved confidence model does not reset the k–value when an agent changes group. Although the details of the two models are different the memory dependent rates of changing opinion have the consequence that some agents are changing opinion more slowly in both models. Therefore it is reasonable that both models result in fast consensus.

Chapter 4

Conserved confidence model on fully connected networks

4.1 Introduction

We modify our non-conserved confidence voter model interactions to additionally enforce that the agent which changes opinion, now, also reduces their confidence. This means that total confidence is now constant. We ask what affect this change in the model has on both the ODEs of the mean-field model and the average consensus time of the fully connected stochastic model. Our motivation for studying this model is that the modified rule of reducing the confidence of the agent which changes opinion is a natural extension of the non-conserved model studied in Chap. 3.

Previously we found that the non-conserved confidence model consensus time depended on the p value (probability that the less confident agent changes opinion) in the non-conserved confidence model. When $\frac{1}{2} < p < 1$ the consensus time scaled with population size, N, in the same way as the voter model so $\tau_N \simeq N$, with a slower pre-factor for larger p. The $p = 1$ model consensus time is different with a slower exponent of the N scaling, Fig. 3.21a. The mean-field equations (Eq.(3.1), (3.2)) showed a equal coexistence state for $\frac{1}{2} < p < 1$. A heuristic model of the mean confidence and opinion group size highlighted the increasing stability, with p, of this equal coexistence state Fig. 3.27b. This stability can also be explained by the behaviour of the confidence distribution, Sec. 3.7. The difference in the behaviour of the mean confidence when $p < \frac{1}{2}$, Sec. 3.7, explains the fast consensus times, $\tau_N \simeq lnN$, Fig. 3.18.

In this chapter we compare the conserved confidence model to the non-conserved confidence model by finding the average consensus time and the mean-field

equations. We find that the $p > \frac{1}{2}$ regime of the conserved confidence model behaves in a similar way to the $p > \frac{1}{2}$ regime of the non-conserved confidence model, with oscillating opinion group size in the numerical solutions of the mean-field equations and an average consensus time that scales like N. The $p = 1$ conserved model also has similar behaviour to the non-conserved model because there is a slower exponent in the N dependence of the mean consensus time, found from the Monte Carlo simulations of the stochastic model. However we see a very different behaviour of the $p < \frac{1}{2}$ conserved confidence model compared to the non-conserved model. In this chapter we see a non-equal coexistence state reached by the mean-field conserved confidence model. This explains why the average consensus time is τ_N for this regime. No longer is there the fast consensus ($\tau_N \simeq lnN$) that was observed in the non-conserved confidence model. The numerical solutions of the conserved confidence mean-field equations highlight the changes in the confidence distribution that provide a way for the opinion group size and the mean confidence to drive the dynamics to the non-equal coexistence state, and not the consensus state as in the case with the non-conserved confidence model.

4.2 Conserved model definition

A description that captures the rules of the conserved confidence model is that each turn an agent i randomly selects one of its neighbours j. If the agents have the same opinion there is no interaction, but if an agent from group $+$ with confidence m interacts with one from group $-$ with confidence n (and for example the first agent is more confident, $m > n$) then the two possible outcomes of the interaction are:

$$(m,+) \oplus (n,-) \rightarrow (m+1,+) \oplus (n-1,+) \text{ with probability } p,$$

$$(m,+) \oplus (n,-) \rightarrow (m-1,-) \oplus (n+1,-) \text{ with probability } 1-p.$$

And if $m = n$ the outcomes are:

$$(m,+) \oplus (m,-) \rightarrow (m+1,+) \oplus (m-1,+) \text{ with probability } \frac{1}{2},$$

$$(m,+) \oplus (m,-) \rightarrow (m-1,-) \oplus (m+1,-) \text{ with probability } \frac{1}{2}.$$

These are identical to the non-conserved model interaction rules except for the update rule. Now the agent who changes their opinion also reduces their confidence by one. This means that in every interaction there is one agent which increases their confidence by one and one agent that reduces their own confidence. Therefore the

total confidence of all the agents is conserved. The total confidence will not change from the initial conditions.

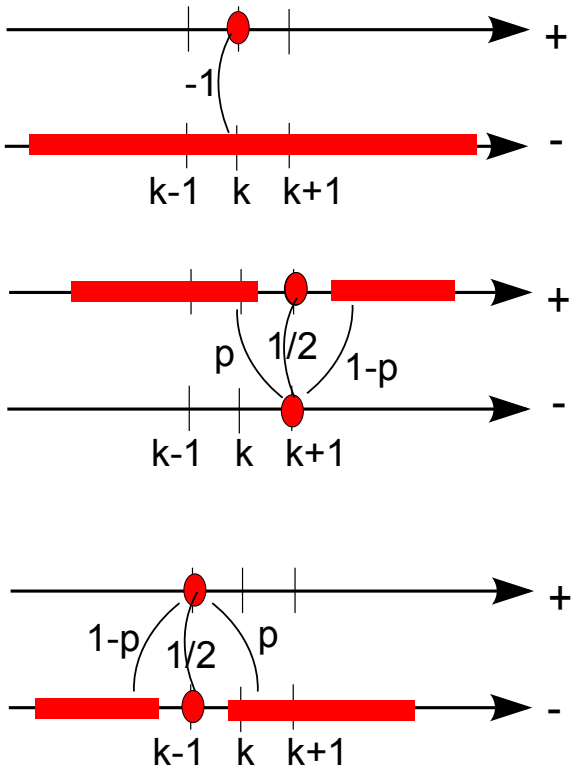

Figure 4.1: Diagram representing the conserved confidence model, on a fully connected network, possible updates for the agents with confidence k and group $+$. The two confidence groups are represented by the two lines and the confidence values $k-1$, k and $k+1$. The full equation for the ODE is given in Eqn. (4.1).

The equations of the fully connected conserved confidence model can be represented by the Fig. 4.1. We notice that the terms like $f_k - f_{k-1}$ found in the non-conserved model no longer appear. This means that when we sum over k to obtain F or ρ the terms are different.

4.3 Mean-field equations

The ODEs of the confidence distributions, $f_k^{\pm}$ are

$$\begin{aligned}\frac{d}{dt}f_k^+ =& -f_k^+F_\infty^- + f_{k-1}^+\left[pF_{k-1}^- + (1-p)G_{k-1}^- + \frac{1}{2}f_{k-1}^-\right] \\ &+ f_{k+1}^-\left[pG_{k+1}^+ + (1-p)F_{k+1}^+ + \frac{1}{2}f_{k+1}^+\right]\end{aligned} \tag{4.1}$$

$$\begin{aligned}\frac{d}{dt}f_k^- =& -f_k^-F_\infty^+ + f_{k-1}^-\left[pF_{k-1}^+ + (1-p)G_{k-1}^+ + \frac{1}{2}f_{k-1}^+\right] \\ &+ f_{k+1}^+\left[pG_{k+1}^- + (1-p)F_{k+1}^- + \frac{1}{2}f_{k+1}^-\right]\end{aligned} \tag{4.2}$$

The equation, Eq. (4.1), captures the gain and loss terms for all the possible changes to f_k^+ (and Eq. (4.2) for f_k^-). The first term in Eq. (4.1) is represented in the first case of Fig. 4.1 and terms 2, 3, and 4 are the second case, and terms 5, 6 and 7 are the third case. We re-write the ODEs (Eq.(4.1), (4.2)) using $G_k^+ = F_\infty^+ - F_k^+ - f_k^+$ and $F_\infty = \sum_{j=-\infty}^{+\infty} f_j$. So the equation for the + opinion distribution can be written

$$\begin{aligned}\frac{d}{dt}f_k^+ =& (f_{k-1}^+ - f_k^+)F_\infty^- + p(f_{k+1}^-F_\infty^+ - f_{k-1}^+F_\infty^-) \\ &+ (2p-1)\left[f_{k-1}^+F_{k-1}^- - f_{k+1}^-F_{k+1}^+ + \frac{1}{2}(f_{k-1}^+f_{k-1}^- - f_{k+1}^-f_{k+1}^+)\right]\end{aligned} \tag{4.3}$$

The ODE for the proportion of agents with confidence k for the conserved model, Eqn. (4.3), is different to the same ODE for the non-conserved model, Eqn. (3.1). This is understandable because the model definitions are different so the update rules for the agents are different. When $p = \frac{1}{2}$ we see from Eqn. (4.3) that the ODEs simplify and that

$$\frac{d}{dt}f_k^+ = \frac{1}{2}f_{k-1}^+F_\infty^- - f_k^+F_\infty^- + \frac{1}{2}f_{k+1}^-F_\infty^+. \tag{4.4}$$

When $f_k^+ = f_k^- \quad \forall k$ then

$$\frac{d}{dt}f_k^+ = \frac{1}{2}(f_{k-1}^+ - 2f_k^+ + f_{k+1}^+)F_\infty^+. \tag{4.5}$$

We find the equations for the density of group + using Eqn. (4.3),

$$\begin{aligned}\frac{d}{dt}\rho^+ &= \sum_{k=-\infty}^{\infty} \frac{d}{dt} f_k^+ \\ &= \sum_{k=-\infty}^{\infty} (f_{k-1}^+ - f_k^+)F_\infty^- + p(f_{k+1}^- F_\infty^+ - f_{k-1}^+ F_\infty^-) \\ &\quad + (2p-1)\left[f_{k-1}^+ F_{k-1}^- - f_{k+1}^- F_{k+1}^+ + \frac{1}{2}(f_{k-1}^+ f_{k-1}^- - f_{k+1}^- f_{k+1}^+)\right]\end{aligned} \tag{4.6}$$

Using the boundary conditions, $f_{\pm\infty}^{\pm}(t) = 0 \quad \forall t$, we find

$$\frac{d}{dt}\rho^+ = (2p-1)\sum_{k=-\infty}^{\infty} f_{k-1}^+ F_{k-1}^- - f_{k+1}^- F_{k+1}^+, \tag{4.7}$$

and therefore

$$\frac{d}{dt}\rho^+ = (2p-1)\sum_{k=-\infty}^{\infty} f_k^+ F_k^- - f_k^- F_k^+. \tag{4.8}$$

It is apparent that when $p = \frac{1}{2}$ the density of both group + and - are constant, because $\frac{d}{dt}\rho = 0$ from Eqn. (4.8). We notice that this is similar to the non-conserved confidence model where the opinion group is also constant when $p = \frac{1}{2}$, Eqn. (3.3). In both cases this is reasonable because the mean-field model captures the average dynamics of individual updates that increase either group with probability exactly $\frac{1}{2}$ as in the voter model.

We write the dynamic equations for the cumulative confidence distribution, $F_k^{\pm}$, using the ODE Eqn. (4.3) and find that the equation, Eqn. (4.9),

$$\begin{aligned}\frac{d}{dt}F_k^+ &= \sum_{j=-\infty}^{k-1} \frac{d}{dt} f_j^+ \\ &= \sum_{j=-\infty}^{k-1} (f_{j-1}^+ - f_j^+)F_\infty^- + p(f_{j+1}^- F_\infty^+ - f_{j-1}^+ F_\infty^-) + \\ &\quad (2p-1)\left[f_{j-1}^+ F_{j-1}^- - f_{j+1}^- F_{j+1}^+ + \frac{1}{2}(f_{j-1}^+ f_{j-1}^- - f_{j+1}^- f_{j+1}^+)\right].\end{aligned} \tag{4.9}$$

We use the boundary conditions of the confidence distributions, $f_{\pm\infty}^{\pm} = 0 \quad \forall t$ and

re-write the sums to find the cumulative confidence dynamic equations

$$\begin{aligned}\frac{d}{dt}F_k^+ =& - f_{k-1}^+ F_\infty^- + p(F_k^- F_\infty^+ - F_{k-1}^+ F_\infty^-) \\ &+ (2p-1)\frac{1}{2}\sum_{j=-\infty}^{k-1}(-f_{k-1}^+ f_{k-1}^- - f_k^+ f_k^-) \\ &+ (2p-1)\sum_{j=-\infty}^{k-1}\left[f_{j-1}^+ F_{j-1}^- - f_{j+1}^- F_{j+1}^+\right].\end{aligned} \tag{4.10}$$

We notice that Eqn. (4.10) is different to the non-conserved model Eqn. (3.4). We expect that the two models will have different ODEs for the cumulative confidence, F_k, in general because the definitions of the interactions are different, for example the conserved model reduces the confidence of one agent in every update while the non-conserved model does not.

We find the ODEs of the mean confidence, again using the boundary conditions, and the definition of

$$\begin{aligned}\frac{d}{dt}\mu^+ &= \sum_{k=-\infty}^{\infty} k\frac{d}{dt}f_k^+ \\ &= \sum_{k=-\infty}^{\infty} k(f_{k-1}^+ - f_k^+)F_\infty^- + pk(f_{k+1}^- F_\infty^+ - f_{k-1}^+ F_\infty^-) \\ &\quad + (2p-1)k\left[f_{k-1}^+ F_{k-1}^- - f_{k+1}^- F_{k+1}^+ + \frac{1}{2}(f_{k-1}^+ f_{k-1}^- - f_{k+1}^- f_{k+1}^+)\right].\end{aligned} \tag{4.11}$$

Using both the boundary conditions for the confidence distribution and rearranging the sums we find that

$$\begin{aligned}\frac{d}{dt}\mu^+ =& (1-2p)F_\infty^+ F_\infty^- + p(\mu^- F_\infty^+ - \mu^+ F_\infty^-) \\ &+ (2p-1)\sum_{k=-\infty}^{\infty}(f_k^+ F_k^- + f_k^- F_k^+ + f_k^+ f_k^-) \\ &+ (2p-1)\sum_{k=-\infty}^{\infty} k(f_k^+ F_k^- - f_k^- F_k^+).\end{aligned} \tag{4.12}$$

We notice that the ODE for the mean confidence in the conserved confidence model, Eqn. (4.10), is very different to that of the non-conserved confidence model Eqn. (3.6). This is because the ODEs for the confidence distributions f_k^+, in the con-

served Eqn. (4.1) and non-conserved Eqn. (3.1) confidence models, are so different. This difference arises from the model definitions where the agent losing an interaction, in the conserved model, will reduce their confidence, but in the non-conserved model they do not. Therefore in the conserved confidence model every interaction will result in one agent gaining confidence and one agent losing confidence. So the change in total confidence at every update is zero, so we know that $\frac{d}{dt}\mu^+ = -\frac{d}{dt}\mu^-$, where we have previously defined $\frac{d}{dt}\mu^+ = \sum_{k=-\infty}^{\infty} k \frac{d}{dt} f_k^+$. The total confidence in the system is not conserved in the non-conserved model and we see this in the increasing mean confidence, for example in Fig. 3.4a. However the total confidence is always conserved in the conserved model, as seen in the numerical solutions of the ODEs for a range of p values, Fig. 4.2.

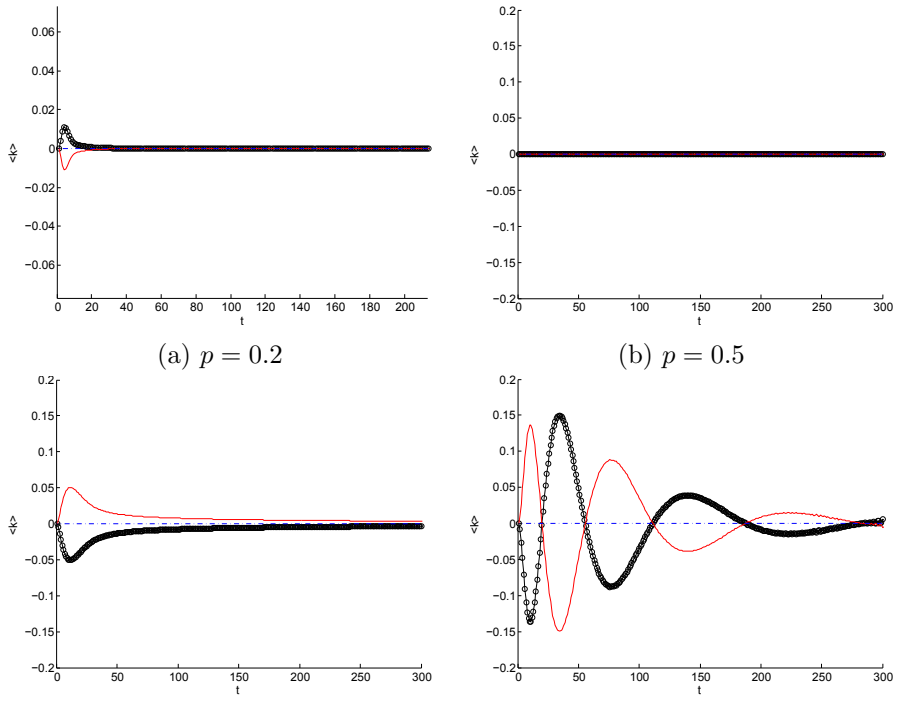

(a) $p = 0.2$ (b) $p = 0.5$

(c) $p = 0.8$ (d) $p = 1$

Figure 4.2: The mean confidence $\mu^{\pm}(t)$ from numerical solutions of the ODEs for the conserved confidence model (Eq.(4.1), (4.2)). We see that although the confidence for opinion group + (black circles) and group − (red line) change the total mean confidence is constant (blue dashed line) for (a) p=0.2, (b) p=0.5, (c) p=0.8, and (d) p=1, as expected from the model definition of interactions increasing one agents confidence and decreasing another agents confidence.

4.4 Mean-field ODEs $p = \frac{1}{2}$

We firstly find the numerical solutions of the ODEs (Eq.(4.1), (4.2)) when $p = \frac{1}{2}$. We use the same initial conditions as previously used in when finding the numerical solutions of the ODEs for the non-conserved confidence model Chap. 3. The initial condition is all agents with zero confidence and the proportion of agents in each opinion group defined, and allocate a higher proportion of agents in one opinion group, for example $\rho^+(t=0) = 0.7$, $\rho^-(t=0) = 0.3$. We find the change in group size is zero, Fig. 4.3a, as expected from Eqn. (4.8). We also see that the confidence appears to diffuse from the initial condition in the plot of increasing snap-shots of the confidence distributions of both opinion groups, Fig. 4.3b.

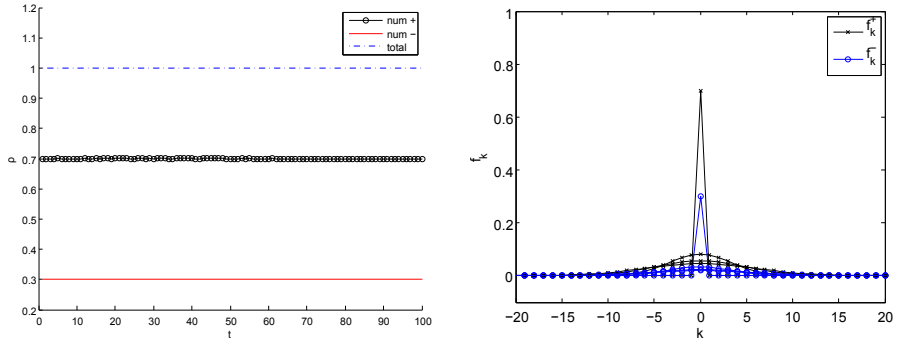

(a) ρ (b) f_k

Figure 4.3: $p = \frac{1}{2}$ conserved model mean-field equations (Eq.(4.1), (4.2)) numerical solutions. (a) The group size ρ dynamics with ρ^+ (black circles), ρ^- (red line) and total population $\rho^+ + \rho^-$ (blue dotted line) plotted. (b) The confidence distributions for three snapshots.

4.4.1 Solution of $p = \frac{1}{2}$ model

To understand the behaviour of the confidence distribution when $p = \frac{1}{2}$ we solve Eqn. (4.1) for f_k using the Fourier Transform. We consider the conserved model when $p = \frac{1}{2}$ and the initial condition has non-equal densities for groups + and - at $k = k_0$. So $f_k^+(t=0) = \delta(k=k_0)A$ and $f_k^-(t=0) = \delta(k=k_0)B$. We assume $A \neq 0$, $B \neq 0$, they are constant and $A \neq B$. We know from the analytical results that when $p = \frac{1}{2}$, the densities $\rho^\pm$ are constant. (Where $\rho^\pm = \sum_{-\infty}^{\infty} f_k^\pm$). So in this case $\rho^+(t) = A$ and $\rho^-(t) = B$. The ODEs are, when $p = \frac{1}{2}$,

$$\frac{\partial}{\partial t} f_k^+ = \frac{1}{2} f_{k-1}^+ F_\infty^- - f_k^+ F_\infty^- + \frac{1}{2} f_{k+1}^- F_\infty^+, \tag{4.13}$$

and

$$\frac{\partial}{\partial t} f_k^- = \frac{1}{2} f_{k-1}^- F_\infty^+ - f_k^+ F_\infty^+ + \frac{1}{2} f_{k+1}^+ F_\infty^-. \tag{4.14}$$

We substitute $A = F_\infty^+$, $B = F_\infty^-$, take a continuous approximation of the confidence distribution $f(k,t) \simeq f_k(t)$. We also use the approximations

$$f_{k+1}^\pm = f_k^\pm + \frac{\partial}{\partial k} f^\pm + \frac{\partial^2}{\partial k^2} f^\pm, \qquad f_{k-1}^\pm = f_k^\pm - \frac{\partial}{\partial k} f^\pm + \frac{\partial^2}{\partial k^2} f^\pm.$$

So we can rewrite the ODEs as

$$\begin{aligned} \frac{\partial}{\partial t} f^+ = & - f^+ B + \frac{1}{2}\left(f^+ - \frac{\partial}{\partial k} f^+ + \frac{1}{2}\frac{\partial^2}{\partial k^2} f^+ \right) B \\ & + \frac{1}{2}\left(f^- + \frac{\partial}{\partial k} f^- + \frac{1}{2}\frac{\partial^2}{\partial k^2} f^- \right) A, \end{aligned} \tag{4.15}$$

and

$$\begin{aligned} \frac{\partial}{\partial t} f^- = & - f^- A + \frac{1}{2}\left(f^- - \frac{\partial}{\partial k} f^- + \frac{1}{2}\frac{\partial^2}{\partial k^2} f^- \right) A \\ & + \frac{1}{2}\left(f^+ + \frac{\partial}{\partial k} f^+ + \frac{1}{2}\frac{\partial^2}{\partial k^2} f^+ \right) B. \end{aligned} \tag{4.16}$$

We take the Fourier Transform where $\hat{f}^\pm(m,t) = \mathcal{F}[f^\pm(k,t)] = \int_{-\infty}^{\infty} f^\pm(k,t) e^{-imk} dk$. So in Fourier space

$$\frac{\partial}{\partial t}\hat{f}^+ = -\hat{f}^+ B + \frac{B}{2}\left(\hat{f}^+ + im\hat{f}^+ - \frac{1}{2}m^2\hat{f}^+ \right) + \frac{A}{2}\left(\hat{f}^- - im\hat{f}^- - \frac{1}{2}m^2\hat{f}^- \right) \tag{4.17}$$

and

$$\frac{\partial}{\partial t}\hat{f}^- = -\hat{f}^- A + \frac{A}{2}\left(\hat{f}^- + im\hat{f}^- - \frac{1}{2}m^2\hat{f}^- \right) + \frac{B}{2}\left(\hat{f}^+ - im\hat{f}^+ - \frac{1}{2}m^2\hat{f}^+ \right) \tag{4.18}$$

We let $c(m) = \frac{1}{2}(-1 + im - \frac{m^2}{2})$ and $d(m) = \frac{1}{2}(1 - im - \frac{m^2}{2})$

$$\partial_t \begin{bmatrix} \hat{f}^+ \\ \hat{f}^- \end{bmatrix} = \begin{bmatrix} Bc(m) & Ad(m) \\ Bd(m) & Ac(m) \end{bmatrix} \times \begin{bmatrix} \hat{f}^+ \\ \hat{f}^- \end{bmatrix} \tag{4.19}$$

We now diagonalize the matrix in Eqn. (4.19) rewritten for brevity as $\partial_t \bar{f} = \mathbf{A}\bar{f}$, in order to decouple the partial differential equations for $\hat{f}^+$ and $\hat{f}^-$. We let $\bar{y} = [y_1 \quad y_2]'$ and $\mathbf{M}$ be the diagonal matrix so $\partial_t \bar{y} = \mathbf{M}\bar{y}$. We let $\mathbf{P}$ be a matrix of

the eigenvectors of matrix $\mathbf{A}$ and $\mathbf{M}$ be the matrix of eigenvalues on the diagonal. Now we let $\bar{y} = \mathbf{P}^{-1}\bar{f}$, so $\bar{f} = \mathbf{P}\bar{y}$, and also $\mathbf{M} = \mathbf{P}^{-1}\mathbf{A}\mathbf{P}$ and $\mathbf{A} = \mathbf{P}\mathbf{M}\mathbf{P}^{-1}$. We therefore write $\partial_t \bar{f} = \mathbf{A}\bar{f} = \mathbf{P}\mathbf{M}\mathbf{P}^{-1}\bar{y}$, so $\partial_t \mathbf{P}\bar{y} = \mathbf{P}\mathbf{M}\mathbf{P}^{-1}\mathbf{P}\bar{y}$ and $\mathbf{P}\partial_t\bar{y} = \mathbf{P}\mathbf{M}\bar{y}$ so $\partial_t\bar{y} = \mathbf{M}\bar{y}$ is required to decouple the equations. We find $\mathbf{M}$ by finding the eigenvalues of the matrix in Eqn. (4.19). We have

$$\lambda_\pm = \frac{(A+B)}{2}c \pm \frac{1}{2}\sqrt{(A+B)^2c^2 - 4AB(c^2-d^2)} \tag{4.20}$$

and can write

$$\partial_t \begin{bmatrix} y_1 \\ y_2 \end{bmatrix} = \begin{bmatrix} \lambda_+ & 0 \\ 0 & \lambda_- \end{bmatrix} \times \begin{bmatrix} y_1 \\ y_2 \end{bmatrix} \tag{4.21}$$

so

$$y_1(m,t) = D_1(m)e^{\lambda_+ t} \tag{4.22}$$

and

$$y_2(m,t) = D_2(m)e^{\lambda_- t} \tag{4.23}$$

where D_1 and D_2 are constant in time, and are found using the Fourier Transform of the initial conditions ($f_k^+(t=0) = \delta(k=0)A$ and $f_k^-(t=0) = \delta(k=0)B$) we write down the initial conditions in Fourier space

$$\hat{f}^+(m,0) = Ae^{-imk_0}, \tag{4.24}$$

and

$$\hat{f}^-(m,0) = Be^{-imk_0}. \tag{4.25}$$

We now construct the matrix from the eigenvectors, such that

$$\begin{bmatrix} \hat{f}^+(m,t) \\ \hat{f}^-(m,t) \end{bmatrix} = \begin{bmatrix} 1 & 1 \\ \frac{\lambda_+ - Bc}{Ad} & \frac{Bd}{\lambda_- - Ac} \end{bmatrix} \times \begin{bmatrix} y_1(m,t) \\ y_2(m,t) \end{bmatrix}. \tag{4.26}$$

Thus the initial conditions can be rewritten

$$D_2(m) = Ae^{imk_0} - D_1(m), \tag{4.27}$$

and

$$D_1(m) = \left(Be^{-imk_0} - \frac{Bc - \lambda_-}{d}e^{-imk_0}\right)\left(\frac{Ad}{\lambda_- - \lambda_+}\right). \tag{4.28}$$

And using Eqn. (4.26) we find that

$$\hat{f}^+(m,t) = y_1(m,t) + y_2(m,t), \tag{4.29}$$

and

$$\hat{f}^{-}(m,t) = \frac{Bc-\lambda_{+}}{Ad} y_1(m,t) + \frac{Bc-\lambda_{-}}{Ad} y_2(m,t). \tag{4.30}$$

We solve for $f^{\pm}$ using an inverse Fourier Transform in *Matlab* and compare this with the numerical results of the ODEs (Eq.(4.1), (4.2)) for the same time, $t = 80$, in Fig. 4.4. Finding the inverse Fourier Transform results in the confidence distributions f_k^+ and f_k^-, for the time chosen. Therefore we have found the exact confidence distribution for the $p = \frac{1}{2}$ case of the conserved confidence model when the initial conditions are all agents with zero confidence and one opinion group larger (e.g. $\rho^+(t=0) = 0.6$).

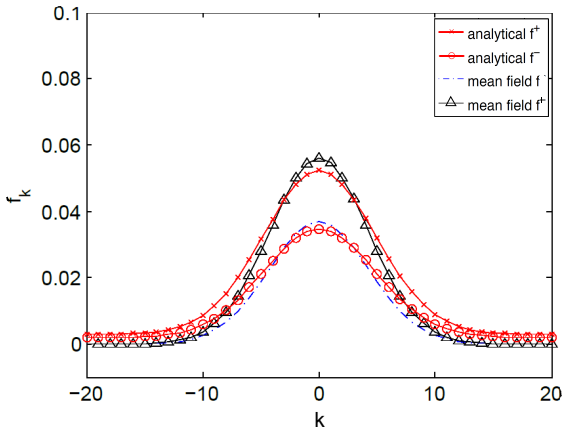

Figure 4.4: Fully connected conserved confidence model with $p = \frac{1}{2}$. Comparison, at $t = 60$, of the numerical results of the full ODEs: f^- (blue dotted line) and f^+ (black triangles) with the solution of the analytical equation: f^- (red circles) and f^+ (red crosses). Initial condition is all agents with zero confidence and $\rho^+(t=0) = 0.6$, $\rho^-(t=0) = 0.4$.

4.5 Mean-field ODEs $p > \frac{1}{2}$

Now we consider the mean-field equations (Eq.(4.1), (4.2)) when $p > \frac{1}{2}$. Previously we found that the non-conserved confidence model has mean-field equations (Eq.(3.1), (3.2)) which give rise to oscillations in the opinion group dynamics, Fig. 3.15b. Now we find that the conserved model numerical solutions of the mean-field equations (Eq.(4.1), (4.2)) also give rise to damped oscillations of the opinion group size, Fig. 4.5a. Once again we find that the confidence distributions converge towards a single distribution, Fig. 4.5b. This is initially surprising. We have introduced the conservation of confidence to our model. One might consider that this

would restrict the oscillations of of the group size and the mean confidence seen in the non-conserved model. However these features of the dynamics are still present. We suggest that the features of the dynamics seen when $p > \frac{1}{2}$ continue to act in the non-conserved model because the process which drives the oscillations still occurs. This process, previously discussed in detail, Sec. 3.7, and observed in the the heuristic model, Sec. 3.8.

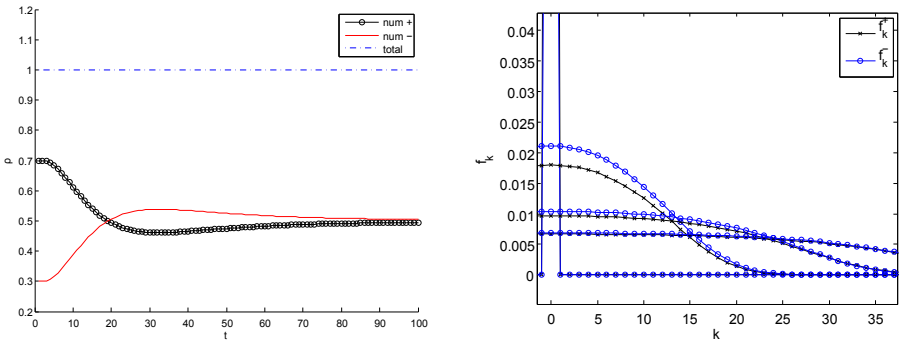

(a) ρ (b) f_k

Figure 4.5: Fully connected conserved confidence model with $p = 0.9$. (a) Group size ρ^+ (black circles), ρ^- (red line), total (blue dotted line). (b) Confidence distribution f^+ (black crosses), f^- (blue full circles) for three snapshots.

4.5.1 $p > \frac{1}{2}$, long-time scaling regime

We notice that when $p > \frac{1}{2}$ in the conserved confidence model with fully connected network we reach a state with equal distributions in the large time limit, Fig. 4.5b. This is the same model behaviour seen in the $p > \frac{1}{2}$ case of the non-conserved confidence model. Even though we have changed the interaction step of the model to include the reduction of confidence of one agent the $p > \frac{1}{2}$ model behaviour is the same. We investigate this regime by taking a scaling limit. Therefore we write $f_k^+ = f_k^- \quad \forall k$ and recall that $F_k = \sum_{j=-\infty}^{k-1} f_j$ and the boundary conditions are $f_{-\infty}(t) = 0 \quad \forall t$. Therefore the ODEs for the cumulative confidence, F_k, become

$$\begin{aligned} \frac{\partial}{\partial t} F_k = \quad & (p-1) f_{k-1} F_\infty + p f_k F_\infty \\ & + (2p-1)\left[-f_k F_k - f_{k-1} F_{k-1} + \frac{1}{2} f_k f_k + \frac{1}{2} f_{k-1} f_{k-1} \right]. \end{aligned} \tag{4.31}$$

Now we remember that $f_k = F_{k+1} - F_k$ so

$$\begin{aligned}\frac{\partial}{\partial t}F_k = \quad & (p-1)(F_k - F_{k-1})F_\infty + p(F_{k+1} - F_k)F_\infty \\ & + (2p-1)[-(F_{k+1} - F_k)F_k - (F_k - F_{k-1})F_{k-1}] \\ & + (2p-1)\left[\frac{1}{2}(F_{k+1} - F_k)f_k + \frac{1}{2}(F_k - F_{k-1})f_{k-1}\right].\end{aligned} \tag{4.32}$$

Now we let $\frac{dF}{dk} = F_{k+1} - F_k$ so that

$$\frac{\partial}{\partial t}F_k = (2p-1)\left[\frac{\partial F}{\partial k}(F_\infty - 2F) + \frac{\partial F}{\partial k}\frac{\partial F}{\partial k}\right], \tag{4.33}$$

and assume that terms of power 2 or higher in $\partial F/\partial k$ are small, so

$$\frac{\partial}{\partial t}F_k = (2p-1)\left[\frac{\partial F}{\partial k}(F_\infty - 2F)\right]. \tag{4.34}$$

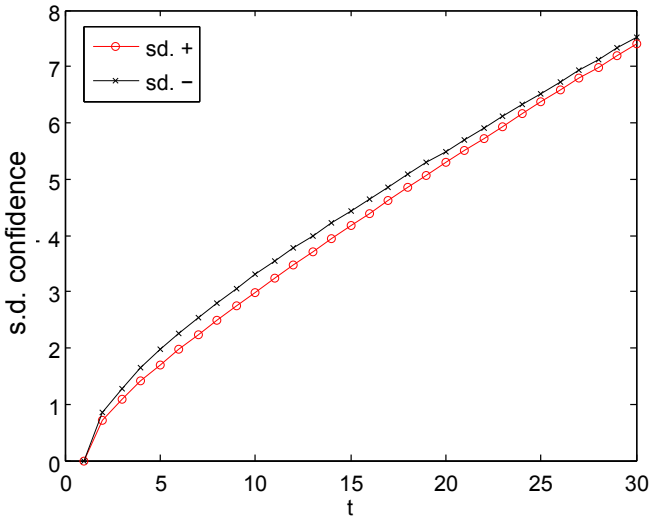

Figure 4.6: Conserved confidence model: when $p = 0.8$ the standard deviation of the confidence is linear in time.

We recall that the width of the confidence distributions increase with time, Fig. 4.5b, and we see that this increase is linear in time, Fig. 4.6, therefore we take a scaling solution with the change of variables $x = kt^{-1}$. We let

$$F(k,t) = \phi(x),$$

and $0 \leq \phi(x) \leq \rho$. Because this is the long-time solution for the $p > \frac{1}{2}$ case, and we have seen that the dynamics in the conserved confidence model converge to give $\rho^+ = \rho^- = \frac{1}{2}$, Fig. 4.5a. We therefore have the upper limit of $\phi(\infty) = \rho = \frac{1}{2}$. We use the following:

$$\frac{\partial}{\partial t} = \frac{d}{dx}\frac{dx}{dt} = -\frac{x}{t}\frac{d}{dx}, \quad \frac{\partial}{\partial k} = \frac{d}{dx}\frac{dx}{dk} = \frac{x}{k}\frac{d}{dx}.$$

Therefore the equation for $\phi(x)$ is

$$-x\phi = (2p-1)\left[\phi'(\phi(\infty) - 2\phi)\right]. \tag{4.35}$$

Using the boundary conditions $\phi(-\infty) = 0$ and $\phi(\infty) = \frac{1}{2}$ and the monotonicity of the cumulative function we find that the equation for $\phi(x)$ is

$$\phi(x) = \frac{1}{2}\left[\phi(\infty) + \frac{x}{2p-1}\right] \tag{4.36}$$

when $x_- < x < x_+$. And $\phi(x) = 0$ when $0 < x < x_-$. And $\phi(x) = 1$ when $x_+ < x$. We find that $x_- = -(p - 1/2)$ and $x_+ = p - \frac{1}{2}$ by using the boundary conditions of ϕ which are $\phi(+\infty) = \frac{1}{2}$ and $\phi(-\infty) = 0$.

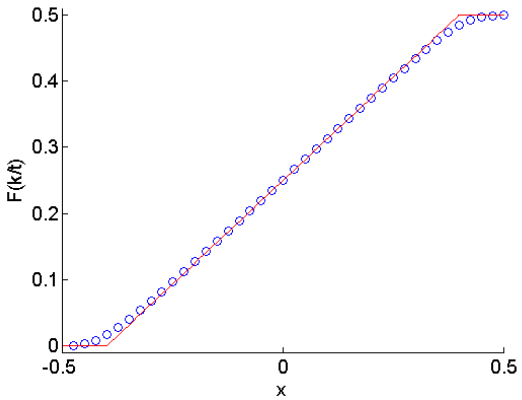

Figure 4.7: The cumulative confidence, F for $p = 0.9$ at late time, $t = 400$ (blue circles) compared to the analytical result for the long time distribution (red line). Both plotted against the confidence rescaled by time, $x = k/t$.

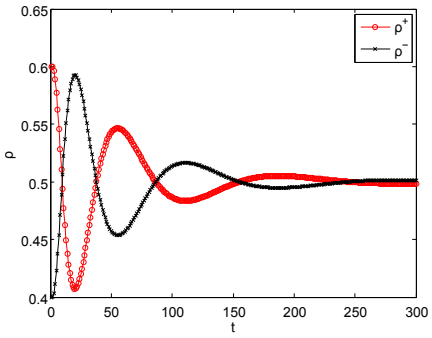

Figure 4.8: Numerical solutions of opinion group size, $\rho(t)$, from the mean-field equations (Eq.(4.1), (4.2)), when $p = 1$, and the initial conditions are all agents with zero confidence and $\rho^+(t = 0) = 0.6$.

4.6 Mean-field results $p = 1$

We find the opinion group density ρ from the numerical solution of the mean-field equations (Eq.(4.1), (4.2)) for the $p = 1$ case of the conserved confidence model, Fig. 4.8. We notice that there are damped oscillations in the opinion group size that were also present in the $p = 1$ non-conserved confidence model, Fig. 3.9b. Furthermore the oscillations in the opinion group size are stronger in the $p = 1$ conserved confidence model when compared to $p = 0.9$ conserved model, Fig. 4.5a. In the non-conserved model we found that the $p = 1$ case also gave stronger oscillations of the opinion group than the other $p > \frac{1}{2}$ cases. The consensus time of the stochastic non-conserved confidence model when $p = 1$ had a different exponent in the N dependence to the other p cases. The basis of the oscillations in the dynamics of the confidence and the group size was highlighted in the the section on the heuristic model, Sec. 3.8, and the qualitative difference in the $p = 1$ model behaviour shown. We therefore expect that the consensus time for the stochastic conserved confidence model may have a different exponent to the other $p > \frac{1}{2}$ cases. We find the mean consensus times in section Sec. 4.8

4.7 Mean-field ODEs $p < \frac{1}{2}$

We now consider the numerical solutions of the mean-field equations for the conserved model (Eq.(4.1), (4.2)) with $p < \frac{1}{2}$. Previously we found that the mean-field equations for the non-conserved model (Eq.(3.1), (3.2)) when $p < \frac{1}{2}$ showed dynamics that reach consensus for the opinion group that was in the initial majority, Fig. 3.14. To illustrate how the dynamics are different in the conserved model we plot the results for $p = 0$. Other models with p values less than 1/2 give qualita-

tively similar results so we select $p = 0$ to show the type of dynamics as this value is the lowest possible in the model.

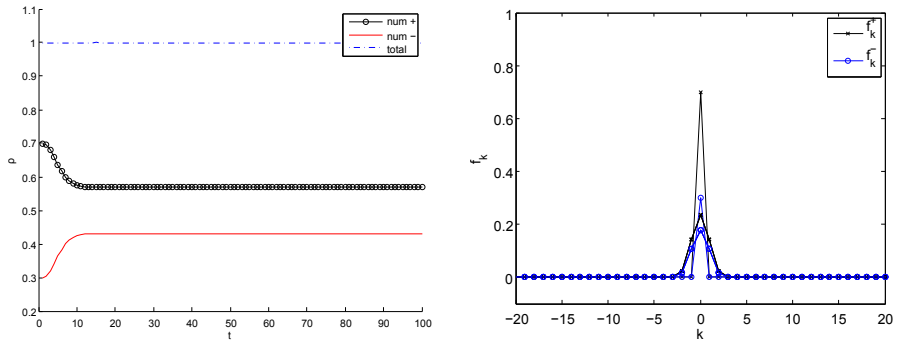

(a) ρ (b) f_k

Figure 4.9: Fully connected conserved confidence model with $p = 0$. (a) Group size ρ^+ (black circles), ρ^- (red line), total (blue dotted line). (b) Confidence distribution f^+ (black crosses), f^- (blue full circles) for three snapshots.

We find that the dynamics of the group behaviour, when $p < \frac{1}{2}$, in the conserved confidence model is different to the non-conserved confidence model. In the mean-field non-conserved model had dynamics where the system goes to the consensus state determined by the opinion of the initial majority, Fig. 3.14. Now the conserved model results, Fig. 4.9a, show dynamics of the opinion group size does not indicate movement to consensus for the initial majority. Instead the majority group reduces in size to a constant size which is not zero, not equal to the other opinion group, and also not equal to the fixed point in the non-conserved model ($\rho = 0.5$). The confidence distribution snap shots, Fig. 4.9b, show that neither distribution approaches zero, and neither do they converge to single distribution. Overall the conserved model gives very different dynamics for the opinion group size, when $p < \frac{1}{2}$, compared to the non-conserved model.

4.7.1 $p < \frac{1}{2}$ long-time confidence distribution

We consider the long-time confidence distribution of the $p < \frac{1}{2}$ case. We see that when $p < \frac{1}{2}$ the dynamics do not reach a consensus state for one population, Fig. 4.9a. The numerical solutions of the mean-field equations of the conserved confidence model (Eq.(4.1), (4.2)) with initial conditions of both groups with the same confidence value but non-equal numbers of agents, result in the two distributions of similar shape, Fig. 4.10a. The distributions are linearly scaled versions of one another, Fig. 4.10b. So we can write $f_k^+(t = \infty) = \frac{1}{c} f_k^-(t = \infty)$.

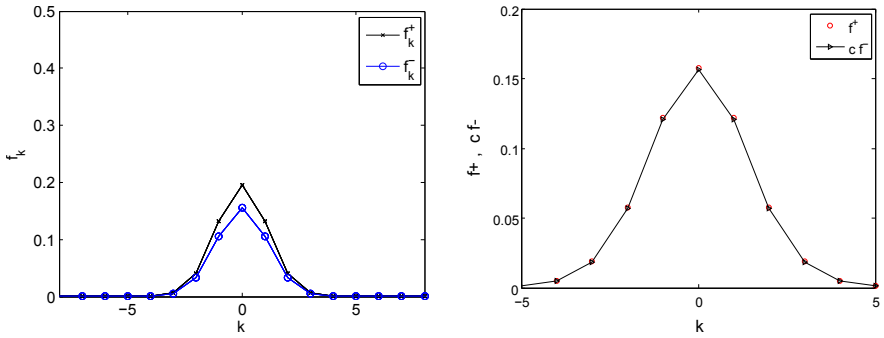

(a) f^+, f^- (b) f^+, cf^-

Figure 4.10: Fully connected conserved confidence model, numerical results of the mean-field equations (Eq.(4.1), (4.2)) with $p = 0$. The confidence distribution at a very late time $t >> 1$ ($t = 1000$). The distributions have neither reached zero, nor consensus, nor converged to the same distribution.

We substitute in $f_k^- = cf_k^+$, into Eqn. (4.1), and take the sum over confidence to find the dynamics of the cumulative confidence distribution F_k to give

$$\begin{aligned}\frac{d}{dt}F_k =& 2c\,[1/2(-f_{k-1}f_{k-1} + f_k f_k) - p(f_{k-1}F_{k-1} - f_{k-1}G_{k-1}) \\ & -p(f_k F_k - f_k G_k) - f_{k-1}G_{k-1} + f_k F_k]\,.\end{aligned} \tag{4.37}$$

4.8 Monte Carlo simulations - consensus times

We now find the mean consensus time for the stochastic version of the conserved confidence model to compare with those of Chap.3. Previously we found that the $p = \frac{1}{2}$ non-conserved model had consensus times that scaled with system size, N, the same way that the voter model does, $\tau_N \simeq N$. We found that the approach to consensus when $p < \frac{1}{2}$ was quicker and $\tau_N \simeq lnN$, Fig. 3.18. And we found that when $p = 1$ consensus time was very slow $\tau \simeq N^{1.4}$, Fig. 3.20b.

Now we find, using the same stochastic simulation method we used for the non-conserved model, that the consensus time results for the conserved model are in general different to the non-conserved model. We see that the $p = \frac{1}{2}$ model gives a mean consensus time that scale s with N the same way that the voter model does, Fig. 4.11. This is the same as the non-conserved model. We find that the $p < \frac{1}{2}$ models give different results. No longer do they give consensus times faster than the voter model, but reach consensus with time like voter model does and $\tau_N \simeq N$. We would expect that the conservation of the confidence may prevent the dynamics from being qualitatively different when $p = 1$. However the consensus time for the conserved model when $p = 1$ is the same as the non conserved model and we find

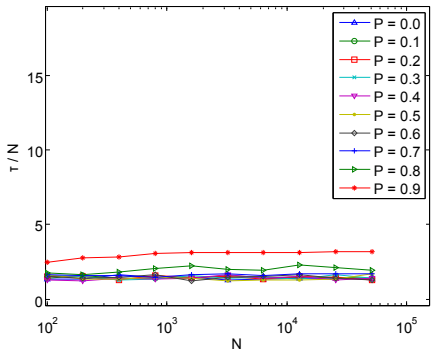

Figure 4.11: The mean consensus time, τ_N for the stochastic conserved confidence model scaled by N. Results averaged over 500 simulations. We see the same N dependence, $\tau_N \propto N$ for both $p < \frac{1}{2}$, $p = \frac{1}{2}$, and $\frac{1}{2} < p < 1$

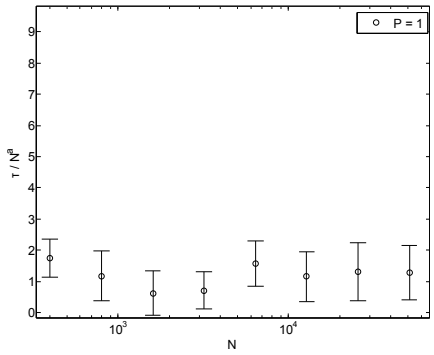

Figure 4.12: The mean consensus time, τ_N for the stochastic conserved confidence model with $p = 1$, scaled by N^a, where $a = 1.37$. Exponent found using linear least squares fitting. Results averaged over 500 simulations.

that $\tau_N \simeq N^{1.37}$, Fig. 4.12. This is less surprising when we consider that the mean-field equations for $p > \frac{1}{2}$ show the oscillation in group size. Where for the model with $p = 1$ we find that the exponent, $\tau_N \simeq N^a$, with a linear least squares fit using *Matlab*, and find that with 95 percent confidence bounds $a = 1.37(\pm 0.05)$. We find that the mean consensus time of the stochastic conserved confidence model depends on p, Fig. 4.13. The consensus time depends on p when $p > \frac{1}{2}$ and the greater p is the greater the consensus. To understand the increase in consensus time when $p > \frac{1}{2}$ we find the ensemble average of the stochastic model in the next section.

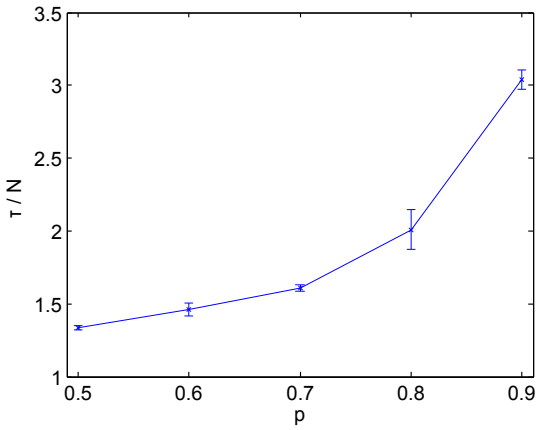

Figure 4.13: The mean consensus time of the stochastic conserved confidence model, on fully connected network, when $N = 6400$, for 1000 simulations, for a range of $\frac{1}{2} < p < 1$.

4.9 Ensemble average of stochastic model results compared to mean-field solutions

We find the dynamics of the stochastic results for the conserved model, by averaging over simulations. We compare these with the mean-field equations (Eq.(4.1), (4.2)) for models with $p = \frac{1}{2}$, $p > \frac{1}{2}$ and $p < \frac{1}{2}$. We inspect the dynamics of the opinion group size, ρ to provide understanding of the consensus time results found in the previous section, Sec. 4.8. We also discuss the confidence distributions, obtained from the numerical results of the mean-field solutions, to help explain the dynamics of the opinion group size $\rho^{\pm}(t)$.

4.9.1 $p = \frac{1}{2}$ conserved model stochastic dynamics

We find that the $p = \frac{1}{2}$ model has ensemble average dynamics of the groups size and the mean confidence of the opinion groups seen in the numerical solutions of the mean-field equations (Eq.(4.1), (4.2)) Fig. 4.3b and Fig. 4.3a respectively. We see that the confidence distribution has a shape which is symmetric about the initial condition of zero confidence, Fig. 4.14a.

4.9.2 $p > \frac{1}{2}$ conserved model stochastic dynamics

We see that the dynamics of the opinion group size given by the ensemble average for the stochastic model simulation results are the same as the numerical results of the mean-field equations (Eq.(4.1), (4.2)) for $p = 0.9$ and $p = 1$, Fig. 4.15a. We see there is agreement even when the number of simulations used in the ensemble

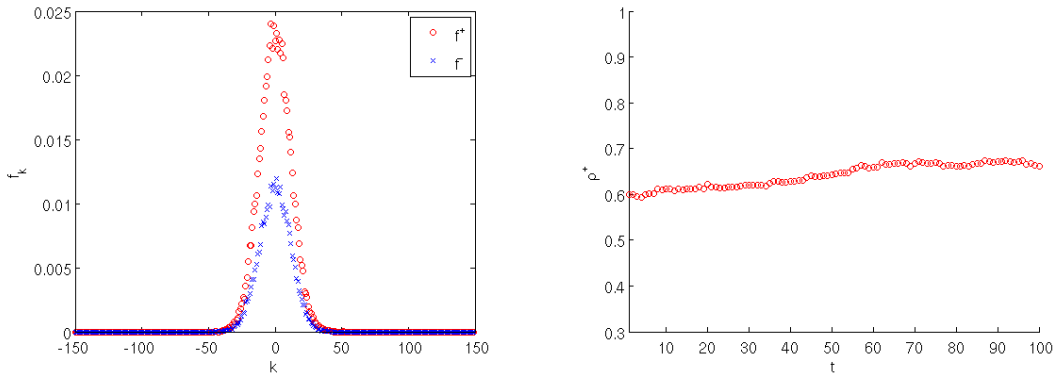

(a) f_k (b) $n^+/N = \rho^+$

Figure 4.14: Conserved confidence model: when $p = \frac{1}{2}$ the average distribution of confidence (over 10 simulations) at a late time (t=10) is centred about zero confidence. And the mean dynamics of the group size (over 10 simulations), ρ, are flat in agreement with the mean-field voter model, Fig. 4.3a.

average is relatively low (25). The discrepancy at later times is small and purely a result of the low number of simulations. That we have agreement between these two results in the conserved model is to be expected because we saw agreement between the ensemble average of simulation results and the numerical results of the mean-field equations (Eq.(3.1), (3.2)) for the non-conserved model, Fig. 3.15a.

The $\frac{1}{2} < p < 1$ case, Fig. 4.15a, has damped oscillations in, ρ, opinion group size and we have shown this case reaches an equal coexistence state, Sec. 4.5.1. We also see that there is non-monotonic behaviour in the mean confidence μ, Fig. 4.2c. The total confidence is constant as expected in this model with conserved confidence for each interaction consequence, one agent increase their confidence by one and the other agent in the interaction reduces their confidence by one.

Furthermore there is stronger oscillations of ρ seen in the $p = 1$ model, Fig. 4.15b than the $p = 0.9$ case. There are also stronger oscillations in the mean confidence for $p = 1$, Fig. 4.2d. The qualitative result of stronger ρ oscillations was also seen in the non-conserved confidence model, Fig. 3.16b. The model behaviour that results in the size of the oscillations in the opinion group size that are greater when p is closer to $p = 1$, explains why the pre-factor of the consensus time increases with p (when $p > \frac{1}{2}$), Fig. 4.13. We now explain that behaviour qualitatively by examining the confidence distribution and referring to the analysis of the heuristic model for the non-conserved case 3.8. We have seen that a heuristic model of the non-conserved confidence model captures the dynamics for both the $p < \frac{1}{2}$ case and the $p > \frac{1}{2}$. We saw that the mean confidence, and therefore the maximum confidence,

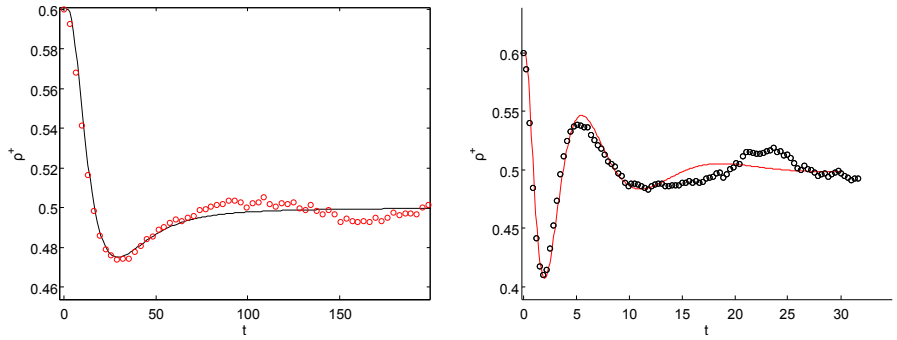

(a) (b) $n^+/N = \rho$

Figure 4.15: Conserved confidence model: when $p = 1$ the proportion of agents with opinion +, ρ^+, averaged over 25 simulations (circles) follow damped oscillations and follow the dynamics of the mean-field equations (Eq.(4.1), (4.2)) for the conserved model, for (a) $p = 0.9$, mean-field equations (black line) and (b) $p = 1$, mean-field equations (red line).

have dynamics coupled with the opinion group size that give rise to oscillations in both when $p = 1$. For the conserved model we now highlight the changes in the confidence distribution which allow this model to also create dynamics with oscillating opinion group and mean confidence.

We plot the confidence distribution very soon after the start of the dynamics, from the numerical solutions of the mean-field equations (Eq.(4.1), (4.2)), for the case with $p = 1$ and all agents start with zero confidence. Initially ρ^+ is 0.6, Fig. 4.16a. We see that as the dynamics progress the proportion of agents with close to maximum confidence of the minority group has increased to be greater than the majority group, Fig. 4.16b and zoomed in Fig. 4.16c. The ability for the minority group to increase their mean confidence faster than the majority group was highlighted in the heuristic model for the non-conserved model Sec. 3.8. The greater proportion of agents with near maximum confidence in the minority group are zealot-like. They are very likely to win their interactions with the (large) proportion of lower confident agents from the majority group when $\frac{1}{2} < p < 1$ and will always win their interactions with those lower confident agents when $p = 1$. These interactions will now dominate the dynamics and create growth in the size of the minority group (i.e. ρ^- increases). This is the reason for the start of the oscillation in the opinion group size. The increase in the minority group will be faster when p is closer to 1, and fastest when $p = 1$. When the minority group has grown larger than the old majority the process repeats itself with the new minority increasing their mean confidence and gaining a proportion of the most confident agents. This process repeats with the distributions becoming ever more similar, Fig. 4.16d, until the

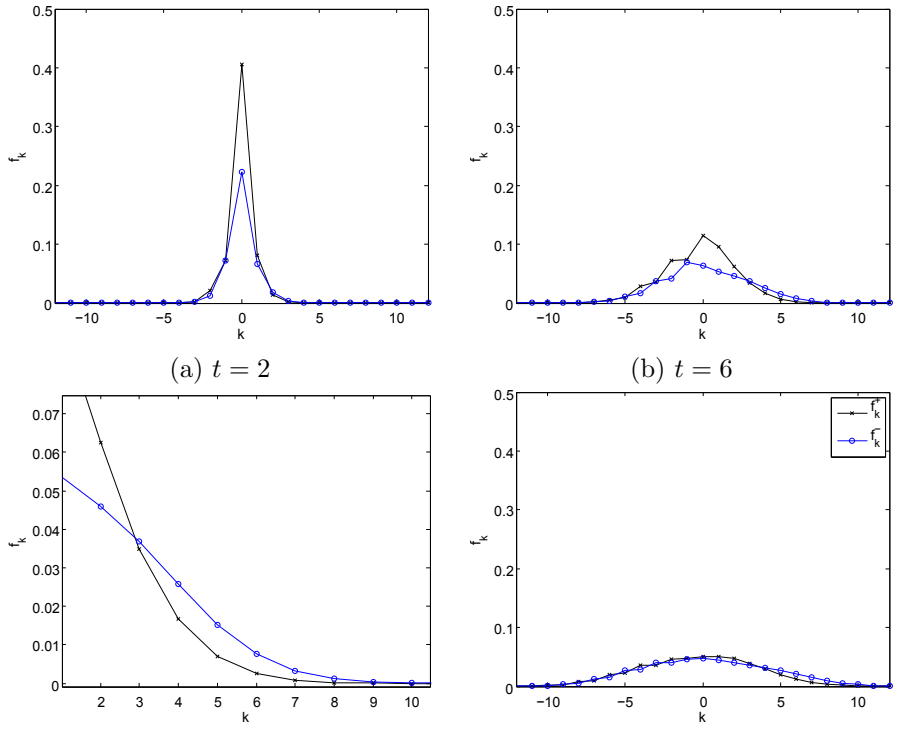

(a) $t = 2$ (b) $t = 6$

(c) $t = 6$ zoom (d) $t = 10$

Figure 4.16: Confidence distributions, f_k, of the conserved confidence model, with $p = 1$, numerical solutions of the mean-field ODEs (Eq.(4.1), (4.2)) (a) $t = 2$ and (b) $t = 6$ (c) $t = 6$ zoomed in (d) $t = 10$.

equal coexistence fixed point is reached. The key difference between $p = 1$ and $p = 0.9$ is that in the individual interactions the agents with more confidence will always win their interactions in the $p = 1$ case, but only with high probability in the $p = 0.9$ model. This is the same process seen in the non-conserved model and the heuristic model of the non-conserved case. Although a globally conserved confidence means that total confidence is constant it does not prevent the maximum confidence for the minority exceeding that of the majority and facilitating the oscillations in opinion group size.

4.9.3 $p < \frac{1}{2}$ conserved model stochastic dynamics

We find that the $p < \frac{1}{2}$ model has ensemble average opinion group size ρ dynamics, Fig. 4.17, that are the same as the mean-field dynamics for $p < \frac{1}{2}$, Fig. 4.9a. The opinion group size of the majority decreases and then levels off. This explains the consensus time result of $\tau_N \simeq N$ for $p < \frac{1}{2}$ in the conserved model. There is no fast movement in the majority to consensus (as seen in the non-conserved confidence model when $p < \frac{1}{2}$ Fig. 3.14) nor does it approach the equal coexistence state (as seen in the non-conserved Fig. 3.15a and conserved model Fig. 4.5a when $p > \frac{1}{2}$, but instead it approaches a non-equal coexistence state. So when we consider the stochastic model we see that the in the conserved model, unlike the non-conserved model, the system is not driven to consensus by deterministic dynamics, so we do not see a $\tau_N \simeq lnN$ fast consensus. Rather the system relies on fluctuations to get out of the unequal coexistence state, preferred by the mean-field dynamics, to reach consensus state. Hence it is plausible that the $\tau_N \simeq lnN$ result seen in the non-conserved model is not shared by the conversed model.

We now discuss the result that for $p < \frac{1}{2}$ the consensus time is $\tau_N \simeq N$. We will refer to the mean-field equation results to clarify the details of the discussion. We are explaining the mean consensus time of the stochastic model using the results from the mean-field equations (Eq.(4.1), (4.2)). This is only possible because we have shown that the ensemble average of the stochastic model satisfy the mean-field equations (for both this model and the non-conserved model) on fully connected networks. We have identified that the opinion group dynamics do not go to consensus. Nor do they go to the equal coexistence state in the non-conserved model (when $p > \frac{1}{2}$). Instead the move towards a new fixed point between the two, Fig. 4.17. Also the specific dynamics in the mean confidence are different in the $p < \frac{1}{2}$ case, Fig 4.2a, as the majority group has a mean confidence greater than the minority group, in contrast to the $p > \frac{1}{2}$ case.

Both the opinion group of these results and the consensus times are explained

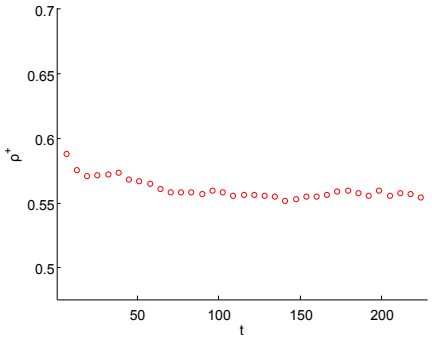

Figure 4.17: Ensemble average of the dynamics of opinion group size, ρ of the conserved confidence model, when $p = 0.2$ (over 50 simulations), $\rho = n^+/N$. Initial conditions are opinion group + with 60 percent of the population, $N = 6400$. We see that the ensemble average opinion group size agrees with the numerical solutions of the mean-field equations (Eq.(4.1), (4.2)) for $p < \frac{1}{2}$, Fig. 4.9a. Furthermore it is completely different to the non-conserved model dynamics which approach consensus quickly Fig. 3.14.

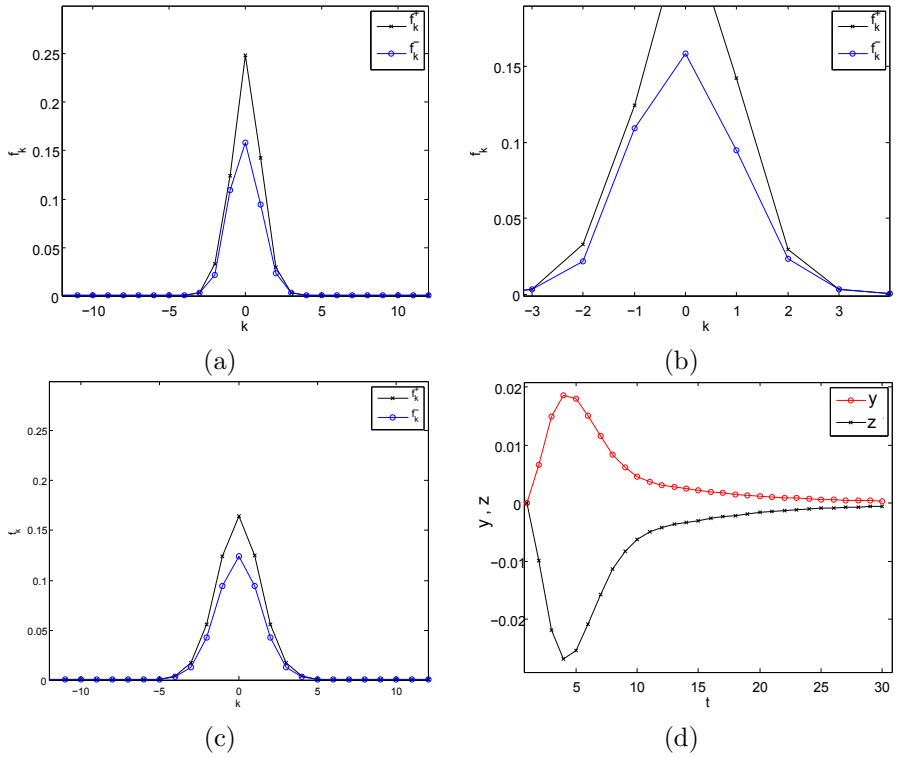

Figure 4.18: Confidence distributions, f_k, of the conserved confidence model, with $p = 0.2$, numerical solutions of the mean-field ODEs (Eq.(4.1), (4.2)) (a) $t = 5$ and (b) $t = 5$ zoomed in (c) $t = 50$. (d) the mean confidence per agent, $\mu^+/\rho^+(t)$ (red dots) and $\mu^-/\rho^-(t)$ (black dots).

by the confidence distributions created by the conserved model dynamics when $p < \frac{1}{2}$. We see that from the initial conditions of all agents with zero confidence and a majority (60 percent) of agents with opinion + the minority distribution is quickly (at $t = 6$) non-symmetric, Fig. 4.18a. This is more transparently seen in the zoomed in section of, Fig. 4.18b. What has occurred is that the minority group have interacted at a rate (relative to their group size) faster than the majority group. The agents which have been persuaded to join their group − from the majority + lose confidence in the interaction. These new converts are the agents with confidence $k = -1$ that make the minority group non-symmetric about $k = 0$. The dynamics mean that those with less confidence are more likely to win conversations so that the minority group continues to convert agents form the majority group. We also notice that the minority group has agents with minimum confidence which are not the agents with the most negative confidence, Fig. 4.18a. The majority group continues to have agents with the most negative confidence. This explains why the opinion group size does not oscillate, as seen in the non-conserved model. There are no 'negative-confidence-zealot-like' agents with the most negative confidence, analogous to the zealot-like agents (with largest positive confidence). Therefore there is no mechanism in the dynamics for the minority group to rapidly convert enough of the majority group to turn itself into the new majority. Instead the minority group stays the minority and the dynamics reach a new equilibrium where the original majority has fewer agents than in the initial conditions but is still the majority group, as seen in the long-time snapshot Fig. 4.18c. We describe this as a non-equal coexistence state, because the dynamics have not reached a consensus state and not reached the equal coexistence state reached when $p > \frac{1}{2}$ in both the conserved and non-conserved confidence models.

4.10 Conclusions

We defined the conserved confidence model which is an adaption of the non-conserved confidence model studied in Chap. 3. We found numerical solutions of the mean-field equations (Eq.(4.1), (4.2)) and the average consensus time to find the effect that change in the model definition has on the consensus time. The numerical solutions of the mean-field equations (Eq.(4.1), (4.2)) reveal that the model reaches a non-equal coexistence state when $p < \frac{1}{2}$, Fig. 4.9a. This is different to the non-conserved model which reaches consensus quickly, Fig. 3.14. The dynamics of the opinion group size of the conserved model with $\frac{1}{2} < p < 1$, Fig. 4.5a, were qualitatively the same as the non-conserved model, Fig. 3.9a. In both models an equal coexistence

state is reached. The opinion group size dynamics of the model with $p = 1$ was also showed similarities between the two models because both the conserved model and the non-conserved model have the strongest oscillations at this p value.

The confidence distribution obtained from the numerical solutions of the mean-field equations (Eq.(4.1), (4.2)) when $p > \frac{1}{2}$ showed the same behaviour in the conserved model, Fig. 4.16b, as the non-conserved model, Sec. 3.7. The minority group attained a proportion of agents with confidence higher than any other agent so became zealot-like. The minority were then able to quickly persuade many agents from the majority and this explains the oscillations in the opinion group size. Therefore the mean consensus time obtained from Monte Carlo simulations of the stochastic conserved model when $\frac{1}{2} < p < 1$ had the same N dependence as the non-conserved model and when $p = 1$ there was a slower exponent to the N dependence, so $\tau_N \simeq N^a$ where $a = 1.37$. This exponent was different to the non-conserved model because the details of the two models are different to the dynamics are only qualitatively the same.

The consensus time when $p < \frac{1}{2}$ for the conserved model was $\tau_N \simeq N$, very different to the fast, $\tau \simeq lnN$, consensus in the non-conserved model. The presence of the the non-equal coexistence state in the mean-field version of the model highlights why the dynamics are different. We inspect the confidence distributions and the mean confidence, Fig. 4.18a, to identify differences in the dynamics compared to the non-conserved model, Sec. 3.7. We find that in the conserved model, Fig. 4.18d, there is a non-monotonic change in the average confidence per agent in the opinion groups, reflecting the fact that the proportion of agents with lower k increases faster for the minority group. These lower k–value agents act a little like strong confidence agents, because $p < \frac{1}{2}$, and they convert agents from the majority. Hence we see the majority group lose agents and the minority group gain, Fig. 4.9a. Previously we saw how the generation of zealot-like agents with confidence higher than any other agents in the $p > \frac{1}{2}$ non-conserved model drove the opinion group size to oscillate, Sec. 3.7. However the behaviour in the $p < \frac{1}{2}$ conserved confidence model is different and the populations stabilise at a non-equal coexistence state because no agents from the minority are able to achieve a k–value more extreme (i.e. lower) than any other agent. Therefore the $p < \frac{1}{2}$ conserved model captures behaviours of both regimes of the non-conserved model. There is oscillatory behaviour of the mean confidence and the opinion group size (as seen in $p > \frac{1}{2}$ non-conserved model) but there is also the stabilisation of the confidence distribution (as seen in the $p < \frac{1}{2}$ non-conserved model). This is the reason why the $p < \frac{1}{2}$ conserved model reaches a non-equal coexistence state in the mean-field model and that explains the $\tau_N \simeq N$

consensus time. An extension to this work is to define and solve a heuristic model of the conserved confidence model to identify the strength of the stability of the non-equal coexistence state for different p values.

Chapter 5

Non-conserved confidence model on a regular lattice

5.1 Introduction

In this chapter we make a numerical study of whether the voter model with non-conserved confidence exhibits different behaviour on the spatial network to the fully connected network. One would expect that as dimension increases the model would exhibit behaviour which is more like that found with the mean-field model. Therefore we investigate both the 2d and 3d regular lattice results previously found for the non-conserved confidence model on the fully connected network. We know that for $p = \frac{1}{2}$ our model should behave like the voter model because the opinion and confidence dynamics are decoupled by the specific choice of p. Therefore we expect that the $p = \frac{1}{2}$ 3d model will give $\tau \simeq N$ and 2d model, $\tau \simeq NlnN$. Therefore, at least for $p = \frac{1}{2}$, we expect that the critical dimension of the voter model with non-conserved confidence is 2d, and that the spatial model in 3d has a consensus time which scales in the same way as the complete graph. The purpose of the numerical investigations in this chapter is to decide whether this remains true for $p \neq \frac{1}{2}$ where the complete graph predicts very different behaviour for $p > \frac{1}{2}$ and $p < \frac{1}{2}$.

We find that the $p < \frac{1}{2}$ model has different results on the 2d regular lattice to the completely connected graph. The fully connected model results indicated that the consensus time was relatively fast for this parameter choice, Fig. 3.18. We find that on a spatial network the consensus times are now slow. While the $p > \frac{1}{2}$ model has results which are not the same on 2d, they are increasingly similar in 3d to the fully connected network results. This suggests that as the dimension increases the $p > \frac{1}{2}$ model becomes more similar to the fully connected model. Based on our

findings, we conjecture that the voter model with non-conserved confidence has a critical dimension that is 3d when $p > \frac{1}{2}$.

5.2 Spatial Model definition

The model is defined in the previous Chap. 3. There is one alteration to the model in this Chapter: we place the agents on the vertices of a regular lattice, with periodic boundary conditions. Therefore each agent has the same number of neighbours in each case. For example in the 2d model each agent has exactly four neighbours.

Recent work on spatial adapted voter models has shown that both models with a small number of heterogeneous agents (through the inclusion of an intermediate state) [11] [16] and a model with the inclusion of memory that creates effective intermediate states [15] result in coarsening dynamics characterised by effective surface tension This is different to the original voter model coarsening process which is purely driven by interfacial noise. We seek to compare our non-conserved spatial model with the non-conserved model on a fully connected network, Chap. 3, therefore do not undertake the same analysis recently made in this literature.

5.3 Monte Carlo simulations of nonconserved model in 2d

We simulate the non-conserved confidence model on a 2d regular lattice with periodic boundary conditions. The initial conditions for each simulation are that all agents have zero confidence and each agent has an equal probability of starting with opinion + or opinion -, so on average half the agents with opinion + and half with opinion - distributed randomly through the 2d spatial structure. We simulate 1000 times to find the mean consensus time. We follow the method for simulating the stochastic model as described in the section on Monte Carlo simulations 3.5.

5.3.1 Monte Carlo simulations in 2d $p = \frac{1}{2}$

The mean consensus time for the voter model on a regular 2d lattice has been shown to be $\tau_n \simeq NlnN$, [14]. Therefore we compare our results to this result. We plot the mean consensus time for our non-conserved confidence model with $p = \frac{1}{2}$ divided by the appropriate scale for the expected result, $NlnN$, Fig. 5.1. We have scaled the mean stochastic results for our model by the expected result, so expect to find a straight line for the range of population sizes (N) if the results agree. We find that there is good agreement between our mean simulation times and the expected result,

Fig. 5.1. We plot a comparison of the mean consensus time results when scaled by N and by $NlnN$ in order to show the extent to which logarithmic corrections are visible in our simulations of the model on 2d. We notice that the result scaled by $NlnN$ gives us a result which agrees with the original voter model, and reflect that if this were not the case then the $p > \frac{1}{2}$ consensus time results for the 2d model would be much more tricky to investigate. We see that the snapshot of a single simulation shows a pattern of agents with the same opinion that has a very coarse boundary Fig. 5.2. This is typical of the behaviour of the voter model on 2d.

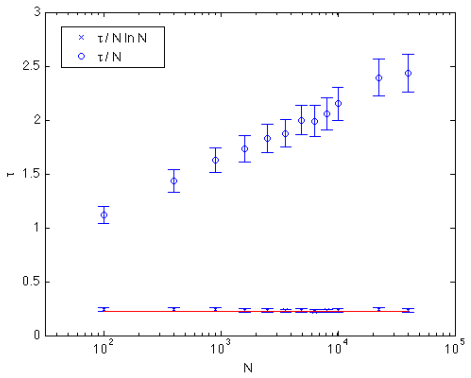

Figure 5.1: Nonconserved confidence: We see that, as expected, the $p = \frac{1}{2}$ model gives mean consensus times, on the 2d lattice, that scale like $NlnN$. This is in agreement with the result for the voter model in 2 dimensions and agrees with the constant also. Blue crosses (x) are mean consensus time for 1000 simulations, blue error bars are 3 standard error (SEM) and the red line is $(2/\pi)(ln(2))$ the analytical constant for 2d voter model.

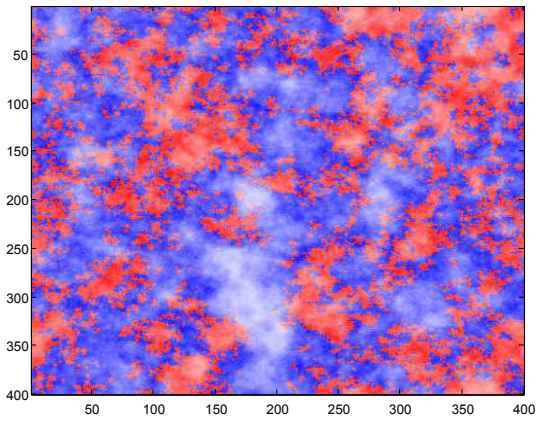

Figure 5.2: Snapshot of a single simulation of the non-conserved confidence model on a 2d square lattice, with $p = \frac{1}{2}$ (time $t = 1000$). Opinion group + (red) and − (blue) with confidence k (increasing darkness of colour) displayed. Random initial conditions equal numbers in each opinion group and of all agents with zero confidence and $N = 160000$.

We also consider the dynamics of the Monte Carlo results and compare these with the dynamics of the fully connected model results. We see that ensemble of simulations show that the dynamics of the proportion of agents with opinion + is unchanging, Fig. 5.3a. This is the same as the result for the fully connected model (mean-field result) Fig. 3.9a. Although this result is trivial, because we know the average magnetisation is conserved in any dimension when $p = \frac{1}{2}$, it is instructive to find this result because we have shown that even the mean-field equations (Eq.(3.1), (3.2)) exhibit non-trivial dynamics for $p \neq \frac{1}{2}$ where the magnetisation is not conserved as shown in the $\rho(t)$ dynamics, Fig. 3.14 and Fig. 3.15a).

We also find the the mean confidence increases linearly, Fig. 5.3b, and the confidence distribution drifts with an increase in confidence and has a width that increases, Fig. 5.3c. This is comparable with the fully connected result that $p = \frac{1}{2}$ model resulted in linear mean confidence, Fig. 3.4a, and confidence distribution followed the dynamics of a drift with diffusion, Fig. 3.4c.

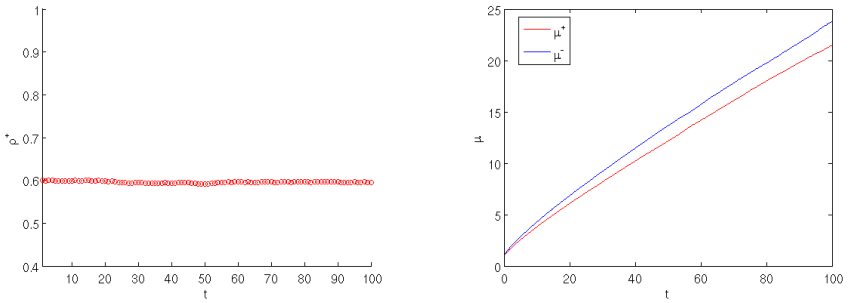

(a) $\rho^+(t)$ (b) $\mu(t)$

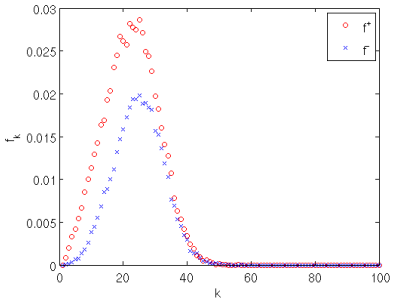

(c) f_k at $t = 100$

Figure 5.3: Ensemble average of the stochastic non-conserved confidence model simulations with $p = \frac{1}{2}$ on 2d. (a) $\rho^+(t)$ opinion group size. (b) $\mu(t)$ mean confidence. (c) ensemble f_k confidence distribution, of 10 simulations, at a late time ($t = 100$).

5.3.2 Monte Carlo simulations in 2d $p < \frac{1}{2}$

We find that when $p < \frac{1}{2}$ there is a different result to the fully connected network. Mean consensus time in the fully connected model were relatively fast and $\tau \simeq lnN$.

We now consider the model of non-conserved confidence when $p < \frac{1}{2}$ on a regular 2d lattice. In this case the less confident agents are more likely to persuade their neighbours. We found the mean consensus time for the same model on a fully connected network and noticed that the dependence on the population size was qualitatively different to the same result for the voter model, Fig. 3.18. Consensus was quicker in the fully connected model with $0 \leq p < \frac{1}{2}$ than the voter model. Now we find the mean consensus time when the $p < \frac{1}{2}$ model is on a regular 2d lattice with periodic boundary conditions and initial conditions of all agents with zero confidence and each agent equally likely to start with opinion + or opinion -. We find that the consensus time is now much slower, for example when $p = 0.2$ the mean consensus time dependence on population size N is slower than $\tau \simeq N$ Fig. 5.4a. The difference in the consensus times between the $p = 0.2$ and the $p = \frac{1}{2}$ models (both on 2d) are shown in Fig. 5.4b where we see that the model with lower

p has a much slower consensus time for all but the smallest population size where boundary effects will play a part (the periodic boundary conditions mean that an island of one opinion the length of the system size will help the dynamics reach consensus more quickly).

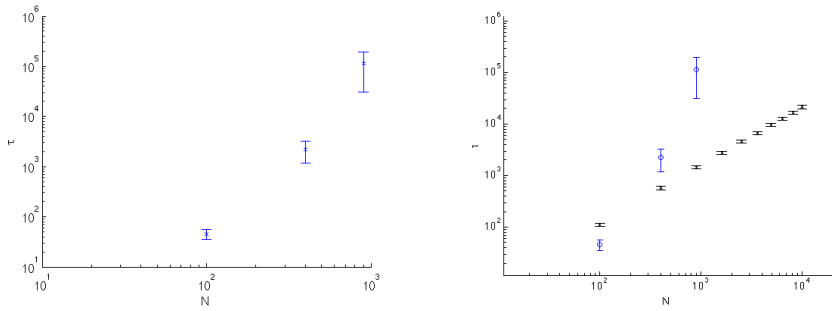

(a) (b)

Figure 5.4: Mean consensus time, τ_N, for different population sizes N for the non-conserved confidence stochastic model, for 1000 simulations, with $p = 0.2$, simulated on a 2d square lattice. (a) $p = 0.2$. (b) $p = \frac{1}{2}$ (black dot) plotted for comparison with $p = 0.2$ (blue circle) results. Initial conditions of zero confidence and equal numbers of agents with opinion + and opinion −. Error bars are 3 standard error (SEM).

We find the ensemble average of the stochastic model dynamics, Fig. 5.5a, move towards consensus but do not reach consensus quickly as seen in the mean-field equation (Eq.(3.1), (3.2)) results for the fully connected model, Fig. 3.14. We identify regions that look like islands in the spatial model simulation, Fig. 5.5b

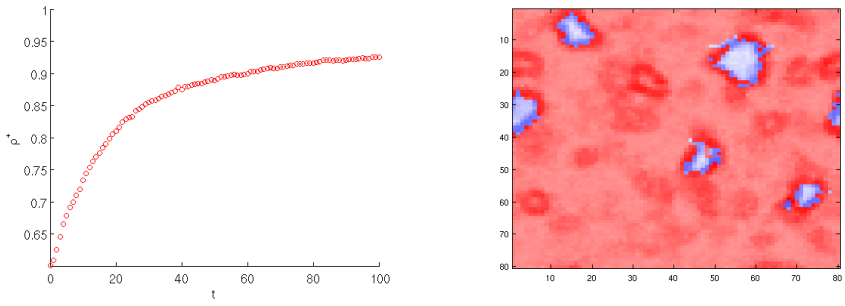

(a) $\rho^+(t)$ (b) snapshot at $t = 100$

Figure 5.5: Non-conserved confidence stochastic model on 2d square lattice, with $p = 0.2$. (a) Ensemble average $\rho^+(t)$ from 5 simulations. (b) Snapshot of confidence and opinion state at late time $t = 100$ (opinion + red, − blue and colour intensity corresponds to confidence. Initial conditions $\rho^+(t = 0) = (0.6)N$, where $N = 6400$.

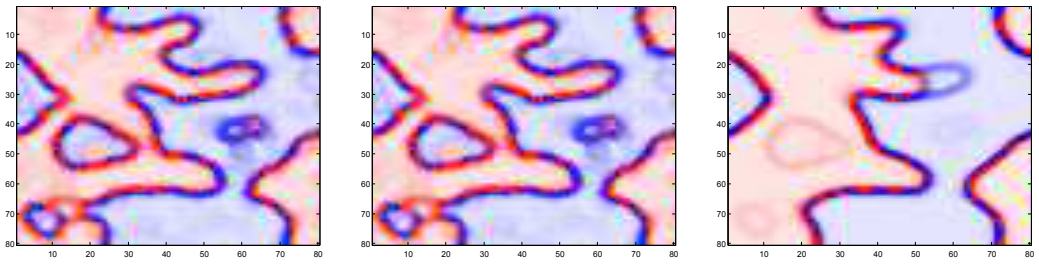

(a) $t = 180$. (b) $t = 200$, (c) $t = 350$

Figure 5.6: Non-conserved confidence stochastic model on 2d square lattice, with $p = 0.2$. Snapshots of confidence and opinion state at times (a) $t = 180$, (b) $t = 200$, (c) $t = 350$, (opinion + red, − blue and colour intensity corresponds to confidence. Initial conditions $\rho^+(t = 0) = (0.5)N$, where $N = 6400$.

We now consider the regions present in the nonconserved 2d model, by obtaining snapshots of a single simulation with initial conditions of all agents with zero confidence and exactly half the agents with opinion +, Fig. 5.6. We plot the group and confidence information at a single snapshot for a single simulation. Group + is red and group - is blue. The greater the strength of the colour the more confidence an agent has. The simulation is for a model with $p = 0.2$, $N = 6400$ are taken at three times through the simulation. We notice in Fig. 5.6a that there are regions of low confidence (light colour) separated by boundaries of high confidence (dark colour). The boundary regions are adjacent to the low region of the same colour, e.g. red (opinion, opinion +). These regions of low confidence are relatively stable. They remain in the state for a relatively long time compared to the speed of dynamics that initially occur in the simulations where the spatial structures are formed from the random initial conditions. It takes a large fluctuation in the opinions of the agents for the regions to change. We see an example of a region changing colour (opinion) in the three figures which show increasingly late time snapshots, Fig.s 5.6a, 5.6b, 5.6c. The regions are a group of agents of the same opinion with low confidence surrounded by borders of high confidence. The borders are next to to regions of the same opinion type. So a region of low confidence of opinion group + (red) is surrounded by a high confidence band which is adjacent to a high confidence band of opinion − (blue). That − band is next to a region of − agents of low confidence. The regions of low confidence are relatively stable because of the choice of p, i.e. they are less likely to change their opinion in individual interactions. Therefore the spatial structure helps prevent the dynamics reach a fast consensus observed in the fully connected model. The effect of the presence of these structures is inherently spatial and has no analogue in the fully connected model.

5.3.3 Monte Carlo simulations in 2d $\frac{1}{2} < p$

We have shown that $p = \frac{1}{2}$ model mean consensus times are the same as the comparable result for the voter model. We now test whether the $p = 0.6$ mean consensus time also follow a $NlnN$ result. We see that the mean consensus time for the $p = 0.6$ model scales like $NlnN$ but with a different pre-factor to the $p = \frac{1}{2}$ model Fig. 5.7. We see that a $NlnN$ is a much better scaling than N even when p is greater, for example $p = 0.7$, Fig. 5.8.

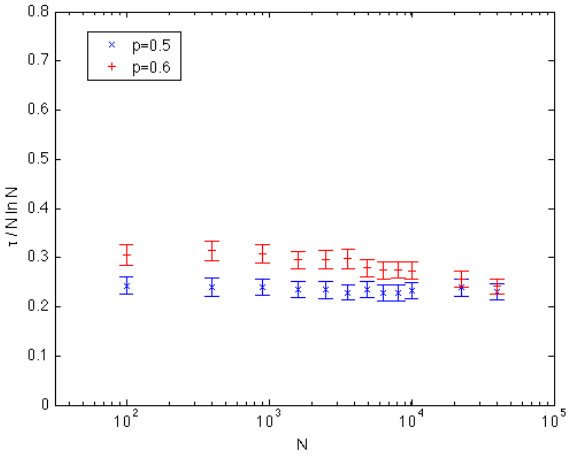

Figure 5.7: Mean consensus time τ_N scaled by $NlnN$ of the non-conserved confidence model on 2d with $p = 0.6$ (red +), $p = \frac{1}{2}$ (blue x) for 1000 simulations. Error bars 3 standard error (SEM).

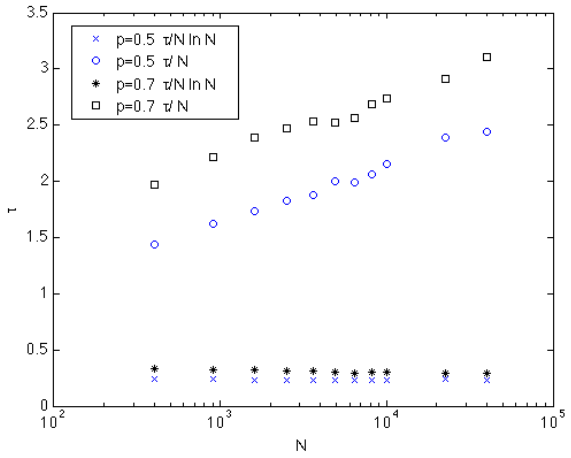

Figure 5.8: Mean consensus time τ_N, for the non-conserved confidence model, plotted scaled by N for $p = \frac{1}{2}$ (blue circle) and $p = 0.7$ (black square) and also scaled by $NlnN$ for $p = \frac{1}{2}$ (blue cross) and $p = 0.7$ (black star). We see that the $p = 0.7$ (black) model gives mean consensus times, on the 2d lattice, that scale in a way which is not the same as N. The result for the $p = \frac{1}{2}$ (blue) model is shown for reference.

While numerics cannot definitively establish the true scaling, particularly when logarithms are involved, the numerical evidence is strongly suggestive of an $NlnN$ scaling for $p > \frac{1}{2}$, Fig. 5.7, but this becomes less convincing as p approaches 1, i.e. $p = 1$ in Fig. 5.9a. See later work for the model behaviour at $p = 1$, see Sec.5.3.4. We also identify that in Fig. 5.9b increasing the p value increase the consensus time. This is a similar behaviour to the one seen in the fully connected model.

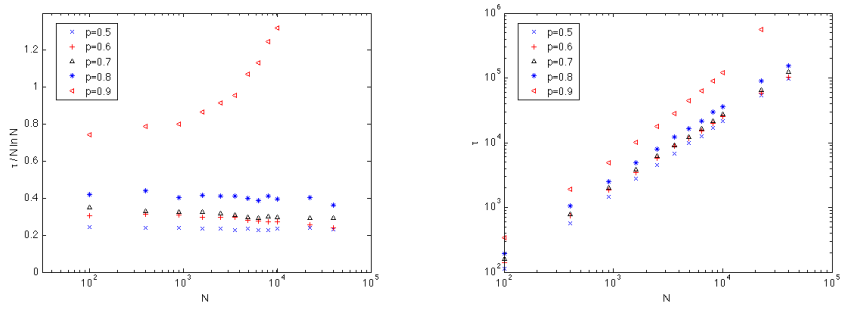

(a) τ scaled by $NlnN$ (b) τ

Figure 5.9: Mean consensus time τ_N, for the non-conserved confidence model on the 2d lattice, (a) τ_N scaled by $NlnN$ for a range of p values, (b) τ_N for the same range of p values.

We explore why the result for consensus time should be similar to the voter model, when $\frac{1}{2} < p < 1$, by illustrating a single simulation with + agents shown as red and - agents shown as blue. The stronger the colour displayed the greater the relative confidence at that time. Colour strength is not an absolute measure because over time the confidence values increase, and it is the relative confidence which determines the probability of which agent will be persuasive in the individual interactions. We plot the group and confidence information for a single time in a single simulation for $p = 0.9$ at times far into the simulation, but not close to consensus, when $t = 900$, Fig. 5.10 (when $N = 1000$ and initial conditions were all agents with zero confidence and each agent randomly allocated to group + (red) or group - (blue)).

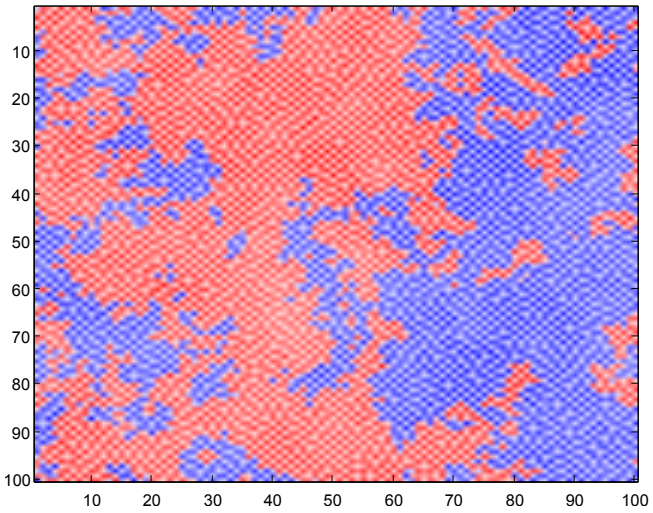

Figure 5.10: Illustration of the state at a snapshot, $t = 900$, where agents in group + are red and agents in group - are blue. The strength of the colour is the agent's relative confidence. The model is the non-conserved confidence model with $p = 0.9$, on a regular 2d lattice with periodic boundary conditions with $N = 1000$. Initial conditions were all agents with zero confidence and each agent randomly allocated to group + (red) or group - (blue).

We find that when $p > \frac{1}{2}$ there is a chequer board effect in the confidence levels of the agents. We notice two aspects of the snapshot of $p = 0.9$ on 2d, Fig. 5.10 that: there are regions of all blue (opinion -) and regions of all red (opinion +) agents; and there is pattern of alternate high and low confidence, which locally looks like a chequerboard. We consider the local dynamics. In this model, where $p > \frac{1}{2}$ the interactions are such that a more confident agent will persuade those around them (their four neighbours). As a consequence of this a confident agent (for example

red, i.e. group +) will persuade the four neighbours around them over time and increase their own confidence at the same time. As a result a small region of red agents grows. However the agents they persuaded did not gain confidence so the region of red agents also has agents with more confidence each with four neighbours with lower confidence, Fig. 5.10. There is a finite probability, $1 - p$, that the less confident agent will win the interactions so it is on average that the more confident agents are more persuasive when $p > \frac{1}{2}$.

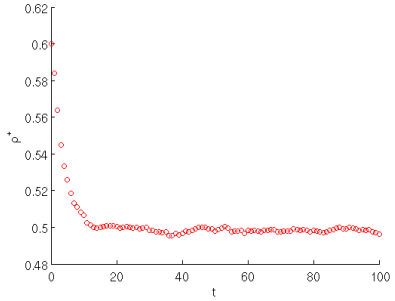

Figure 5.11: Ensemble average of $\rho^+(t)$ for the $p = 0.9$ model on 2d lattice, for simulations with initial conditions of zero confidence and $\rho^+(t = 0) = 0.6N$, $\rho^-(t = 0) = 0.4N$, $N = 6400$, and randomly distributed in the lattice. (a) proportion of agents ($\rho^+ = n^+/N$) does not oscillate strongly (as seen in the fully connected model, Fig. 3.15b).

In the fully connected model we observed oscillation in the group size for $p > \frac{1}{2}$, Fig. 3.15a. In the 2d model we see that there is not the same qualitative behaviour, Fig. 5.11. We will test whether the model on a 3d lattice gives results that are more similar to the 2d model (no oscillations) or the fully connected model (with oscillations) in a later section, Sec. 5.4.2.

5.3.4 Monte Carlo simulations in 2d $p = 1$

We find that when $p = 1$ the simulations do not reach consensus even with the stochastic fluctuations in single simulations. This is because the simulations develop to structures where persistent arrangements exist. An example of a persistent arrangement of alternating high and low confident agents, i.e. dark and light in adjacent places on the 2d grid was found Fig. 5.12.

These low confidence agents (light colour) are repeatedly persuaded to join alternate opinion groups. They never have the chance to increase their own confidence. They are always interacting with agents of higher confidence and $p = 1$ determines that the most confident agent successfully persuades the less confident

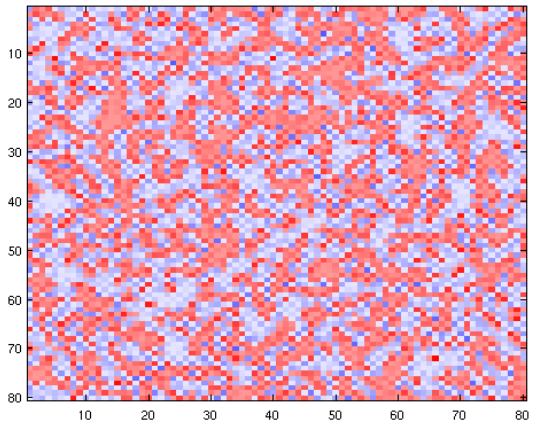

Figure 5.12: Snap shot of the non-conserved confidence model on 2d lattice with $p = 1$, at $t = 110$. The light blue and white squares are agents with low confidence and opinion choice $-$ and the dark blue are high confident agents in the same group. The $+$ opinion group are red and the dark red agents have high confidence (and light red are low confidence). Random initial conditions of all agents with zero confidence and equal number of each opinion group.

ones in every interaction, Fig. 5.13. Furthermore we notice that the group proportion has dynamics that remain away from consensus, and close to 50 percent in both opinion groups Fig. 5.14a. We see that the mean confidence oscillates, Fig. 5.14b, which is comparable with the fully connected model (mean-field) dynamics also showing ρ oscillation, Fig. 3.15b.

This result is different to the fully connected model coexistence state. We have identified a coexistence fixed point from where the stochastic dynamics are unable to reach consensus. The choice of $p = 1$ means that locally stable regions can never order into a state of all $+$ (red) or all $-$ (blue). Each interaction between a confident agent and a non-confident neighbour reinforces the more confident agent with certainty. This is not seen in the $p = 0.9$ model because there is some finite probability that the more confident agent loses interactions so there is a small probability that temporarily stable regions similar to that shown in Fig. 5.13 will order and therefore consensus can be reached. This highlights a qualitative difference between the $p = 1$ model and the $\frac{1}{2} < p < 1$ models in 2d. Therefore the coexistence fixed point is abnormally stable when $p = 1$, compared to the other $p > \frac{1}{2}$ values. We have previously identified $p = 1$ model as displaying behaviour different to the other p value non-conserved models in the fully connected model. The distribution of confidence values when $p = 1$ is abnormal, when compared to all the other

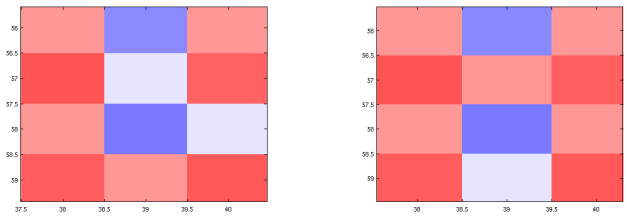

(a) 2d, $p = 1$, $t = 98$. (b) 2d, $p = 1$, $t = 108$.

Figure 5.13: Two different late time snap shots of the $p = 1$ model on 2d. The white squares are agents with low confidence and opinion choice $-$ (blue) and the dark blue are high confident agents in the same group. The $+$ opinion group are red and the dark red agents have high confidence (and light red are low confidence).

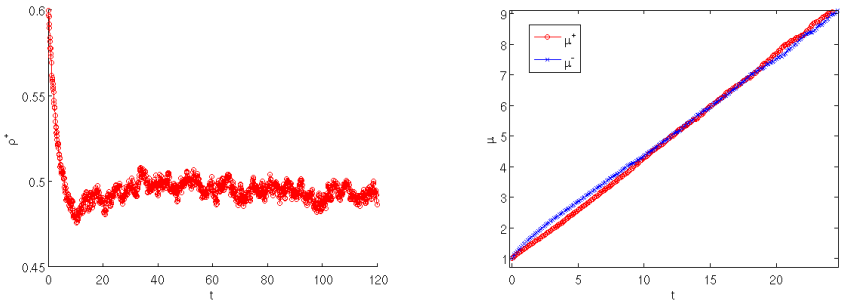

(a) $\rho^+(t)$ (b) $\mu(t)$

Figure 5.14: Dynamics of a simulation of the non-conserved confidence model with $p = 1$ on a 2d square lattice (a) $\rho^+(t)$ the proportion of agents with opinion $+$. (b) $\mu(t)$ mean confidence. With initial condition of all agents with zero confidence and 60 per cent agents with opinion $+$, and $N = 6400$.

$p > \frac{1}{2}$ models, (seen in the numerical results of the mean-field equations Eq.(3.1), (3.2)) Fig. 3.11a and that there are oscillations in the opinion group mean-field equation results, see Fig. 3.9b and ensemble average of the stochastic model results, see Fig. 3.16b. Furthermore the reduced ODE model also displays behaviour which is abnormal at $p = 1$ compare to the other p choices, see Sec. 3.8. Therefore the qualitative jump seen at $p = 1$ in the fully connected model consensus time results, Fig. 3.20b, is in the context of this model behaviour.

5.4 Monte Carlo simulations of non-conserved model in 3d

Now we simulate the non-conserved confidence model on a 3d regular lattice, again with periodic boundary conditions. As in the 2d lattice simulations we choose the initial conditions for each simulation to be all agents with zero confidence and each agent with an equal probability of starting with opinion + or opinion -, so on average half the agents with opinion + and half with opinion - distributed randomly through the 2d spatial structure. We simulate repeatedly with different random seeds to find the mean consensus time. The mean consensus time for the voter model on a regular 3d lattice is $\tau_n \simeq N$, [14]. Therefore we compare our $p = \frac{1}{2}$ model results to this. We notice that the ambiguity in the plots arise from the finite size effects, not a lack of simulations.

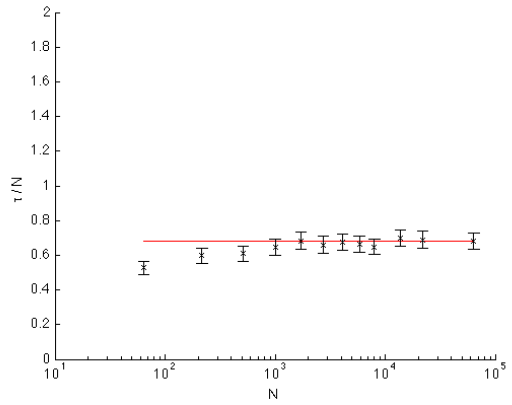

Figure 5.15: Mean consensus time τ_N for the non-conserved confidence model on 3d lattice with $p = \frac{1}{2}$, scaled by population size N. We find that the mean consensus time is the same as the voter model and $\tau \simeq N$. We fit by hand a (red line) a constant which is 0.68.

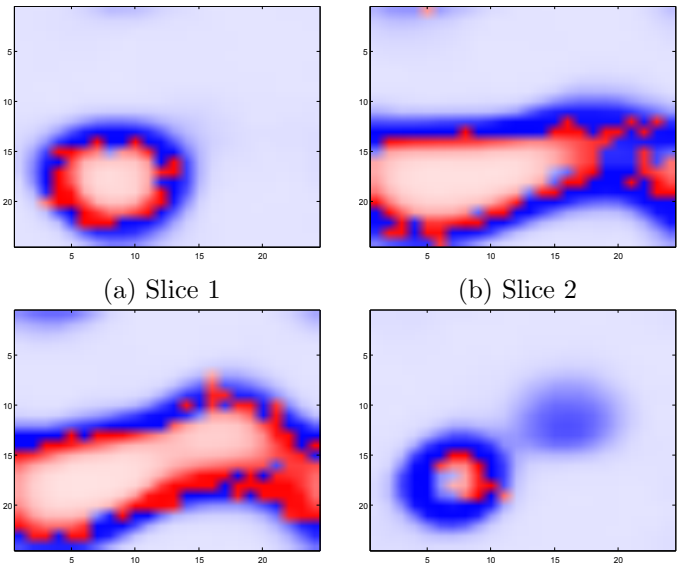

(a) Slice 1 (b) Slice 2

(c) Slice 3 (d) Slice 4

Figure 5.16: Snapshots of the confidence and opinion of a 3d non-conserved confidence model with $p = 0.2$. Each slice is 10 lattice spaces lower moving down through the 3d lattice. Opinion group + (red) and − (blue) with the stronger of colour indicating greater confidence, k, levels. Initial conditions are 50 percent of the population with opinion + and all agents with zero confidence, $N = 900$.

5.4.1 Monte Carlo simulations in 3d $p < \frac{1}{2}$

We find spatial structures in the 3d model, Fig. 5.16, that are analogues of those in the 2d model, Fig. 5.6b. Once again there are structures of bands of high k–values separating regions of low k–value. This is understandable because it is the low k–value agents which change opinion less often because $p < \frac{1}{2}$.

5.4.2 Monte Carlo simulations in 3d $\frac{1}{2} < p$

We find that in 3d the mean consensus time found from average results of the Monte Carlo simulations for $p = \frac{1}{2}$ agree with the voter model result of $\tau \simeq N$, Fig. 5.17b. We also find that the $p = 0.7$ mean consensus result is also comparable with the N and with a prefactor that is greater than that for the $p = \frac{1}{2}$ result, Fig. 5.17a.

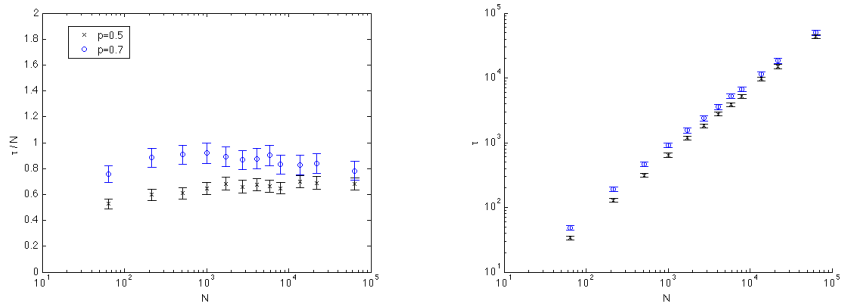

(a) τ compensated by N (b) τ

Figure 5.17: Mean consensus time for the 3d model, given population size N, (a) τ compensated by N, (b) τ, for $p = \frac{1}{2}$ (black cross) and $p = 0.7$ (blue circle). Error bars are 3 standard error (SEM) and results averaged over 1000 simulations

We find that that on a 3d lattice the ensemble average dynamics of the stochastic model results demonstrate oscillations in the opinion group size Fig. 5.18. This result is comparable with the fully connected model stochastic results which also show a damped oscillation in the opinion group Fig. 3.15b.

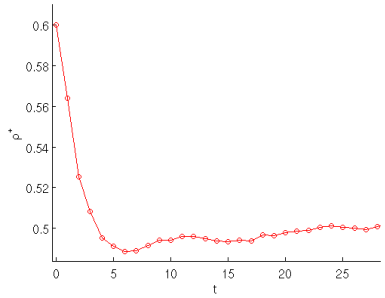

Figure 5.18: Ensemble average of $\rho^+(t)$ for the non-conserved confidence model on a 3d lattice, with $p = 0.9$, of (a) opinion group size $\rho^+(t)$, with initial conditions of zero confidence and $\rho^+(t = 0) = 0.6N$, $\rho^-(t = 0) = 0.4N$, $N = 6400$, and randomly distributed in the lattice. Ensemble average over 50 simulations.

5.5 Conclusions

We found that in 2d the $p = \frac{1}{2}$ model has mean consensus time, found from the average of the Monte Carlo simulation results, that is the same as the voter model in 2d, Fig. 5.1. The ensemble average of the opinion group size, $\rho^+(t)$, is flat, Fig. 5.3a, the change in mean confidence is linear Fig. 3.4a, and the distribution of confidence values appears to follow the dynamics of drift with diffusion Fig. 3.4c. These are results commensurate with the mean-field ODEs (Eq.(3.1), (3.2)) mean confidence

Fig. 3.4a and confidence distribution Fig. 3.4c results.

The $p < \frac{1}{2}$ model behaves very differently on a regular lattice than the fully connected model. The consensus times are slower than the comparable result in the fully connected model. Previously we found that the confident voter model on fully connected network with $p < \frac{1}{2}$ had relatively short consensus times and $\tau_N \simeq lnN$, Fig. 3.18. The same model on the 2d regular lattice gives a qualitatively different result, Fig.5.4a which is superlinear in N. When $p < \frac{1}{2}$ in the 2d cases we notice spatial structures are present in the dynamics, Fig. 5.6. Similar structures are also seen in the dynamics of the 3d model Fig. 5.16. These show regions of low confidence surrounded by borders of high confidence. The borders are adjacent to regions of the same opinion type. So a region of low confidence of opinion group $+$ is surrounded by a high confidence band which is adjacent to a high confidence band of opinion $-$. That $-$ band is adjacent, on the other side, to a region of $-$ agents of low confidence. These regions of low confidence are relatively stable because of the choice of p, i.e. low confidence agents are less likely to change their opinion. This helps explain the longer consensus times observed in the spatial model than the fully connected model.

We notice that the spatial structures may indicate that the coarsening process is different in the the non-conserved model on spatial networks to the voter model on spatial networks. That spatial voter models with memory and multiple states coarsen with effective surface tension has been shown recently [11] [15] [16]. Therefore our results agree with this finding. Our model has explicit intermediate states in the sense that there are many k–values that the agents take during the simulations. Therefore a natural extension to this work is to measure the density of interfaces to understand the nature of the coarsening at different times in the simulations for the spatial non-conserved model.

With $p > \frac{1}{2}$ on a 2d lattice we found that the dynamics of the group size, $\rho^+(t)$ i.e. proportion of agents with opinion $+$, Fig. 5.11, are qualitatively different to the same result for the mean-field model on the fully connected network, Fig. 3.15a. The damped oscillations seen in the ODEs (Eq.(3.1), (3.2)) describing the ensemble average for the mean-field model are not present. However when the model is on a 3d lattice it appears that the damped oscillations return, Fig. 5.18. This suggests that as we move from 2d to 3d the dynamics are more similar to the fully connected model, a result that is reinforced by the mean consensus time results. When $1 > p > \frac{1}{2}$ on the $d = 2$ lattice there is strongly suggestive numerical evidence that mean consensus time is $\tau_N \simeq N$, Fig. 5.9a. This is less convincing as p approaches 1, and seems to fail at $p = 1$ when the dynamics are qualitatively different due to the presence

of locally stable configurations Fig. 5.13. When $p > \frac{1}{2}$ on 3d the mean consensus time is $\tau \simeq N$, Fig. 5.17a. This is the same as the fully connected model consensus time result, Fig. 3.20a. Therefore the dynamics and the consensus time results both suggest that as the model dimension increases from 2 to 3 the model behaves in a way which is increasingly like the fully connected model.

We find that the $p = 1$ model dynamics achieve locally stable configurations which prevent consensus Fig. 5.13. This explains the opinion group dynamics which oscillate about the equal coexistence fixed point Fig. 5.14a. The dynamics are prevented from reaching consensus by these local configurations which reinforce themselves in interactions between more confident agents becoming increasingly confident with certainty (because $p = 1$). This is qualitatively different to the 2d models with other $p > \frac{1}{2}$ values because these have a finite probability that the more confident agent loses an interaction and the stable region does not persist. We found that behaviour which was qualitatively different to the other p values was also shown in the $p = 1$ fully connected model in the opinion group dynamics Fig. 3.16b and the distribution of confidence values obtained after a long time Fig. 3.11a. This all suggests that the coexistence fixed point (at $\rho^+ = \frac{1}{2}$) is indeed abnormally stable for $p = 1$ as highlighted by the jump in the mean consensus time at $p = 1$ in the fully connected model Fig. 3.20b. The original voter model has only two, symmetric, absorbing states: consensus for one of the two groups. Our non-conserved fully connected model displays persistent diversity on average. The ensemble average results of the fully connected stochastic model reach the coexistence fixed point (of $\rho^+ = \frac{1}{2}$) Fig. 3.16b. This is reached on average because individual simulations of the fully connected stochastic model do reach consensus due to random fluctuations. However the persistent diversity observed in the non-conserved confidence $p = 1$ 2d model Fig. 5.14a can be compared with the non-consensus absorbing state in the Axelrod model, Chap. 6. In the 2d non-conserved model the persistent diversity occurs in individual simulations. Therefore this is more like the coexistence seen in the Axelrod model when no consensus is reached but a persistent state of regions with different opinions is achieved. The difference between the diverse state in the 2d non-conserved confidence model is that interactions continue to occur, and an absorbing state is not reached, whereas the Axelrod model can reach a frozen state with diversity, one of the many absorbing states that can be reached in that model.

We also note that the local spatial structures present in the 2d model which favour repeated interactions between very high confidence agents and low confidence agents gives an insight into why the fully connected model behaves differently when $p = 1$ compared to $p < 1$. The stability of the structure is a consequence of the

preference in the dynamics to develop agents which have opinions that are relatively low and therefore quickly change opinion. This provides a higher proportion of the agents in the fully connected model who swap groups quickly and helps explain the strong oscillations in the opinion group size.

We have not investigated in this work the correlation lengths in the results of the spatial model. We have seen that the models with different p regimes result in spatial structures that are different. Therefore an analysis of the spatial results is an natural extension to the work presented here. We suggest that it would be of interest to measure both the correlation lengths and the number of defects. Finding the correlation length as a function of time in order to establish the coarsening laws is another further extension to the results presented.

Overall the question of whether the spatial model behaves similarly to the complete graph does not have an entirely simple answer. In many respects the answer is 'yes' for $p \geq \frac{1}{2}$ and 'no' for $p < \frac{1}{2}$ where spatially long lived structures play an important role in the dynamics. In particular they prevent the fast consensus times seen in the complete graph model dynamics when $p < \frac{1}{2}$.

Chapter 6

Biased Axelrod model

6.1 Introduction

We have shown how the introduction of heterogeneity as confidence held by agents affects our modified voter model. Now we introduce heterogeneity into the Axelrod model with confidence in specific opinions, through the introduction of biased opinions. We seek to understand whether these model changes modify the consensus time and whether the likelihood the system will reach coexistence states is altered.

In this chapter we introduce the modifications made to the Axelrod model to create both the Biased Outcome and Biased Topic models. We summarise the simulations and highlight the results for firstly the Biased Outcome model and secondly the Biased Topic model. Finally we summarise the results of both models together. We note here that the Axelrod model is made of agents, each with a vector of F 'opinions' (synonymous with 'features'), each opinion with q 'choices' (synonymous with 'traits'). The terms 'features' and 'traits' are the usual terminology of the Axelrod model. In this Chapter we focus on our novel modifications to this model and therefore use these terms here.

We discussed a range of modifications made to the Axelrod model in Chapter 2. Features in the standard Axelrod model are homogeneous in two respects. Firstly when an interaction has taken place all the features which are not shared between the agents are equally likely to be copied (one agent adopts the trait from the other for the feature being updated). Secondly before any interaction takes place each feature contributes equally to the likelihood of interaction. We modify both of these rules separately. Where the interaction is interpreted as a conversation our model modifications can be described as adding biases to the conversations between individuals.

The agents within the Axelrod model update as a result of interactions that include the concept of social influence [21]. Additionally the interaction rules mean that if agents are more similar then they are more likely to interact, those incorporating also the effect of homophily [44]. We provide two modifications of the Axelrod model. We link opinions (features) so that if one is shared between agents then the other is more likely to be updated than the other, regular, opinions. Motivation for linking the features in our adapted Axelrod model comes from the empirical research that shows that some opinions are correlated [20]. Separately we include a weighted bias to opinions in the interaction stage of the Axelrod model. The consequence of the bias is that the weight of importance of that opinion when deciding whether to interact is greater. There is motivation for this model characteristic from the research that highlights that not all personality traits are equal [2].

There has been research, discussed in Chap. 2, on modifying the way the features are included in the interaction step of the Axelrod model. Research found that the system was more likely to reach a coexistence state due to the introduction of both an external field acting as a mass media influence, [24], and the introduction of 'generalized other' and a 'filtered global media' [55]. The 'generalized other' model includes an hypothesised fifth neighbour that has the same influence over an agent as their actual four neighbours. The fifth neighbour has the most preferred trait of each feature and is therefore a generalised agent. The filtered global media model is different. An agent is only influenced by their four real neighbours however the update will only occur if the trait of the influencing agent is the same trait as the plurality (the most common traits of all the agents). In this way agents are only able to update through the filter of the plurality that represents the global media. Although different models, both of these models implicitly place a restriction on the features that agents own features are able to interact with (for at least some proportion of the interactions). The consequence of this restriction is to increase the ability of the system to reach a disordered (coexistence) frozen state. Research by Gonzalez et. al. [25] has also shown that consensus is favoured, i.e. more likely to be reached, when there is a low level of interactions with the media. In other work Parravano et. al. [51] modified the probability of interaction so that the size of the overlap (over the opinions, features) has a threshold below which no interaction occurs between the two agents. This constraint on the occurrence of interactions resulted in the system reaching consistently reaching states with a smaller fraction of the agents in the largest cultural group.

The changes we make to the Axelrod model involve introducing heterogeneity to the opinion space at the interaction stage. One of our modifications is to introduce

bias in favour of features determining the probabilities of which feature to update. Because research has shown that in other models that change the opinion space that an agent can interact with, through a global media [24] [25] [55] can effect the type of frozen state that the system reaches we may imagine that our change will change the typical type of frozen state the system reaches.

The other modification introduces a bias in favour of features when calculating the probability of interacting. Research has shown that a model with modified interaction probability [51] changes the typical number of agents in the largest cultural group therefore one might imagine that our changes may effect the proportion of agents in the largest region (i.e. the size of the largest region).

One would expect that linking features may result in the type of frozen state being reached by the simulations of the model being changed. One could imagine that the consequence would be an effective reduction in the number of features and the consequence on the type of frozen state would be that expected for the original Axelrod model with the reduced number of features. To test this we find the typical frozen state for the simulations for a range of F.

6.2 Axelrod Model Extensions: Biased Conversations

Our extensions to the Axelrod model concern the interaction stage of the simulations. The Axelrod model assumes that all features are equally important and also all equally likely to be changed upon interaction. However this is not born out in everyday experience. Firstly an individual is more likely to copy a feature of their neighbour if they already share a related feature. There are two key features which are intrinsically related, for example political views and media preference. It is possible that it is more likely that an individual will be inclined to engage in discussion about media types with someone who has the same political preference and so would be more open to having their opinion on media choice influenced by that person.

The context of the second model alteration is that there is likely to be a subject that is more important, topical, or interesting. So that an individual is more likely to interact because they share a specific feature, for example religion (feature 1). So, regarding homophily, certain features are likely to be more important than others in influencing whether individuals interact. Our novel model extensions therefore consider two separate aspects of the interaction stage. We were interested to understand if modifications to the local interactions affected the dynamics of the simulation or the phase transition between final state consensus and fragmentation. Our first modification is a bias over which features are updated when an interaction

does take place. The separate second change is to the probability of two individuals interacting based on which features of the cultural state they share.

6.3 Simulation steps

We summarise the generic simulation steps taken for a generic Axelrod model, on a 2d regular lattice so each agent has four neighbours, highlighting where the subsequent modified model simulations are different.

1. Select an agent i at random.
2. Select a neighbour, j, at random.
3. Find P_i the probability of interaction: Either
    - Calculate the probability of interaction by the overlap (the number of features for which the agents share traits) divided by the total number of features, $P_i = m/F$, or
    - use the Biased Topic model rules to determine P_i (described in Section 6.5.1).
4. With probability P_i update the agent i in the next step, and with probability $(1 - P_i)$ do not update the agent and return to the first step.
5. Choose a feature to update, either:
    - select a feature (which has different trait between the two agents) at random, and agent i copies the trait of that feature of agent j (so that if there are $F^{'}$ features which have a different trait between the two agents then each of those has a $1/F^{'}$ chance of being the feature that is updated in agent i), or
    - select the feature with the Biased Outcome model rules (detailed in Chapter 6.4.1).
6. Return to the first step (unless the system is frozen).

We note that time recorded in the simulation results corresponds to the time taken for one single interaction to have the chance of occurring. Where $\delta t = 1$ and each iteration of the simulation steps was δt. The network of agents is a 2d lattice for all simulations performed.

6.4 Simulation 1: Biased Outcome Model

In the original Axelrod model there is is equal likelihood to update each feature not shared by the two individuals interacting. However in the modified model the outcome is biased towards linked features. The parameter α tunes between the original situation and the modified one. When α is zero the model is the original Axelrod model and when the parameter is one the linked features are the only ones with non-zero probability of being selected to be adopted. When there is more than one pair of linked features then all the linked features with one trait shared between the two agents are more likely to be updated. Features are always linked in separate pairings so that any feature is only ever linked to at most one other.

6.4.1 Biased Outcome Model rules

We only modify the step where the feature, to copy the trait of the other agent, is chosen. In the original Axelrod model each feature which has a different trait between the two agents (where the number of these for any given pair of agents is $F^{'}$) has $1/F^{'}$ chance of being selected to be modified.

We introduce the parameter α which specifies how much more important linked features are in the interaction. When agents share a trait between a feature the linked feature is more likely to be updated, by an amount specified by α. The new weighting of the probabilities of which feature is to be updated is determined by α. When $\alpha = 0$ all features not shared between the agents are equally likely to be updated in the interaction, as in the original Axelrod model. The extreme case of $\alpha = 1$ determines that the only features which can be updated are those features not shared between the agents and which are also linked to features which are shared. The parameter α increases simply and linearly the weight allocated to the linked features (not shared and linked to features which are shared) while reducing the weight allocated to all other features (not shared between the two agents). Our modifications (detailed in Appendix B) mean that specific features have an increase in the chance that they are chosen to be updated, proportional to α. These are features which fulfil the three-fold criteria: being linked; having different traits between the agents; and their linked feature having a shared trait between the agents. Correspondingly those other features which have different traits between the agents have their probability of selection reduced by an amount proportional to α (these are features which have different traits between the agents but are either not linked or their linked feature does not have a shared trait between the agents).

6.4.2 Pairing rules

For the following model cases we used the simplest pairing rules:

- When a single pair of agents was linked we chose features 1 and 2. We use the term 'single pair' to summarise this case.
- When, for example, 5 pairs of agents were linked we paired the features simply 1 and 2, 2 and 4, 5 and 6, 7 and 8, 9 and 10. We refer to this as 'fully paired'.
- In models with an odd number of features, e.g. $F = 5$, the most pairs of linked features possible were created, whilst ensuring any feature was paired with at most one other feature. For example paring 1 and 2, 3 and 4 in the case where $F = 5$. We also refer to this as 'fully paired'.

In each cases the modification made was the same for all the agents in the simulation.

6.4.3 Results of simulations of the Biased Outcome Model

We ran simulations of the model to obtain the average outcomes for a range of model size, N, along with F and q choices. The Biased Outcome model differs from the Axelrod model in the way that features are treated in the update rules of of the model. Therefore we obtained novel results demonstrating the mean frequency of change of each feature during the simulations. Specifically we measured the mean rate of change of each feature throughout the simulations. We ran one thousand simulations of the same size model to obtain the rate of change of features. We performed these simulations for two models: 10 features and 2 traits; and one with 10 features and 15 traits.

We chose to run the Biased Outcome models with $\alpha = 1$ to test largest possible effect of the model modifications. That is with the outcome of the interactions most strongly determined by the linked features.

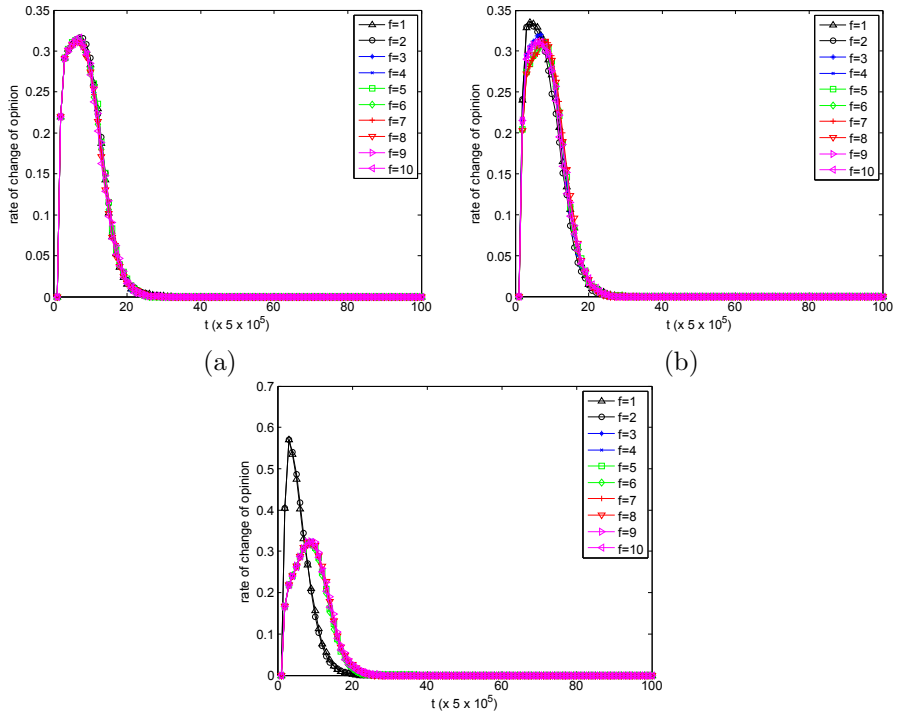

Figure 6.1: Rate of change of each feature for models with F = 10, q=15 for (a) the Axelrod model ($\alpha = 0$) (b) Biased Outcome model with 5 pairs of linked features and $\alpha = 1$ (c) Biased outcome model with one single pair of linked features (feature 1 and feature 2) with $\alpha = 1$.

The Axelrod model and the model with 5 pairs of linked features demonstrated behaviour where all features changed with roughly the same frequency, see Fig. 6.1a and 6.1b, 6.2a and 6.2b.

However the model with a single pair of linked features demonstrated different behaviour. Here the two linked features changed more frequently than the other features for the early part of the simulation (see Fig. 6.1c and 6.2c). These models therefore reached a stage where all agents had the same respective choices for feature 1 and feature 2. The other features continued to change until the whole system reached a frozen state.

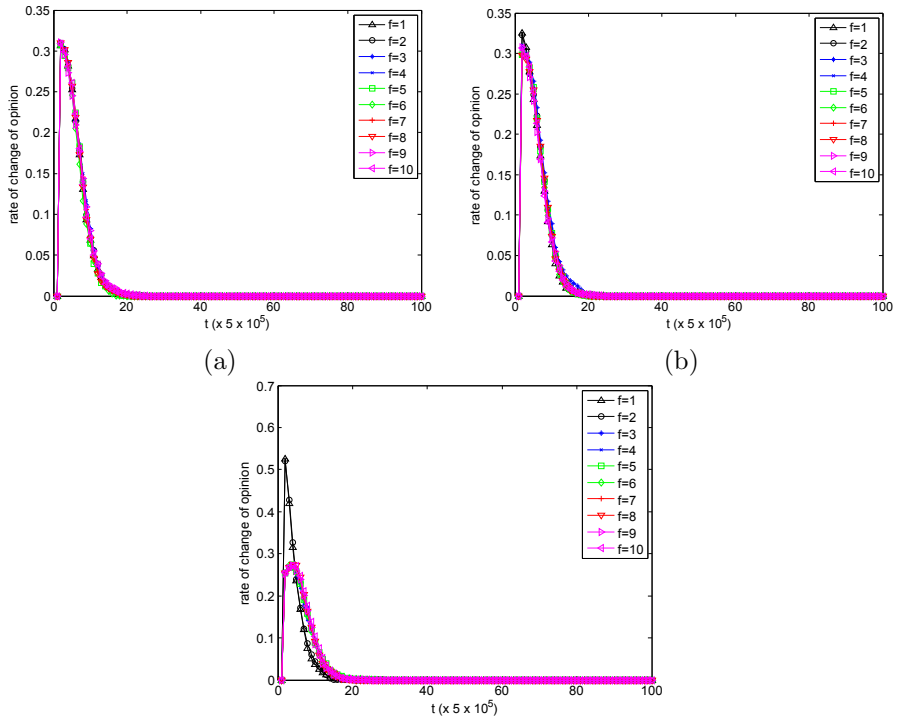

Figure 6.2: Rate of change of each feature for models with F = 10, q=2 for (a) the Axelrod model ($\alpha = 0$) (b) Biased Outcome model with 5 pairs of linked features and $\alpha = 1$ (c) Biased outcome model with one single pair of linked features (feature 1 and feature 2) with $\alpha = 1$.

Models with few features (relative to the number of traits) end in a frozen state of fragmented regions. At the population level the dynamics of the Axelrod and modified models with linked features showed the same behaviour. The plots of the dynamics with models of 10 features made of 5 pairs of linked features demonstrate this, see Fig. 6.3. We notice a small discrepancy in the results for the early times. This is not the focus of our work here but this is of potential interest and related to finite size effects. We have seen how linking the features effects the dynamics of the models when only a single pair of features are linked. However we also want to determine the possible effect of linking 2 or all features on the type of frozen states reached and the time it takes the simulations to reach these.

Previous analysis of the Axelrod model has focused on the effect of tuning the number of traits, q, [4]. When the number of features, F, is held constant it has been observed that there is a phase transition between consensus and fragmented frozen final states when q is increased [4]. The type of end state of the simulation depends on both F and q. Therefore it is also possible to observe a change in the

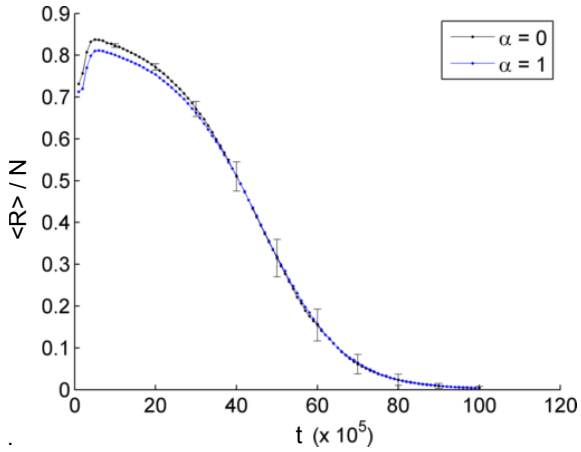

Figure 6.3: The mean number of cultural regions for (1000) simulations of models with five pairs of linked features (and 15 traits each). The original Axelrod model is given by $\alpha = 0$ and the fully linked pairs are with $\alpha = 1$. The error bars are the 3σ range of the 1000 simulations and we see that for the majority of the simulation time the models give the same mean number of regions.

type of final state reached by fixing q and varying the number of features, F. The linked features affect the outcome of which features are updated. Therefore it was more appropriate to observe a change in the behaviour of the dynamics considering models with different numbers of features. Our expectation was that including linked features would result in dynamics corresponding to a model with an altered number of features. So we chose to fix q and vary F. This provides a transition in the type of final state observed, from fragmented regions with smaller F to consensus with larger F.

The model choices were made in order to show the phase transition from fragmented frozen state (with fewer features) to consensus frozen state (with more features). Therefore we chose a model with q = 50 to have a range of F over which to observe the phase transition. Simulation times for these models are longer than simpler models (with fewer features) so these were averaged over 100 simulations only.

For simulations of 900 agents on a periodic lattice we observed that models with a larger number of features (compared with the number of traits) go to consensus, see Fig. 6.4a. Furthermore we note that the time to consensus is comparable for the Axelrod and fully linked models with the same parameter choices, Fig. 6.5.

In order to test the type of frozen state, with a large number of simulations, for a model with both fully connected features and a single pair we used a model with

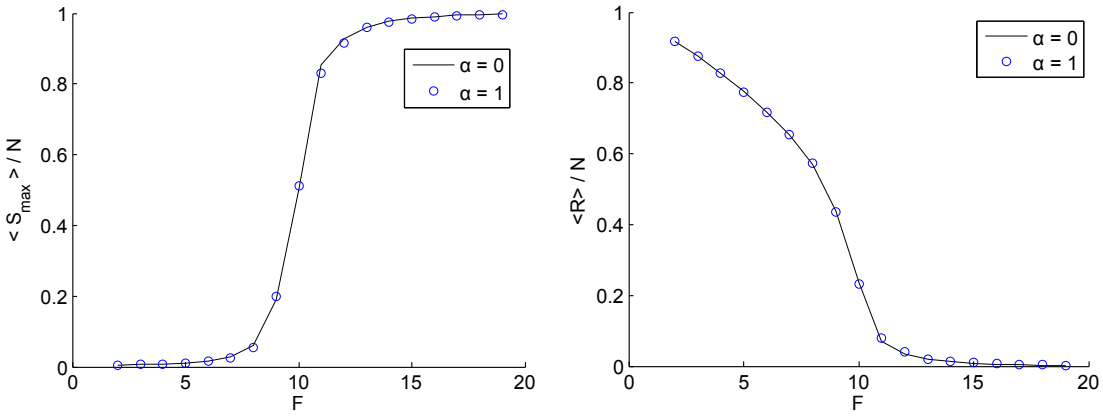

(a) (b)

Figure 6.4: (a) Mean size of the largest cultural region in the frozen state, and (b) mean number of cultural regions, both (relative to the system size, N=900 agents) for a model with q=50, for both Axelrod model ($\alpha = 0$) and a Biased Outcome model with fully connected pairs of features with $\alpha = 1$. Averaged over 100 simulations. While keeping the number of traits fixed, on average consensus is reached by models with more features, while frozen fragmented states are reached by those with fewer features, for both models.

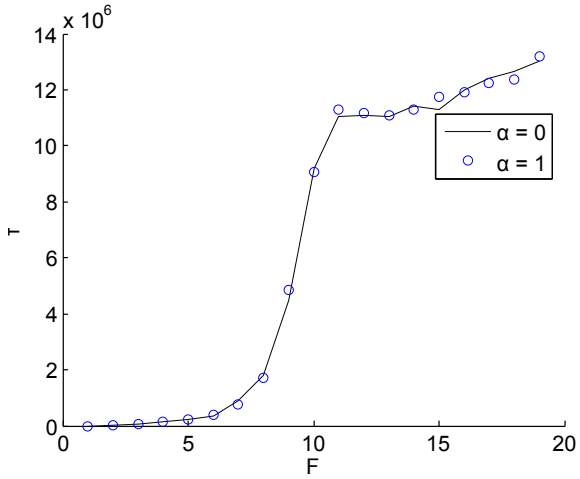

Figure 6.5: Mean freezing times for a model with q=50 (N=900 agents) averaged over 100 simulations for both the Axelrod model ($\alpha = 0$) and a Biased Outcome model with fully connected pairs of features and $\alpha = 1$. The consensus times for both models are comparable and they increase with increasing number of features, i.e. with model complexity.

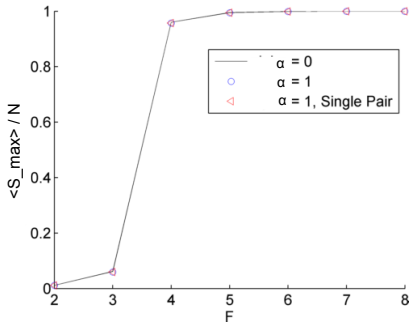

Figure 6.6: Mean size of the largest cultural region in the frozen state divided by the system size ($N = 900$) for an appropriate range of number of features, F, and models with $q = 15$ but three types of linked-ness: (1) the original Axelrod dynamics, i.e. no pairs linked (2) all fully linked pairs and (3) a single linked pair. We see that the mean largest region size in the frozen state is comparable for all three models. Results averaged over 1000 simulations.

q = 15 (giving lower consensus time and therefore shorter simulation times). We tested a model with: a single pair; all features connected in pairs; and the original Axelrod model over a range of features which would demonstrate the transition from fragmented frozen regions to consensus, Fig. 6.6, and found that the three models reach comparable types of frozen states.

6.5 Simulation 2: Biased Topic Model

Here the only step of the simulation which is altered is the way that the probability of interaction is calculated. The model reflected the fact that one topic of conversation is much more important to all the individuals. Therefore this feature carries more importance in the calculation of the likelihood of interaction. The effect of the model alteration is that when the first feature was the same then the two agents are more likely to interact (than in the equivalent Axelrod simulation) and if the first feature is different then the two agents are less likely to interact.

6.5.1 Biased Topic Model rules

The model alteration was that we gave weighting to each of the features. Therefore when the overlap was calculated the was a multiplicative factor for each. This factor was inversely proportional to the cardinality of the feature in the cultural state of the agent, so the first feature is 1, the second is 2 and the third is 3 and so on. Each weighting was raised by an integer power β to enable the effect to be tuned.

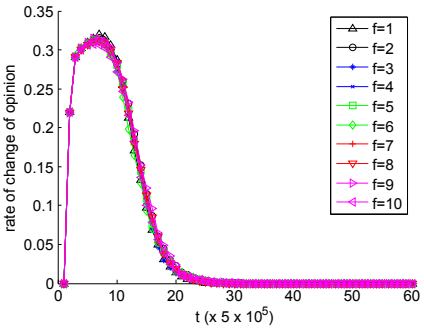

Figure 6.7: Rate of change of each feature for models with $F = 10$, $q = 15$ and $\beta = 0$, i.e. the all features affect the probability of interaction equally.

Therefore the weighting for each can be written as $(1/f)^{\beta}$. The effect is that the weight of the first feature is the largest of all the features. Each subsequent feature has a weighting that is increasingly small. As β is increased the multiplicative factors become smaller and smaller. The effect therefore is that the first feature takes on an increasingly important role in deciding whether the interaction will take place or not for a given two agents at a given time. We studied models with β in the range $0 \leq \beta \leq 3$ and where $\beta = 0$ corresponding to the original Axelrod dynamics. The weights were normalized so that the total probability summed to 1. The modification was the same for all the agents in the population.

6.5.2 Results of simulations of the Biased Topic model

Simulations were performed for an adapted Axelrod model with the alteration described above, with 900 agents, on a square periodic lattice. These models were tested for a range of β, the parameter which increases the relative importance of the first feature when calculating the probability of interaction. We investigated the route to frozen state at the level of individual features. As with the first model modification we noticed that the route to the frozen state is different to that in the Axelrod model. In the Axelrod model each feature gets changed at a similar frequency (see Fig. 6.7) compared with the other features. When the first feature affects the probability of interaction, i.e. $\beta = 3$, this feature is changed less frequently relative to the other features for the initial stages of the simulation (see the first half of Fig. 6.8). Furthermore when the first feature affects the probability of interaction, this feature continues to change longer than all the other features (see the second half of Fig. 6.8).

With more features, e.g. F = 8, consensus was reached, Fig. 6.9. This is

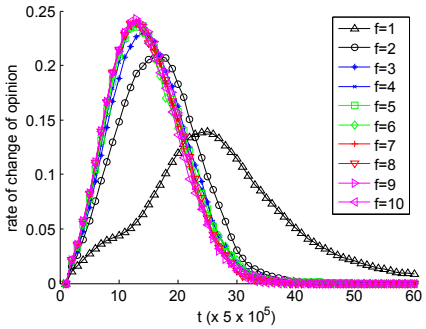

Figure 6.8: Rate of change of each feature for models with $F = 10$, $q = 15$ and $\beta = 3$, i.e. the first feature affects the probability of interaction more than the other features.

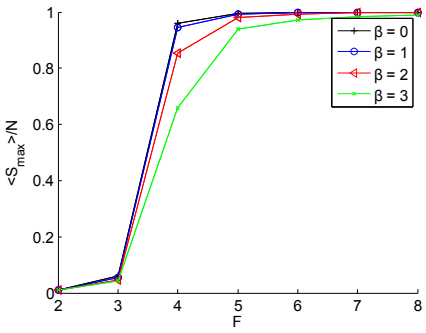

Figure 6.9: Mean size of the largest cultural region in the frozen state (relative to the system size, $N = 900$ agents) for a model with $q = 15$ and a range of F, averaged over 500 simulations. Results are plotted for models with the parameter $\beta = 0, 1, 2, 3$ which prescribe the relative importance of the first features affecting the probability of interaction, relative to the other features.

expected in the original Axelrod model because the number of features relative to the number of traits means there are enough possibilities for a non-zero overlap to allow the dynamics to reach consensus. That we also find consensus on average for the model with heavily weighted feature importance in calculating the probability of interaction is non-trivial. The alteration to the interaction step means that the dynamics are necessarily altered but it is not to be expected that the type of frozen state reached will necessarily be the same as the original Axelrod model. We observed that the other method for testing the type of consensus (i.e. measuring the number of regions in the frozen state divided by the total number of agents, $N = 900$) demonstrates the same result: type of frozen states are the same on average between the models. This was the same for all values of β tested. Also with a

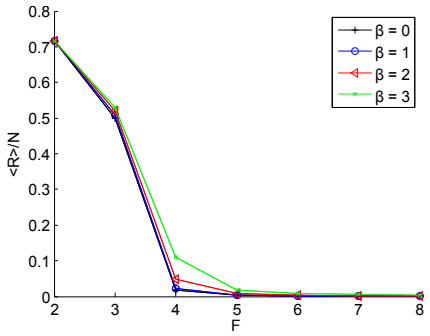

Figure 6.10: Mean number of the largest cultural regions in the frozen state (relative to the system size, $N = 900$ agents) for a model with $q = 15$ and a range of F, averaged over 500 simulations. Results are plotted for models with the parameter $\beta = 0, 1, 2, 3$ which prescribe the relative importance of the first features affecting the probability of interaction.

low number of features, e.g. F = 2 there was a frozen state of different fragmented cultural regions. Again this was the same for all values of β tested.

We also found that the more emphasis there is on the first feature the longer the simulation takes to get to its frozen state, see Fig. 6.11. Additionally it takes longer for a model with more features to get to its frozen state (consensus) than it does for a model with fewer features to gets to its frozen state (fragmented). This is to be understood as a modification to the rates that the agents update in an inhomogenous way across the population. Each pair of agents that interact calculate their probability of interaction given the comparison of their opinion states. The weighting of the importance of the first feature means that this is a lower probability for agents that do not share the same trait for this first feature. However agents that do share the same trait for the first feature have a relatively higher probability of interacting. This means that the rates of interaction will be higher in groups of agents that happen to share the trait of the first feature and one would suspect they would reach local consensus. It it possible to imagine that these regions may either prevent the population reaching consensus however we know they do not because the type of frozen state reached is the same as in the original Axelrod model Fig.s 6.9, 6.10. Also it is possible to imagine that the change in rates for the interactions will enable the system to reach consensus faster. However we find the opposite which is that as β increases and there is greater homogeneity in the probability of interaction between agents with different opinion states the consensus time (or time to frozen coexistence state) increases greatly Fig. 6.11

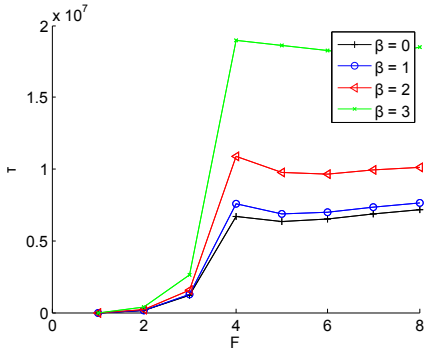

Figure 6.11: Mean freezing time for a model with, $N = 900$ agents, $q = 15$ and a range of F, averaged over 500 simulations. Results are plotted for models with the parameter $\beta = 0, 1, 2, 3$ which prescribe the relative importance of the first features affecting the probability of interaction.

6.6 Conclusions

We compared the original Axelrod with our modified version that introduced static heterogeneity to the opinion space. We found that the model with the heterogeneity over the probability of which feature is updated, the Biased Outcome model, reached the same typical types of frozen state as the Axelrod model, Fig. 6.4a 6.4b for the case where all pairs were linked. One would imagine that the consequence of linking features would cause the dynamics to follow the same typical behaviour as an Axelrod model with a reduced number of features. Therefore we found results for models with fixed q and varied F. However the type of consensus reached was coexistence in the adapted model when the choice of F resulted in coexistence in the Axelrod model, and the same for the F values that resulted in consensus, Fig. 6.4a 6.4b. We found that the time taken by the system to reach the frozen states in the stochastic simulations were comparable between the adapted model and the original Axelrod model, both for fully linked features Fig. 6.5, and a single pair of linked features, Fig. 6.6. Therefore overall the Axelrod model was still able to reach the consensus or coexistence states in the same average time despite the introduction of the heterogeneity in the opinion space, affecting the which feature was updated.

Recent research has shown that introducing heterogeneity to the opinion space at the interaction stage through a global media [24] [25] [55] can effect the type of frozen that the system reaches. We therefore conclude that the heterogeneity we introduced was not only different in the detail of the model changes made to the original Axelrod model but also the resulting effect on the system dynamics.

Our second model modification was to introduce heterogeneity to the prob-

ability of interacting. We found that introducing a bias on the influence of the features contributions to the probability of interaction gave a clear slowing down of the consensus time when compared to the original Axelrod model, Fig. 6.11. Despite this difference the type of frozen state reached was the same between the two models, Fig. 6.9, 6.10.

A different model that modified interaction probability has been studied [51]. The result of reducing the probability of interaction through the introduction of a threshold of similarity between agents before an interaction can take place was that the typical number of agents in the largest cultural group was reduced. However our results, Fig. 6.9 suggest that Axelrod model is robust to the heterogeneity which we introduced in our model.

The heterogeneity we introduced to our modified voter model, Chap. 3 was different to the heterogeneity we implemented in our adapted Axelrod model. In our voter model it is dynamic and at the level of agents. The heterogeneity we introduce into the Axelrod model is static and at the level of features. We suggest that the dynamic aspect of the changes to the voter model help the system reach a coexistence state: it is the changes in the confidence distributions that enable the coexistence state to be reached in the mean-field model and as a consequence, we suggest, the consensus time in the finite size model is affected. However the heterogeneity to the opinion space is static in the the Axelrod model. And we find the Axelrod model is resilient to the model changes of heterogeneity that we introduced.

Chapter 7

Conclusions

Our research goal was to investigate the effects of various forms of heterogeneity on the voter and Axelrod models, and explore the importance of coexistence states. We used the average consensus time found from Monte Carlo simulations to test the effect of our introduction of heterogeneity to these models.

7.1 Non-conserved confidence model

We introduced the non-conserved confidence model in Chap. 3. In this model all agents hold a confidence in their current opinion and interactions between agents result in the less confident agent changing opinion with probability p, while the more confident agent increases their confidence. In this way we have introduced heterogeneity to the original voter model through dynamic confidence which is coupled to the voter dynamics. We compared the $p = \frac{1}{2}$ model, where the confidence values are decoupled from the opinion dynamics, to the reference case of the voter model. We found that when the more confident agents are less likely to change opinion and $\frac{1}{2} < p < 1$ the mean consensus time of the stochastic model is increased relative to the voter model although it still scales with N Fig. 3.20a. We found at $p = 1$ there is a slower, exponent and $\tau_N \simeq N^a$ where $a \approx 1.4$, Fig. 3.21a. The case when the less confident agents are less likely to change opinion is $p < \frac{1}{2}$ and in this case we found that the mean consensus time is fast, $\tau_N \simeq lnN$ Fig. 3.18, when compared to the standard voter model.

We found when $\frac{1}{2} < p$ the numerical solutions of the mean-field equations (Eq.(3.1), (3.2)) show that system reaches an equal coexistence state and found scaling solutions for these long time confidence distributions, where the confidence distributions of the two groups converge to a single distribution Sec. 3.4.5. These

equal coexistence states are only present in the mean-field model. In the finite size model the stochasticity allows the system to reach consensus. Furthermore we create and solve a 3 dimension heuristic model, capturing the same qualitative behaviour as the full ODEs (Eq.(3.1), (3.2)), see Sec. 3.8. We found the stability of the coexistence state, Fig. 3.27b, and highlight that when $\frac{1}{2} < p$ the coexistence state is attractive but repulsive when $p < \frac{1}{2}$. Also when $p = 1$ the absorbing state is the most attractive of all the p values. We suggest this behaviour at the mean-field level is a reason for the different consensus times we found.

We highlight the dynamic creation of zealot-like agents, who are more confident than all other agents, at least for some time, when $p > \frac{1}{2}$ in the full ODEs Sec. 3.7. We provide a narrative description that describes the effect of the changing confidence distribution that incorporates the effect of the zealot-like agents. They help the minority group persuade many agents to leave the majority rapidly and this helps explain the oscillations in the opinion group size in the mean-field model Fig. 3.15b, 3.16b. We also found a non-zero proportion of weak-willed agents (with zero confidence) in only the $p = 1$ case Fig. 3.11a. We suggest that these agents also contribute to the strong oscillations observed in the opinion group when $p = 1$.

In Chap. 2 we identifed research by Lambiotte [36] that studies a simple model with the inclusion of vacillating voters captures the same model element of weak-willed agents. The model of vacillating voters has an interaction step where a randomly chosen agent, i, will only stay in the same opinion group if two randomly selected neighbours both share their opinion. If either of the them hold an opposing view to the original agent then i changes opinion. The mean-field model incorporating these weak-willed agents means the dynamics found the zero-magnetisation state, which is equivalent to our equal coexistence state. We note that the model does not include dynamic confidence and has an interaction rule that considers up to two neighbours rather than one. However we identify that the behaviour of the model at a qualitative level is similar. Research by Mobilia et. al. [46] also showed that agents with different propensity to change opinion, i.e. zealots who never change opinion, were able to keep the system near zero magnetisation. Therefore we are able to suggest that the reason for the coexistence state is due to the effect of the dynamic confidence creating relatively different confidence agents.

It is possible to consider the confidence value k to be a counter of the number of times that an agent has interacted and not changed group. Within this view we can compared our fast consensus in the $p < \frac{1}{2}$, seen in the consensus time, Fig. 3.18 to the results of a similar model proposed by Stark et al. [57]. The model that Stark et. al. introduced included a counter that recorded the time since they last

changed opinion. The counter is reset to zero when the agent changes opinion and it increases the probability that an agent will not change, i.e. inertia. They found that consensus time was reduced through the introduction of this inertia. We have also defined a model with state dependent rates. The effect of the k–value in the non-conserved confidence model when $p < \frac{1}{2}$ is that agents with a lower k–value are less likely to change opinion. However in our model it is every time they interact and do not change opinion their confidence, k–value, increases. Also our model does not reset the k–values at anytime. Therefore there are differences in the two models. However it is plausible that the relative changes in the k–values in the non-conserved confidence model capture some of the effects of the model proposed by Stark et al. [57]. Therefore it is reasonable that both models result in fast consensus.

Overall the presence of the coexistence state in the mean-field model, we suggest, is a reason for the model to exhibit the range of consensus times in the the spatial model. The stability of the coexistence state suggests that the consensus time is increased, when attractive and $p < \frac{1}{2}$, and reduced when repulsive and $p < \frac{1}{2}$.

In Chap. 5 we made a numerical study of the non-conserved confidence model on a regular lattice in low dimensions. We compared the consensus times for the spatial model with the fully connected network model. We asked 'does the spatial model behave similarly to the complete graph?'. We compared in 2d the $p = \frac{1}{2}$ consensus time with the reference voter result, and found they are the same, Fig. 5.1. When $\frac{1}{2} < p < 1$ on the $d = 2$ lattice there is strongly suggestive numerical evidence that mean consensus time is $\tau_N \simeq N$, Fig. 5.9a. This is less convincing as p approaches 1, and seems to fail at $p = 1$ when the dynamics are qualitatively different due to the presence of locally stable configurations Fig. 5.13. When $\frac{1}{2} < p$ on 3d the mean consensus time is $\tau \simeq N$, Fig. 5.17a. Therefore mean consensus times for the model in 2d when $\frac{1}{2} < p < 1$ are different to the fully connected model, and in 3d results suggest that they comparable. For the model with $\frac{1}{2} < p < 1$ on a 2d lattice we found that the dynamics of the group size, $\rho^+(t)$ i.e. proportion of agents with opinion +, Fig. 5.11, are qualitatively different to the same result for the mean-field model on the fully connected network, Fig. 3.15a. We found that the damped oscillations seen in the mean-field model are no longer present. When the model is on a 3d lattice it appears that the damped oscillations are present, Fig. 5.18. We suggest that as we move from 2d to 3d the dynamics are more similar to the fully connected model. This is because as the number of dimensions increases the connectivity in the model increases. As the connectivity increases the model becomes more similar to the fully connected model.

We found that the $p < \frac{1}{2}$ model behaves very differently on a regular lattice

to the fully connected model. The consensus times are superlinear in N, Fig.5.4a. This is different to the fast consensus seen in the non-conserved confidence fully connected model. When $p < \frac{1}{2}$ in the 2d cases we notice spatial structures are present in the dynamics, Fig. 5.6. Similar structures are also seen in the dynamics of the 3d model Fig. 5.16. These are regions of low k–values surrounded by borders of high k–values. These spatial structures may indicate that the coarsening process is different in the the non-conserved model on spatial networks to the voter model on spatial networks. A model with a single intermediate state has been studied on a 2d lattice by Castello et. al. [11]. Their model contained agents labeled A, AB and B, and in 2d they found that the presence of the intermediate agents, AB, caused the dynamics of coarsening to be different to the typical voter model process of interfacial noise. They found that the dynamics with the intermediate state were typical of curvature driven coarsening. The system reached consensus more slowly because the spatial structures created by these dynamics were then dynamically metastable. The non-conserved confidence model on 2d lattice also appears to show that there are spatial structures. This model dynamically creates agents with a range of confidence values. These can be interpreted as intermediate states because these agents are different relative to agents with higher or lower confidence (with respect to the agent interactions). Therefore we tentatively suggest that there may be different coarsening processes to the voter model present in the non-conserved confidence model in 2d. Further work would enable investigation into the type of coarsening present in the non-conserved model in 2d. The study of the concentration (density) of the active interfaces would be an appropriate way to study the type of coarsening present.

The coexistence state observed in the non-conserved and conserved confidence model on a fully connected network is only present in the mean-field model. However the coexistence states present in the Axelrod model are truly absorbing. When $p = 1$ there is a coexistence state that is more like the coexistence states seen in the Axelrod model, because the persistent diversity occurs in individual simulations. The locally stable configurations observed, Fig. 5.13, explain the opinion group dynamics which oscillate about the equal coexistence fixed point Fig. 5.14a. These local configurations reinforce themselves in interactions because more confident agents becoming increasingly confident with certainty (because $p = 1$). This suggests that the coexistence at $p = 1$ is abnormally stable (when compared to the stability of the models with $\frac{1}{2} < p < 1$) in agreement with the finding of the stability in the fully connected model, and the jump in the consensus time N dependence at $p = 1$ to $\tau_N \simeq N^{1.4}$.

Overall the answer to the question whether the spatial model behaves similarly to the complete graph is not an entirely simple one. It depends on the p value, and many respects the answer is 'yes' for $p \geq \frac{1}{2}$ and 'no' for $p < \frac{1}{2}$. In the $p < \frac{1}{2}$ we found that spatially long lived structures play an important role in the dynamics, where they prevent the fast consensus times seen in the fully connected model dynamics.

The most general observed phenomena is that when p increases beyond $p > \frac{1}{2}$ the consensus time increases. This was the result for the fully connected model and the 2d lattice model. We now present intuitive explanations for this model behaviour. A suggested explanation for this behaviour is that as the simulation progresses the agents have a range of confidence values. In general there is an increase in the range of the confidence values in both opinion groups. However in some models there are agents created that are from the minority and have confidence higher than all the agents in the majority opinion group. These are agents with relatively high confidence. Agents in the non-conserved confidence model with zero confidence are those with relatively low confidence as all agents with non-zero confidence are more confident than them. It is the presence of agents with relatively high confidence and agents with relatively low confidence contribute to the observed behaviour. The intuitive understanding is that the agents with the lower confidence repeatedly change opinions and those with relatively high confidence do not change opinion as frequently. These high confidence agents therefore take longer to join the consensus opinion group.

In 2d with $p = 1$ the agents with relatively high and relatively low confidence contribute to locally stable configurations. A pattern of high-low-high-low confidence makes up these local regions. These regions reinforce their configuration through the interactions. Although the low confidence agents repeatedly change opinion the high confidence agents never interact with agents of the same (or higher) confidence. These high confidence agents therefore never change opinion. Therefore consensus is prevented in this $p = 1$ case in 2d. In 2d with $p > \frac{1}{2}$ the agents with different confidence also contribute to the consensus times. With increasing p the more confident agents are more likely to win an interaction an therefore not change their own opinion. The dynamics therefore have agents with relatively low confidence which repeatedly change their opinions. The amount these agents change their opinions increases with p because this increases the likelihood that the less confident agents change opinion. These dynamics give rise to the increasing consensus time in the $p > \frac{1}{2}$ model.

In the fully connected model with $p > \frac{1}{2}$ we have seen that in the mean-field

model the opinion group size changes in a way that depends on p. With increasing values of p the group size changes are more dramatic. The greater the value of p the more agents with lower confidence. These agents mean that when the opinion group sizes change there are more low confidence agents for the high confidence agents from the other opinion group to persuade. The greater the number of low confidence agents the quicker it is for a group of high confidence agents to persuade the other agents. Therefore the opinion group size changes more rapidly in the mean-field model dynamics when there is a higher proportion of low confidence agents. This is reflected in the stochastic model consensus time results which show that and the greater p is the slower the consensus. The jump in consensus time at $p = 1$ is a reflection of the special case, observed in the 2d model, that this is the only model where there is zero probability that a less confident agent will win an interaction. It is a different case in the fully connected model with $p < \frac{1}{2}$. In this case relatively high confidence agents in the minority group, that have confidence of more extreme values than the majority group, are not dynamically created. Therefore the opinion group with the larger number of agents is able to persuade the minority group and reach consensus.

7.2 Conserved confidence model

In Chap. 4 we studied a variation of the non-conserved confidence model which has conserved confidence. Now the interactions include the result that, additionally, the agent that changes opinion reduces their k–value by one. We compared the results of the conserved confidence model on a fully connected network to the non-conserved model. We found that when $\frac{1}{2} < p < 1$ the consensus time scales linearly with N, Fig. 4.5a, and when $p = 1$ it scales as $\tau_N \simeq N^a$ where $a \approx 1.37$. Both of these are comparable with the non-conserved confidence model consensus times. However when $0 < p < \frac{1}{2}$ the consensus time was different and for the conserved confidence model is scaled linearly with N.

In contrast to the fast consensus seen in the non-conserved model we found that the mean-field equations (Eq.(4.1), (4.2)) of the conserved confidence model reaches a non-equal coexistence state when $p < \frac{1}{2}$, Fig. 4.9a. We suggest through discussion of the confidence distributions in Sec. 3.7 that this explains the consensus time. The confidence distributions and the mean confidence, Fig. 4.18a, highlight differences in the dynamics compared to the non-conserved model, Sec. 3.7. We see that the proportion of agents with lower k increases faster in the minority group than the majority. These lower k–value agents act a little like strong confidence agents

(in the $p > \frac{1}{2}$ case), because $p < \frac{1}{2}$ they convert agents from the majority. Hence we see the majority group lose agents and the minority group gain, Fig. 4.9a. In the non-conserved confidence model when $\frac{1}{2} < p$ there was the generation of zealot-like agents with confidence higher than any other agents that drove the opinion group size to oscillate, Sec. 3.7. However the behaviour in the $p < \frac{1}{2}$ conserved confidence model is different and the populations stabilise at a non-equal coexistence state because no agents from the minority are able to achieve a k–value more extreme (i.e. lower) than any other agent. An extension to this work is to define and solve a heuristic model of the conserved confidence model to identify the strength of the stability of the non-equal coexistence state for different p values.

We found that the dynamics of the opinion group size of the conserved model with $\frac{1}{2} < p < 1$, Fig. 4.5a, were qualitatively the same as the non-conserved model, Fig. 3.9a. In both models an equal coexistence state is reached in the mean-field model. We found that in the mean-field model of the $p = 1$ case the opinion group size oscillated more strongly than the other $\frac{1}{2} < p$ cases. This was in qualitative agreement with the behaviour of the opinion group size in the non-conserved model.

We found a non-equal coexistence state in the mean-field conserved confidence model when $p < \frac{1}{2}$, which we suggest is an explanation for the change in the consensus time between this model and the non-conserved confidence model.

7.3 Biased Axelrod model

We introduced a modified Axelrod model that included static heterogeneity to the opinion space. We found that the model with the heterogeneity over the probability of which feature is updated, the Biased Outcome model, reached the same typical types of frozen state as the Axelrod model, Fig. 6.4a 6.4b for the case where all pairs were linked. We presented these results as the plots with fixed q and varied F because one would imagine that the consequence of linking features would cause the dynamics to follow the same typical behaviour as an Axelrod model with a reduced number of features. We found that the type of consensus reached was coexistence in the adapted model when the choice of F resulted in coexistence in the Axelrod model, and the same for the F values that resulted in consensus, Fig. 6.4a 6.4b. Also we found that the time taken by the system to reach the frozen states in the stochastic simulations were comparable between the adapted model and the original Axelrod model, both for both fully linked features Fig. 6.5, and a single pair of linked features, Fig. 6.6. We suggest that the Axelrod model is resilient to the heterogeneity we introduced because overall the Axelrod model was still able

to reach the consensus or coexistence states in the same average time despite the introduction of the heterogeneity in the opinion space, which effected which feature is updated in the interactions. Research has found that introducing heterogeneity to the opinion space at the interaction stage through the introduction of a global media [24] [25] [55] can effect the type of frozen that the system reaches. We note that the heterogeneity we introduced was different to these previous modified Axelrod models.

We also introduced heterogeneity to the probability of interacting in the Axelrod model and we introduced a bias on the influence of the features in their respective contribution to the probability of interaction. We found that this increased the time to frozen state, on average, in comparison to the original Axelrod model, Fig. 6.11. We found that despite the change in the speed of the dynamics the type of frozen state reached was the same between the two models, Fig. 6.9, 6.10. Research on the modified Axelrod model with an altered interaction probability found that the result of reducing the probability of interaction by incorporating a threshold of similarity between agents before an interaction can take place was that the typical number of agents in the largest cultural group was reduced [51]. Our results suggest that Axelrod model is robust to the heterogeneity which we introduced in our model.

7.4 Further Work

There are several natural extensions to the work we have presented in this thesis. The non-conserved confidence model has confidence distributions which could be studied in the extreme $p = 1$ case. Work to found the specific p dependence of the consensus time is possible area of research. Creating a simple model that explains this specific dependence would be the next step after that. Another specific area of extension to this work is the the creation and solution of a heuristic model for the conserved confidence model. Studying the non-conserved confidence model on network structures which are not regular is a possible extension. A natural extension to the work on the spatial model is to measure the density of interfaces to understand the nature of the coarsening at different times in the simulations for the spatial non-conserved model.

Appendix A

Heuristic model

The explicit formulae for the multivariate polynomials appearing on the right hand side of Eqs. (3.28)–(3.30) defining the reduced model in Sec. **??** are detailed below. All of these terms are subleading in the neighbourhood of the coexistence fixed point.

Where $F_Y = F_Y(X, Y, Z)$, $F_Z = F_Z(X, Y, Z)$

$$
\begin{aligned}
F_Y &= -2X^5 + 5X^4 - 4X^3 - 2X^2Y + X^2 - 4XY^2 + 2XY + 2Y^3Z + 2Y^2 + \\
&\left(4XY^2Z - 2Y^2Z + 2X^2YZ - 2XYZ - 2Y + 2X^5Z - 5X^4Z + 4X^3Z - X^2Z\right)|Y| \\
F_Z &= -X^2Y^2Z^2 + X^2 + 2XY^3Z^2 - 2XY - X - Y^3Z^2 + Y + (2p-1)\left[2XY^3Z^2 - Y^3Z^2\right. \\
&+2Y^2Z - 4X^3YZ + 6X^2YZ - 2XYZ + 10XY - 5Y - X^4Z + 2X^3Z - X^2Z + \\
&\left.\left(X^4Z^2 + 4X^3YZ^2 - 2X^3Z^2 - 6X^2YZ^2 + X^2Z^2 + \text{"}XYZ^2 - 12XYZ - 2Y^2Z^2 + 6YZ\right)|Y|\,\right].
\end{aligned}
$$

Appendix B

Axelrod Biased Topic model: update probabilities

In the the Biased Topic model the probability that two individuals will interact is m/F where m is the overlap of the Features, F, between the two agents, i and j, so $m = \sum_{f=1}^{F} \delta_{C_i^f, C_j^f}$. We also define $F^{'}$, the number of features which are different between i and j, i.e. $F^{'} = F - m$.

If two individuals do interact, then we have a probability that a certain feature will be changed, $P(m)$. We define the probability for a linked feature, P_l and a standard feature P_s separately for clarity.

We consider the three possible cases for the linked features. When two agents interact their features are compared. Of the list of features that make up their states we consider features p and q. Where p and q are linked (for example features 1 and 2) there are only three cases:

Case (1) is interesting:

- feature p has a shared trait between the agents
- feature q does not have a shared trait between the agents
- therefore feature q will have a probability of being updated given by P_l
- feature p cannot be updated because it is already shared

Case (2) is the standard situation:

- feature p does not have a shared trait between the agents
- feature q does not have a shared trait between the agents

- therefore features p and q will each have a probability of being updated given by P_s

Case (3) is trivial:

- feature p has a shared trait between the agents,
- feature q has a shared trait between the agents,d
- features p and q cannot be updated because they are both already shared.

We define L to be the number of features that can be updated and satisfy Case (1) above. Therefore if $L = 0$ then there are no features with probability P_l and

$$P_s(m) = \frac{1}{F'}$$

And if $L \neq 0$ we have:

$$P_l(m) = \left(\frac{L}{F'} + \alpha \frac{F' - L}{F'} \right) \frac{1}{L}$$

and

$$P_s(m) = \frac{1 - \alpha}{F'}$$

Where α is the parameter tuning between the original Axelrod model ($\alpha = 0$) and our modified model and α determines how much more important a linked feature (which is different and linked to a feature which is not shared by the agents) is to a feature which is not shared by the agents. When $\alpha = 1$ we can only update a linked feature (which is different and linked to a feature which is not shared by the agents). When $\alpha = 0$ all the features not shared by the agents have equal probability of being updated.

For example if we have 7 features, and all are linked (in this case three pairs), and 3 features have shared traits between the agents then, $m = 3$, $F = 7$, $F^{'} = 4$. Supposing that of the 3 pairs of features that are linked in only one pair is only one of the features is shared by the agents, as seen in the example in Fig. B.1.

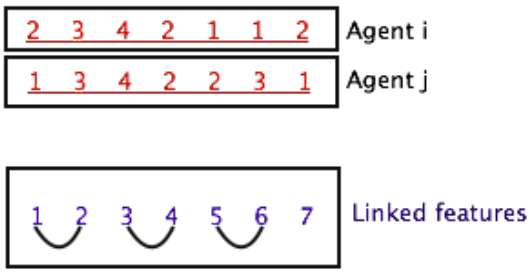

Figure B.1: An example of the states of two agents interacting, and the features which are linked in all agents.

So we have 4 features which are not shared by the two agents, and 3 of these are standard features, and 2 of these are part of linked features. The role of α is to tune between giving equal weight to all 4 features and only weighting the feature which is part of a linked pair and have the other feature the same. For example:

- feature 1 - different between agent i and agent j (linked to 2)
- feature 2 - the same between agent i and agent j (linked to 1)
- feature 3 - the same between agent i and agent j (linked to 4)
- feature 4 - the same between agent i and agent j (linked to 3)
- feature 5 - different between agent i and agent j (linked to 6)
- feature 6 - different between agent i and agent j (linked to 5)
- feature 7 - different between agent i and agent j

So here, features 1, 5, 6 and 7 can be updated with a probability weighting that depends on α. The probabilities for the following features are:

- the feature 1 has probability: $P_l = \left(\frac{1}{4} + \frac{3}{4}\alpha\right)\frac{1}{1}$
- each feature 5, 6 has probability: $P_s = \frac{1}{4}(1-\alpha)$
- and feature 7 has probability: $P_s = \frac{1}{4}(1-\alpha)$

We see that the total probability is 1 because the sum is

$$\sum_{F'} P_l + P_s = P_l \times (L) + P_s \times (F^{'} - L) = 1P_l + 3P_s = \frac{1}{4} + \frac{3}{4}\alpha + \frac{3}{4}(1-\alpha) = 1.$$

Bibliography

[1] T. Antal, S. Redner, and V. Sood. Evolutionary dynamics on degree-heterogeneous graphs. *Physical Review Letters*, 96:188104, 2006.

[2] S. E. Asch. Forming impressions of personality. *Journal of Abnormal and Social Psychology*, 41:258, 1946.

[3] S. E. Asch. Studies of independence and conformity: A minority of one against a unanimous majority. *Psychological Monographs*, 70(1), 1956.

[4] R. Axelrod. The dissemination of culture. *Journal of Conflict Resolution*, 41 (2):203, 1997.

[5] R. Axelrod. *The Complexity of Cooperation*. Princeton University Press, 1997.

[6] L. Behera and F. Schweitzer. On spatial consensus formation: Is the sznajd model different from a voter model? *International Journal of Modern Physics C*, 2003.

[7] E. Ben-Naim, F. Vazquez, and S. Redner. On the structure of competitive societies. *European Physics Journal B*, 26:531, 2006.

[8] E. Ben-Naim, F. Vazquez, and S. Redner. Parity and predictability of competitions. *Jounal of Quantitative Analysis in Sports*, 2(4), 2006.

[9] J. Billy, J. Rodgers, and J. Udry. Adolescent sexual behavior and friendship choice. *Social Forces*, 62:653, 1984.

[10] C. Castellano, M. Marsili, and A. Vespignani. Nonequilibrium phase transition in a model for social influence. *Physical Review Letters*, 85:3536, 2002.

[11] X. Castello, V. M. Eguiluz, and M. San Miguel. Ordering dynamics with two non-excluding options: bilingualism in language competition. *New Journal of Physics*, 8(308), 2006.

[12] D. Centola, J. C. Gonzalez-Avella, V. M. Eguiluz, and M. S. Miguel. Homophily, cultural drift and the coevolution of cultural groups. *Journal of Conflict Resolution*, 51:905, 2007.

[13] P. Clifford and A. Sudbury. A model for spatial conflict. *Biometrika*, 60(3): 581, 1973.

[14] J. T. Cox. Coalescing random walks and voter model consensus times on the torus in zd. *The Annals of Applied Probability*, 17(4):1333, 1989.

[15] L. Dall'Asta and C. Castellano. Effective surface-tension in the noise-reduced voter model. *Europhysics Letters*, 77(60005), 2007.

[16] L. Dall'Asta and T. Galla. Algebraic coarsening in voter models with intermediate states. *Journal of Physics A: Mathematical and Theoretical*, 41:16, 2008.

[17] L. De Sanctis and T. Galla. Effects of noise and confidence thresholds in nominal and metric axelrod dynamics of social influence. *Physical Review E*, 79:046108, 2009.

[18] G. Deffuant, D. Neau, F. Amblard, and G. Weisbuch. Mixing beliefs among interacting agents. *Advances in Complex Systems*, 3:87, 2001.

[19] I. Dornic, H. Chate, J. Chave, and H. Hinrichsen. Critical coarsening without surface tension: The universality class of the voter model. *Physical Review Letters*, 87(4):045701, 2001.

[20] B. Erickson. *Networks, ideologies and belief systems.* Social Structure and network analysis. CA: Sage, 1982.

[21] L. Festinger, S. Schachter, and K. Back. *Social Pressures in Informal Groups: A Study of Human Factors in Housing.* Harper, USA, 1950.

[22] A. Flache and M. W. Macy. Why more contact may increase cultural polarization. *eprint arxiv:physics/0604196*, 2006.

[23] L. Frachebourg and Krapivsky P. L. Exact results for kinetics of catalytic reactions. *Physical Review E*, 53:R3009, 1996.

[24] J. C. Gonzalez-Avella, M. G. Cosenza, and K. Tucci. Nonequilibrium transition induced by mass media in a model for social influence. *Physical Review E*, 72 (065102), 2005.

[25] J. C. Gonzalez-Avella, M. G. Consenza, K. Klemm, V. M. Eguiluz, and M. S. Miguel. Information feedback and mass media effects in cultural dynamics. *The Journal of Artitificial Societies and Social Simulation*, 10(9), 2007.

[26] C. Gracia-Lazaro, L. F. Lafuerza, L. M. Floria, and Y. Moreno. Residential segregation and cultural dissemination: An axelrod-schelling model. *Physical Review E*, 80(046123), 2009.

[27] J. M. Grieg. The end of geography? globalization, communications, and culture in the internal system. *Journal of Conflict Resolution*, 46:225, 2002.

[28] I. L. Janis. Personality correlates of susceptibility to persuasion. *Journal of Personality*, 22:504, 1954.

[29] M. Kearns, S. Judd, J. Tan, and J. Wortman. Behavioral experiments on biased voting in networks. *Proceedings of the National Academy of Sciences*, 106(1347), 2009.

[30] K. Klemm, V. Eguiluz, R. Toral, and M. San Miguel. Role of dimensionality in axelrod's model for the dissemination of culture. *Physica A*, 327(1), 2003.

[31] K. Klemm, V. M. Eguiluz, R. Toral, and M. S. Miguel. Global culture: A noise-induced transition in finite systems. *Physical Review E*, 67:045101, 2003.

[32] K. Klemm, V. M. Eguiluz, R. Toral, and M. San Miguel. Nonequilibrium transitions in complex networks: A model of social interaction. *Physical Review E*, 67:026120, 2003.

[33] K. Klemm, V. M. Eguiluz, R. Toral, and M. Sanmiguel. Global, polarization and cultural drift. *Jounal of Economic Dynamics and Control*, 29:321, 2005.

[34] P. L. Krapivsky and S. Redner. Dynamics of majority rule in two-state interacting spin systems. *Physical Review Letters*, 90:238701, 2003.

[35] P.L. Krapivsky, S. Redner, and E. Ben-Naim. *A Kinetic View of Statistical Physics*. Cambridge University Press, Cambridge, 2010.

[36] R. Lambiotte and S. Redner. Dynamics of vacillating voters. *Journal of Statistical Mechanics Theory and Experiment*, 2007.

[37] N. Lanchier. The axelrod model for the dissemination of culture revisited. *The Annals of Applied Probability*, 22:860, 2012.

[38] B. Latane and S. Wolf. The social impact of majorities and minorities. *Psychological Review*, 88(5):438, 1981.

[39] T. M. Liggett. *Stochastic Interacting Systems: Contact, Voter and Exculsion Processes*. Springer, 1999.

[40] M. W. Macy and R. Willer. From factors to actors: Computational sociology and agent-based modeling. *Annual Review of Sociology*, 28:143, 2002.

[41] N. Masuda, N. Gibert, and S. Redner. Heterogeneous voter models. *Physical Review E*, 82:010103, 2010.

[42] K. I. Mazzitello, J. Candia, and V. Dossetti. Effects of mass media and cultural drift in a model for social influence. *International Journal of Modern Physics C*, 18:1475, 2007.

[43] J. McPherson and L. Smith-Lovin. Homophily in voluntary organizations: Status distance and the composition of face-to-face groups. *American Sociological Review*, 52:370, 1987.

[44] M. McPherson, L. Smith-Lovin, and J. Cook. Birds of a feather: Homophily in social networks. *Annual Review of Sociology*, 27:415, 2001.

[45] M. Mobilia. Does a single zealot affect an infinite group of voters? *Physical Review Letters*, 91:028701, 2003.

[46] M. Mobilia, A. Petersen, and S. Redner. On the role of zealotry in the voter model. *Journal of Statistical Mechanics Theory and Experiment*, (P08029), 2007.

[47] S. Moscovici. Toward a theory of conversion behavior. *Advances in experimental social psychology*, 13:209, 1980.

[48] S. Moscovici and M. Zavalloni. The group as a polarizer of attitudes. *Journal of Personality and Social Psychology*, 12(125), 1969.

[49] D. G. Myers. *Polarizing Effects of Social Interaction*. Group Decision Making. London: Academic Press, 1982.

[50] A. Nowak, J. Szamrej, and B. Latane. From private attitude to public opinion: A dynamic theory of social impact. *Psychological Review*, 97(3):362, 1990.

[51] A. Parravano, H. Rivera-Ramirez, and M. G. Cosenza. Intracultural diversity in a model of social dynamics. *Physica A*, 379:241, 2007.

[52] N. Rhodes and W. Wood. Self-esteem and intelligence affect influenceability: The mediating role of message reception. *Psychological Bulletin*, 111:156, 1992.

[53] T. C. Schelling. Models of segregation. *American Economic Review*, 59:488, 1969.

[54] M. Scheucher and H. Spohn. A soluble kinetic model for spinodal decomposition. *Journal of Statistical Physics*, 53(1):279, 1988.

[55] Y. Shibanai, S. Yasuno, and I. Ishiguro. Effects of global information feeback on diversity - extensions to axelrods' adadptive cultural model. *Journal of Conflict Resolution*, 45:80, 2001.

[56] V. Sood and S. Redner. Voter model on hetrogenous graphs. *Physical Review Letters*, 94:178701, 2005.

[57] H-U. Stark, C. J. Tessone, and F. Schweitzer. Decelerating microdynamics can accelerate macrodynamics in the voter model. *Physical Review Letters*, 101: 018701, 2008.

[58] F. Vazquez and S. Redner. Non-monotonicity and divergent time scale in axelrod model dynamics. *Europhysics Letters*, 78:18001, 2007.

[59] F. Vazquez, P. L. Krapivsky, and S. Redner. Constrained opinion dynamics: freezing and slow evolution. *Jounal of Physics A*, 36:L61, 2003.

[60] F. Vazquez, J. Gonzalez-Avella, M. Eguiluz, and M. San Miguel. Time scale competition leading to fragmentation and recombination transitions in the coevolution of network and states. *Physical Review E*, 76, 2007.

[61] B. Wang, Y. X. Han, L. N. Chen, and K. Aihara. Limited ability driven phase transitions in the coevolution process in axelrod's model. *Physics Letters A*, 373:1519, 2009.